ČESKÉ VYSOKÉ UČENÍ TECHNICKÉ V PRAZE

FAKULTA STROJNÍ

MASTER THESIS

“VIBRATIONAL ANALYSIS AND MATHEMATICAL MODELLING OF VEHICLE SUSPENSION”

2020

ABDULMUHAIAMAN ALWAIR

ABSTRACT

The dilemma faced by a design engineer during the vehicle development program is during the design process, in which he requires, load data representing severe customer usage. During the initial stage, only predicted loads estimated from historical targets are available, whereas the actual loads are not available at in the initial stage but only at the far end of the process. At the same time during the initial stages of the design process changes required are easier and inexpensive whereas they become extremely costly in the latter stages of the process.

For the automobile designers suspension design is a one of the most challenging task as it have view of complex objectives, number of control parameters, and stochastic disturbances. It's a challenging to maintain high standard of ride comfort and good vehicle handling, from worst to best, under all driving conditions. Predicting the load acting on the whole vehicle is currently being researched and is also one of the hot research topic.

The vibration of an on-road vehicle is because of the unevenness of road surface on which we may travel. Vehicle dynamic analysis is important from the view point of ride comfort, safety of passenger and defense vehicle, and overall performance of vehicle.

When a particle or a body or system of connected bodies displaced from its steady state position or from an edge of an equilibrium vibration comes into picture. Most vibrations are not desirable neither in machines, system nor in structures. Vibration produce increase in stresses of material and body, it increases energy loss, and add wear in the system, it increases bearing loads, it created fatigue, create passenger discomfort in vehicles, which is detailed in this work and absorb energy from the system.

In general, a vibrating system consists of a spring, a mass or inertia, and a damper. Spring is used for storing potential energy. Mass or Inertia is used for storing kinetic energy.
Damper is used for energy degradation. An undamped vibrating system involves alternatively transfer its potential energy to kinetic energy and vice versa. In a damped vibrating system, some energy is lost in each vibration cycle and required to be replaced by an external source in order to maintain a steady state of vibration.

There are mainly 3 models used for performing analysis the dynamic behavior of vehicle and its vibration control: The quarter-car model, the half-car model and the full-vehicle model. The simplest representation of a ground vehicle is a quarter-car model with a spring and a damper connecting the body to a single wheel which is in turn connected to the ground via the tire spring.

In automobile industry, NVH (Noise, Vibration and Harness) is an important issue to consider. In designing also NVH is one of the points required (but given less importance). The main techniques for vibration analysis are: Time Domain Analysis, Frequency Spectrum Analysis, Modal Analysis, Finite Element Analysis and Digital Order Tracking. Among these FEA is mostly used nowadays.

ACKNOWLEDGEMENT

I am grateful to my supervisor, **Ing. Musalek Lubomir** for all his guidance and advise during my thesis work and for providing me with insights during the course of the project. I also express my thankfulness to **Ph,D. Ing. Hlavac Vladimir,** along with all the professors I had during my Masters program for the knowledge I gained from them. I would also like to thank my colleagues for their kind co-operation over the course of the program.

Lastly, I am thankful to my parents, my fiancée and my family for their continuous love and support.

Name:

DECLARATION

I declare that this Masters thesis entitled “**Vibrational Analysis and Mathematical Modelling of Vehicle Suspension**” is my own work performed under the supervision of **Ing. Musalek Lubomir**, with the use of the literature and references provided at the end of my Masters thesis.

In Prague 17-01-2020 ……………………

ABDULMUHAIAMAN ALWAIR

TABLE OF CONTENTS

List of Figures

List of Tables

CHAPTER 1. INTRODUCTION

1.1 Basic of Vibration

When a particle or a body or system of connected bodies displaced from its steady state position or from an edge of an equilibrium vibration comes into picture. Most vibrations are not desirable neither in machines or system nor in structures. Vibration produce increase in stresses of material and body, it increases energy loss, and add wear in the system, it increases bearing loads, it created fatigue, create passenger discomfort in vehicles [10], which is detailed in this Thesis and absorb energy from the system.

A system is a combination of elements intended to act together to accomplish an objective. For example, an automobile is a system whose elements are the wheels, suspension, car body, and so forth. Vibration occurs when a system is displaced from equilibrium. The system tends to return to its equilibrium position under the action of restoring forces. The system keeps moving back and forth across its position of equilibrium [10].

Most of our activities in day to day life involve vibration in one form or other. For example, our eardrums vibrate, light waves vibrate, vibration of lungs, the oscillatory motion of larynges and the most important concept, Nothing is Stationary in the Universe – the elements (atoms) vibrates. In recent times, many investigations have been motivated by the engineering applications of vibration, such as the design of control systems. In many engineering systems, a human being acts as an integral part of the system. The transmission of vibration to human beings results in discomfort and loss of efficiency.

In general, a vibrating system consists of a spring, a mass or inertia, and a damper [10] as shown in Fig. 1.1. Spring is used for storing potential energy. Mass or Inertia is used for storing kinetic energy. Damper is used for energy degradation or energy absorption. An undamped vibrating system involves alternatively transfer its potential energy to kinetic energy and vice versa. In a damped vibrating system, some energy is lost in each vibration cycle and required to be replaced by an external source in order to maintain a steady state of vibration.

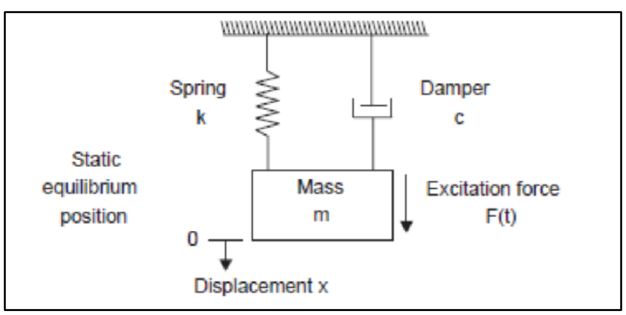

Figure 1. 1 A Simple System of Mass, Spring and Damper

Mechanical Vibration can be classified as shown in Figure 1.2 below [2]:

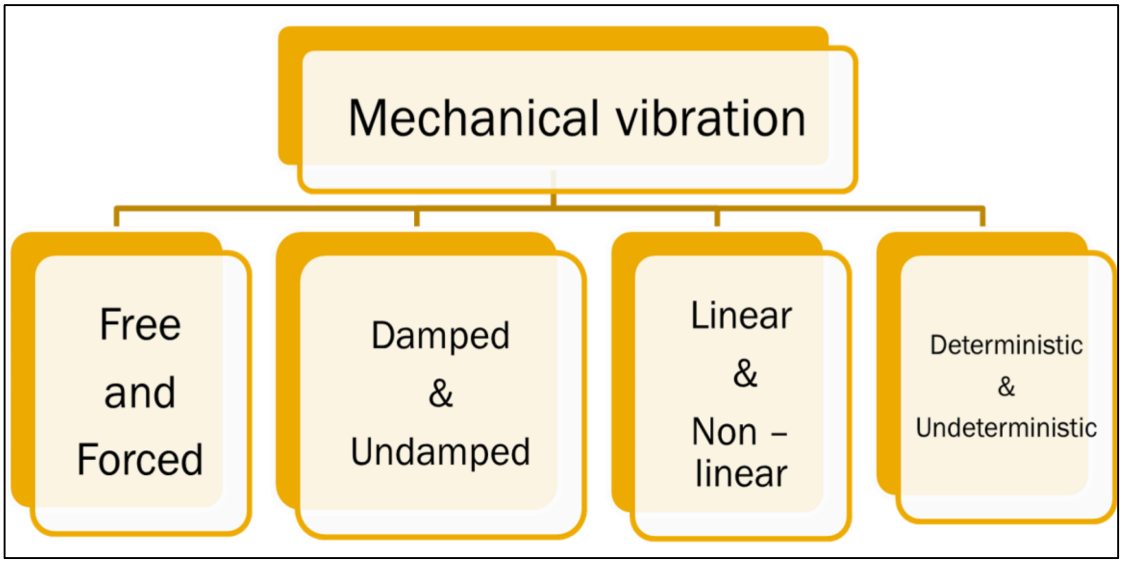

Figure 1. 2 Types of Mechanical Vibration

1) **Free – Vibration**: After an initial disturbance, if a system, is left to vibrate on its own, the ensuing vibration is known as free vibration. There is no external force acting on the system. One of the example of free vibration is the oscillation of a simple pendulum.
2) **Forced – Vibration**: If a system is subjected to a repeating type of external force, the resulting vibration is known as forced vibration. Example of forced vibration is the oscillation that arises in machines such as diesel engines.
3) **Undamped – Vibration**: If energy is not lost or dissipated because of friction or other resistance during oscillation or motion of the system, the vibration is known as undamped vibration.
4) **Damped – Vibration**: If any energy is lost or dissipated because of friction or other resistance during oscillation or motion of the system or in any other way, however, it is called damped vibration.
5) **Linear and Non Linear Vibration**: The spring, mass, and damper are the basic components of a vibratory system. If they behave linearly, the resulting vibration is known as linear vibration. If any of the spring, mass or damper behave nonlinearly, the vibration becomes nonlinear vibration.
6) **Deterministic and Non Deterministic Vibration**: If the amplitude or magnitude of the excitation (force or motion) acting on a vibratory system is known at any given time, the excitation is called deterministic and vibration is called deterministic vibration. In some cases, the excitation is non-deterministic or random; the value of the excitation at a given time cannot be predicted. Wind velocity, road roughness, and ground motion during earthquakes are examples of Non Deterministic Vibration.

1.2 Causes of Vibration

There are various ways we can tell that something is vibrating. Either by touching or by seeing or by hearing a sound or by sensing heat. System vibration can occur in various forms. A machine component may vibrate over large or small distances, quickly or slowly and with generation sound or heat or without generation[2]. System vibration can be intentionally designed having functional purpose. System vibration can be unintended, leading to machine damage. Most times system vibrations are unintended and undesirable.

All machine vibration occurs mainly due to these reasons [5,2]:

a) Repetition of forces
b) Looseness of the equipment in the system
c) Resonance

As in our case, a vehicle vibrates mainly due to road excitation, or due to wear of elements

1.3 Introduction to vehicle

In reality an automobile in its conventional form represents a very complicated vibrating system. It is well known that the rigid mass free in space has 6 degree of freedom;

- 3 translational such as: (a) bobbing up and down; (b) swaying back and forth and (c) moving forward and backward,
- 3 rotational such as: (a) rolling about a longitudinal axis; (b) pitching about lateral axis and (c) yawing about vertical axis.

Since an automobile has 3 such masses viz., (a) the body, (b) the front and rear axles and (c) 8 distinct springs, 4 springs and 4 wheels, it has 18 degrees of freedom.

1.4 Vehicle suspension

The design of vehicle suspension system is a complicated task. The main objective of suspension is to provide soft riding and good handling ability. The suspension design is a compromise between these objectives, depending upon the manufacturer's objective. A properly designed suspension also produces minimum wear on wheels and other parts of the vehicles. The wheels are either mounted conventionally or independently.

There are dynamic forces acting on the vehicle. These forces depend on surface condition and friction between road and wheel, also it depends on the type of wheel. The dynamic forces are Acceleration, braking and steering forces acting on a vehicle. The amount of friction depends on the type and surface of wheel and road as well as the weight of the wheel. Control is lost on any wheel if the dynamic load exceeds the friction and wheel slips.

Moving vehicle encountering road irregularities which is not considered theoretically. According to theory the ideal wheel model should contact ground squarely and should roll without any sidewise force. Besides this vehicle encounters wind just and required directional control. Also, there is a change in weight and acceleration because of large and small bumps and in addition to movable suspension.

Deflections due to small bumps are absorbed by wheels, but that from larger bumps is carried out through wheels to the vehicle suspension system. Suspension if designed properly, for a wide band of deflection, absorbs these deflections and run smoothly. Suspension with limited deflection bounces the vehicle body. The suspension system not only absorb shock and support the automobile system, but it keeps wheel in contact with road.

1.5 Vehicle Vibration

Vibration causes human discomfort. When vehicle is under severe acceleration vibration is increased and hence discomfort, depending upon the amplitude and frequency of vibration. The road roughness creates acceleration of vehicle on vertical direction due to which passengers' experiences pounding. The problem of vehicle vibration is extremely complicated in nature. The real description of road is random in nature. The analysis of vehicle vibration is thus required

When a spring supported mass such as that of motor vehicle chassis is given an impulse, it is set into vibratory motion and it keeps on vibrating until the energy of the impulse completely dies out in overcoming damping forces. The sources of vibration of the vehicles may be due to;

- Road roughness
- Unbalance of engine
- Whirling of shaft
- Cam forces
- Torsional fluctuation, etc.

All vibratory systems have certain natural damping forces. In vehicle suspension the natural damping force is minimum, if coil springs or torsion bars are used, when it is due chiefly to due friction in the joins or bearing of the guiding mechanism. But in no case this damping force is sufficient for a comfortable ride under all condition. Therefore, on passenger cars and buses special damping devices are fitted.

1.6 Vehicle Vibration models

As mentioned earlier the problem of vehicle vibration is extremely complicated in nature since it involves dealing with multi – DoF system. To obtain a deterministic mathematical model idealization has been made to realistic problem. For present analysis in this thesis we assumed that the car travels in horizontal direction of the plane and motion consists of vertical and rotational motion of car body and vertical motion of wheels. The car body is represented by the sprung mass, which is constrained by springs and dampers. The springs consist of suspension springs and wheel springs. The mass of the wheels can also be considered as an unsprung one. The damping is due to suspension system and the wheels.

On the basis of different complexity level, the vehicle is modeled and classified in following main types:

(a) Quarter Car Model (b) Half Car Model

(c) Bicycle Car Model (d) Full Car Model

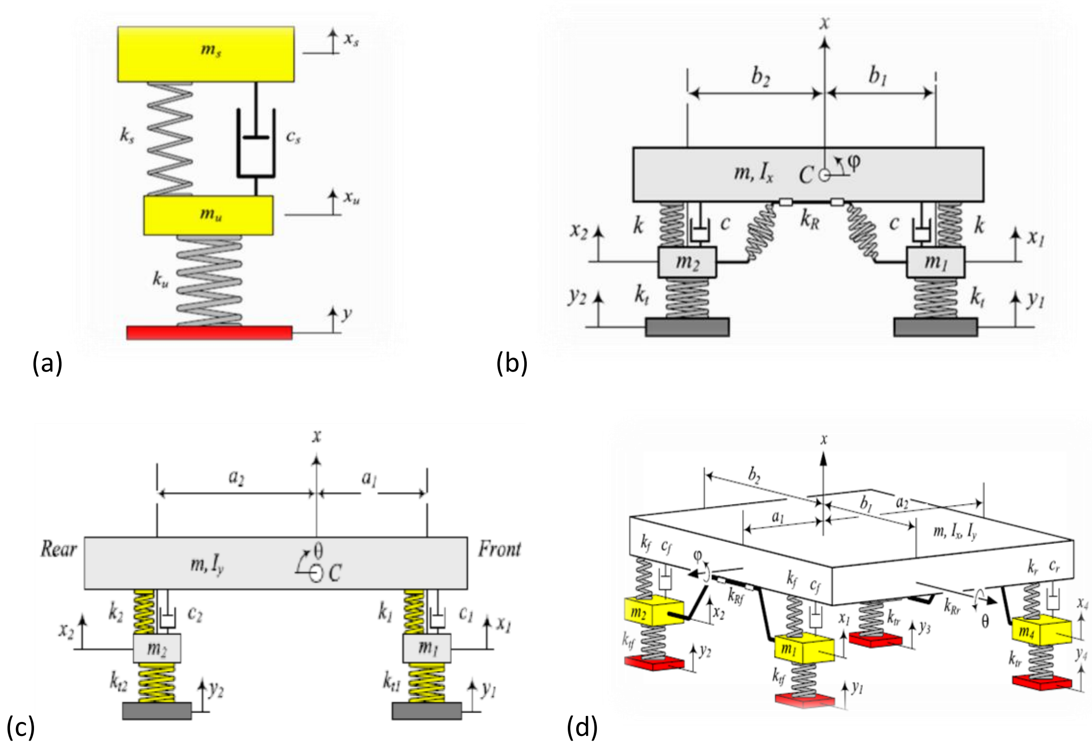

Figure 1. 3 (a) QCM, (b) HCM (c) BCM (d) FCM

1.7 Vibration Analysis

Before going in depth of this topic it is necessary to understand why we monitor vibration. Vibration is of interest mainly due the following reasons [5]:

- Due to long-term exposure to vibration can cause injuries and disease in humans, and back injuries occur due to vibration mainly in the vehicle.
- Vibration can cause discomfort, fatigue, dysfunction in both humans and things we manufacture.
- Vibration can be used for cleaning, etc.
- Vibration can cause noise.

Vibration analysis is a technique or more precisely a methodology by which we analyze the system performance, study the data and predict the reason for such performance. Mainly we analyze for predicting the life cycle, damage in system if occurred, behavior under certain regions, and so on.

Areas of Vibration Analysis [9,11]

- Structural dynamics
- Environmental engineering
- Fatigue analysis
- Vibration monitoring
- Acoustics

Different Vibrational Analysis Techniques [9,11]

- Time Domain Analysis
- Frequency Domain Analysis (FFT, Spectrum)
- Wavelet Transform
- Modal Analysis
- Finite Element Analysis

CHAPTER 2. Problem Statement

2. Problem Statement

Vibration induced in vehicle due to road roughness and its effect on driver, passengers and vehicle itself, is still a critical issue. Although test engineers and handling qualities specialists have dealt with this phenomenon over the past decades, it still is difficult to apprehend and all too often it catches engineers by surprise.

- This research was aimed to find out the causes of road induced oscillation (vibration) and analyzing them by traditional methods and to develop the simulation methods for analyzing. To accomplish this objective, initially development of the vehicle – road dynamic interaction model is required.

- Road roughness, bumps, curves and slopes effects the vehicle on road. Study of these effects on vehicle is considered.

- The repetition and magnitude of vibration is important which create impact on the driver and the speed of vehicle.

- Another supplementary objective of the subject research effort was to develop new concepts and design methods for road profile and vehicle design.

CHAPTER 3: Vehicle Vibrating Model

3.1 Quarter Car Model (QCM)

The most employed and useful model of a vehicle suspension system is a quarter car model, shown in Fig. 3.1. We introduce and examine the quarter-car model in this section. [12]

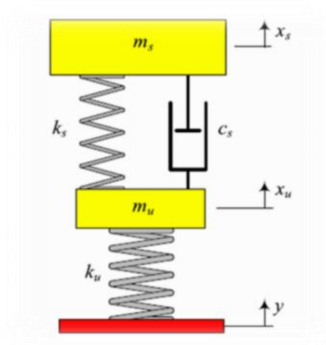

Figure 3.1 Quarter Car Model (QCM)

We represent the vertical vibration of a vehicle using a quarter-car model made of two solid masses, m_s and m_u, called sprung and unsprung masses, respectively. The sprung mass m_s represents $\frac{1}{4}$ of the body of the vehicle, and the unsprung mass m_u represents one wheel of the vehicle. A spring of stiffness k_s and a shock absorber with viscous damping coefficient c_s support the sprung mass. The spring k_s and the damping c_s are called the main suspension of the car. The unsprung mass m_u is in direct contact with the ground through a spring k_u, representing the tire stiffness.

The governing differential equations of motion for the quarter-car model shown in Fig are

$$m_s\ddot{x}_s + c_s(\dot{x}_s - \dot{x}_u) + k_s(x_s - x_u) = 0 \tag{3.1}$$

$$m_u\ddot{x}_u + c_s(\dot{x}_u - \dot{x}_s) + (k_u + k_s)x_u - k_s x_s = k_u y \tag{3.2}$$

Where (y) is the ground excitation.

The proof for the above equation of motion is given below:

The kinetic energy, potential energy, and dissipation function of the quarter car model are

$$K = \frac{1}{2} m_s \dot{x}_s^2 + \frac{1}{2} m_u \dot{x}_u^2 \tag{3.3}$$

$$V = \frac{1}{2} k_s (x_s - x_u)^2 + \frac{1}{2} k_u (x_u - y)^2 \tag{3.4}$$

$$D = \frac{1}{2} c_s (\dot{x}_s - \dot{x}_u)^2 \tag{3.5}$$

Employing the Lagrange method,

$$\frac{d}{dt}\left(\frac{\partial K}{\partial \dot{x}_s}\right) - \frac{\partial K}{\partial x_s} + \frac{\partial D}{\partial \dot{x}_s} + \frac{\partial V}{\partial x_s} = 0 \tag{3.6}$$

$$\frac{d}{dt}\left(\frac{\partial K}{\partial \dot{x}_u}\right) - \frac{\partial K}{\partial x_u} + \frac{\partial D}{\partial \dot{x}_u} + \frac{\partial V}{\partial x_u} = 0 \tag{3.7}$$

We find the equations of motion below.

$$m_s \ddot{x}_s = -k_s (x_s - x_u) - c_s (\dot{x}_s - \dot{x}_u)$$

$$m_u \ddot{x}_u = k_s (x_s - x_u) + c_s (\dot{x}_s - \dot{x}_u) - k_u (x_u - y)$$

Which can be rearranged in matrix form:

$$[m]\, \dot{x} + [\mathrm{C}]\, \dot{x} + [k]\, x = F \tag{3.8}$$

$$\begin{bmatrix} m_s & 0 \\ 0 & m_u \end{bmatrix} \begin{bmatrix} \ddot{x}_s \\ \ddot{x}_u \end{bmatrix} + \begin{bmatrix} c_s & -c_s \\ -c_s & c_s \end{bmatrix} \begin{bmatrix} \dot{x}_s \\ \dot{x}_u \end{bmatrix} + \begin{bmatrix} k_s & -k_s \\ -k_s & k_s + k_u \end{bmatrix} \begin{bmatrix} x_s \\ x_u \end{bmatrix} = \begin{bmatrix} 0 \\ k_u y \end{bmatrix} \tag{3.9}$$

We may add a damper c_u in parallel to k_u, as shown in Fig., to model any damping in tires. However, the value of c_u for the tire, compared to the main suspension damping c_s, is very small, and, hence, we may ignore c_u to simplify the model. Having the damper c_u in parallel to k_u makes it possible to write the equation of motion of the system as

$$m_u \ddot{x}_u + c_u \dot{x}_u + c_s (\dot{x}_u - \dot{x}_s) + k_u x_u + k_s (x_u - x_s) = k_u y + c_u \dot{y} \tag{3.10}$$

$$m_s \ddot{x}_s - c_s (\dot{x}_u - \dot{x}_s) - k_s (x_u - x_s) = 0 \tag{3.11}$$

And in matrix form as:

$$\begin{bmatrix} m_u & 0 \\ 0 & m_s \end{bmatrix} \begin{bmatrix} \ddot{x}u \\ \ddot{\mathrm{x}}\mathrm{s} \end{bmatrix} + \begin{bmatrix} \mathrm{cu} + \mathrm{cs} & -\mathrm{cs} \\ -\mathrm{cs} & \mathrm{cs} \end{bmatrix} \begin{bmatrix} \dot{x}u \\ \dot{\mathrm{x}}\mathrm{s} \end{bmatrix} + \begin{bmatrix} ku + \mathrm{ks} & -\mathrm{ks} \\ -\mathrm{ks} & \mathrm{ks} \end{bmatrix} \begin{bmatrix} \mathrm{xu} \\ xs \end{bmatrix} = \begin{bmatrix} kuy + cu\dot{y} \\ 0 \end{bmatrix} \tag{3.12}$$

The state space is derived as follows:

Consider $x_1 = x_s, x_2 = x_u, x_3 = \dot{x_s}, x_4 = \dot{x_u}$, then the state space model will be obtained as flowing:

$$A = \begin{bmatrix} 0 & 0 & 1 & 0 \\ 0 & 0 & 0 & 1 \\ \frac{-k_s}{m_s} & \frac{k_s}{m_s} & \frac{-C_s}{m_s} & \frac{C_s}{m_s} \\ \frac{-k_s}{m_s} & -(\frac{k_s}{m_u} + \frac{k_t}{m_u}) & \frac{C_s}{m_u} & -\frac{C_s}{m_s} \end{bmatrix} \quad , \quad x = \begin{bmatrix} x1 \\ x2 \\ x3 \\ x4 \end{bmatrix} = \begin{bmatrix} xs \\ xu \\ \dot{x}s \\ \dot{x}u \end{bmatrix}$$

$$B = \begin{bmatrix} 0 \\ 0 \\ 0 \\ \frac{\mathrm{kt}}{\mathrm{ms}} \end{bmatrix} \quad , \quad C = \begin{bmatrix} 1 & 0 & 0 & 0 \\ 0 & 1 & 0 & 0 \\ 0 & 0 & 1 & 0 \\ 0 & 0 & 0 & 1 \\ 1 & -1 & 0 & 0 \end{bmatrix}$$

$$D = [0]$$

<u>Mathematical model's limitations</u>: The quarter-car model contains no representation of the geometric effects of the full car and offers no possibility of studying longitudinal and lateral interconnections. However, it contains the most basic features of the real problem and includes a proper representation of the problem of controlling wheel and wheel–body load variations.

In the quarter-car model, we assume that the tire is always in contact with the ground, which is true at low frequency but is not true at high frequency. A better model must have the possibility of separation between the tire and ground.

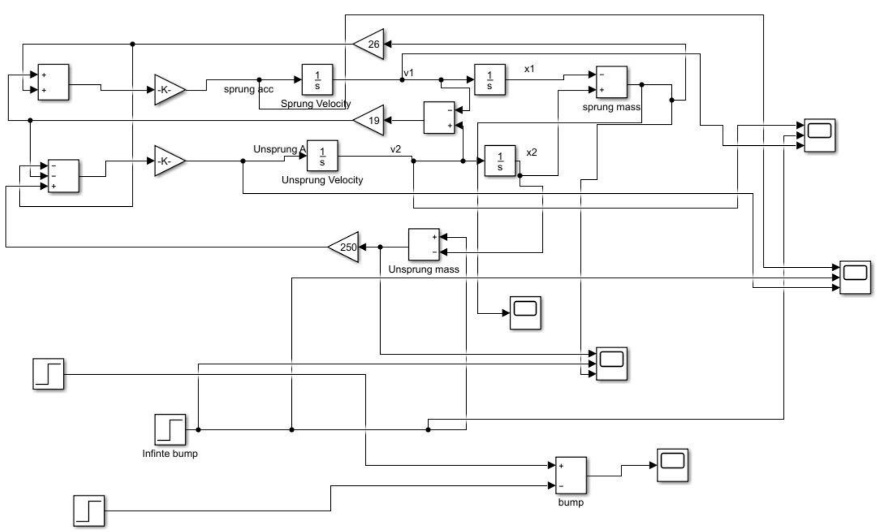

Figure 3.2 Simulink Model of QCM Implemented in MATLAB

3.2 Half Car Model (HCM)

3.2.1 Bicycle Model

Figure 3.3 illustrates the bicycle vibrating model of a vehicle [12,3]. This model includes the body bounce x, body pitch θ, wheels' hops x_1 and x_2, and independent road excitations y_1 and y_2.

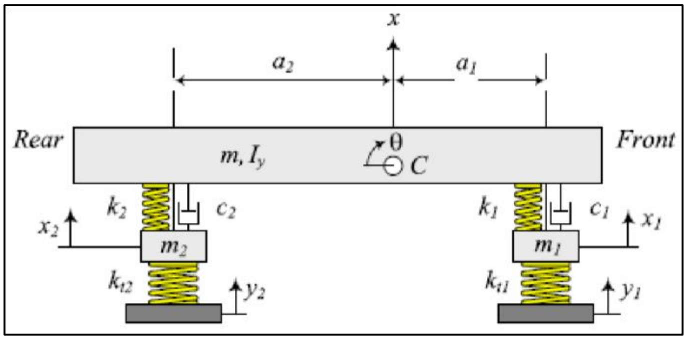

Figure 3. 3 Bicycle Car Model (BCM)

The equations of motion for the bicycle vibrating model of a vehicle are

$$[m]\ddot{x} + [c]\dot{x} + [k]x = F \tag{3.13}$$

Where, $\quad x = \begin{bmatrix} x \\ \theta \\ x1 \\ x2 \end{bmatrix}$

$$[m] = \begin{bmatrix} m & 0 & 0 & 0 \\ 0 & 1y & 0 & 0 \\ 0 & 0 & m1 & 0 \\ 0 & 0 & 0 & m2 \end{bmatrix}$$

$$[C] = \begin{bmatrix} c_1 + c_2 & a_2c_1 - a_1c_2 & -c_1 & -c_2 \\ a_2c_2 - a_1c_1 & {a_1}^2c_1 + {a_2}^2c_2 & a_1c_1 & -a_2c_2 \\ -c_1 & a_1c_1 & c_1 & 0 \\ -c_2 & -a_2c_1 & c_2 & 0 \end{bmatrix}$$

$$[K] = \begin{bmatrix} k_1 + k_2 & a_2k_2 - a_1k_1 & -k_1 & -k_2 \\ a_2k_2 - a_1k_1 & k_1{a_1}^2 + k_2{a_2}^2 & a_1k_1 & -a_2k_2 \\ -k_1 & a_1k_1 & k_1 & 0 \\ -k_2 & -a_2k_2 & 0 & k_2 + k_{t_2} \end{bmatrix}$$

$$F = \begin{bmatrix} 0 \\ 0 \\ y_1k_{t_1} \\ y_2k_{t_2} \end{bmatrix}$$

The Parameters in the above equations are defined as follows

m = half of body mass m_1 = mass of a front wheel m_2 = mass of a rear wheel x = body vertical displacement coordinate x_1 = front wheel vertical displacement coordinate x_2 = rear wheel vertical displacement coordinate θ = body pitch motion coordinate y_1 = road excitation at the front wheel

y_2 = road excitation at the rear wheel

I_y = half of body lateral mass moment

a_1 = absolute distance of C from front axle

a_2 = absolute distance of C from rear axle

The body of the vehicle is assumed to be a rigid bar. This bar has a mass m, which is half of the total body mass, and a lateral mass moment I_y, which is half of the total body mass moment. The front and rear wheels have a mass m_1 and m_2, respectively. The tires' stiffnesses are indicated by different parameters k_{t1} and k_{t2}. The difference is that the rear tires are usually stiffer than the fronts, although in a simpler model we may assume $k_{t1} = 2$. Damping of tires is much smaller than the damping of shock absorbers so, we may ignore the tire damping for simpler calculation.

To find the equations of motion of the bicycle vibrating model, we use the Lagrange method. The kinetic and potential energies of the system are

$$k = \frac{1}{2}m\dot{x}^2 + \frac{1}{2}m_1\dot{x}_1^2 + \frac{1}{2}m_2\dot{x}_2^2 + \frac{1}{2}I_y\dot{\theta}^2 \tag{3.14}$$

$$V = \frac{1}{2}k_{t_1}(x_1 - y_1)^2 + \frac{1}{2}k_{t_2}(x_2 - y_2)^2 + \frac{1}{2}k_1(x - x_1 - a_1\theta)^2 + \frac{1}{2}k_2(x - x_2 + a_2\theta)^2 \tag{3.15}$$

And its dissipation function is

$$D = \frac{1}{2}c_1(\dot{x} - \dot{x}_1 - a_1\dot{\theta})^2 + \frac{1}{2}c_2(\dot{x} - \dot{x}_2 + a_2\dot{\theta})^2 \tag{3.16}$$

Applying the Lagrange equation,

$$\frac{d}{dt}\left(\frac{\partial K}{\partial \dot{q}_r}\right) - \frac{\partial K}{\partial q_r} + \frac{\partial D}{\partial \dot{q}_r} + \frac{\partial V}{\partial q_r} = f_r \quad r = 1,2, \ldots ,4 \tag{3.17}$$

Provides us with the equations of motion:

$$m\ddot{x} + c_1(\dot{x} - x_1 - a_1\theta) + c_2(\dot{x} - \dot{x}_2 + a_2\theta) + k_1(x - x_1 - a_1\theta) + k_2(x - x_2 + a_2\theta) = 0 \tag{3.18}$$

$I_y\ddot{\theta} - a_1c_1(\dot{x} - \dot{x}_1 - a_1\theta) + a_2c_2(\dot{x} - \dot{x}_2 + a_2\theta) - a_1k_1(x - x_1 - a_1\theta) + a_2k_2(x -$
$x_2 + a_2\theta) = 0 \qquad (3.19)$

$m_1\ddot{x}_1 - c_1(\dot{x} - \dot{x}_1 + a_1\theta) + k_{t1}(x_1 - y_1) - k_1(x - x_1 + a_1\theta) = 0$

$m_2\ddot{x}_2 - c_2(\dot{x} - \dot{x}_2 + a_2\theta) + k_{t2}(x_2 - y_2) - k_2(x - x_2 + a_2\theta) = 0 \qquad (3.20)$

This set of equations may be rearranged in matrix form as (3.13).

The state space model can be derived as follows:

Consider $x_3 = x$, $x_4 = \theta$, $x_5 = x_1$, $x_6 = x_2$, $x_7 = \dot{x}$, $x_8 = \theta$, $x_9 = \dot{x_1}$, $x_{10} = \dot{x_2}$

$$A = \begin{bmatrix} 0 & 0 & 0 & 0 & 1 & 0 & 0 & 0 \\ 0 & 0 & 0 & 0 & 0 & 1 & 0 & 0 \\ 0 & 0 & 0 & 0 & 0 & 0 & 1 & 0 \\ 0 & 0 & 0 & 0 & 0 & 0 & 0 & 1 \\ -\frac{k_1+k_2}{m} & \frac{a_1k_1-a_2k_2}{m} & \frac{k_1}{m} & \frac{k_2}{m} & \frac{-c_1+c_2}{m} & \frac{a_1c_1-a_2c_2}{m} & \frac{c_1}{m} & \frac{c_2}{m} \\ \frac{-a_1k_1-a_2k_2}{l_y} & \frac{-k_1a_1^2-k_2a_2^2}{l_y} & \frac{-a_1k_1}{l_y} & \frac{a_2k_2}{l_y} & \frac{a_1c_1+a_2c_2}{l_y} & \frac{-a_1^2c_1+a_2^2c_2}{l_y} & -\frac{a1c1}{l_y} & \frac{a2c2}{l_y} \\ \frac{k_1}{m_1} & -\frac{a_1k_1}{m_1} & -\frac{k_1+k_{t_1}}{m_1} & 0 & \frac{c_1}{m_1} & -\frac{a_1c_1}{m_1} & -\frac{c_1}{m_1} & 0 \\ \frac{k2}{m_2} & \frac{a_2k_2}{m_2} & 0 & -\frac{k_2+k_{t_2}}{m_2} & \frac{c_2}{m_2} & \frac{a_2c_2}{m_2} & 0 & \frac{c_2}{m_2} \end{bmatrix}$$

$$B = \begin{bmatrix} 0 \\ 0 \\ 0 \\ 0 \\ 0 \\ 0 \\ \frac{k_1}{m_1} \\ \frac{k2}{m_2} \end{bmatrix}$$

3.2.2 Half Car model

To examine and optimize the roll vibration of a vehicle we may use a half car vibrating model[12,8,3]. Figure illustrates a half-car model of a vehicle. This model includes the body bounce x, body roll ϕ, wheels hop x_1 and x_2 and independent road excitations y_1 and y_2.

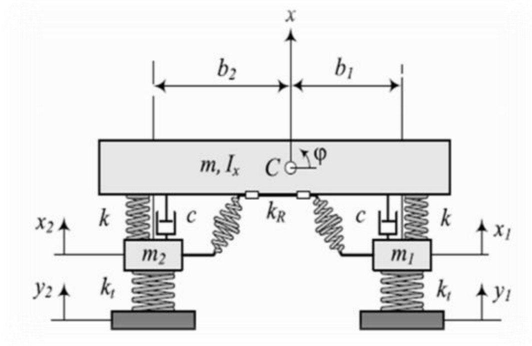

Figure 3. 4 Half Car Model (HCF)

The equations of motion for the half-car vibrating model of a vehicle are

$$m\ddot{x} + C(\dot{x} - \dot{x}_1 + b_1\dot{\varphi}) + C(\dot{x} - \dot{x}_2 - b_2\dot{\varphi}) + K(x - x_1 + b_1\varphi) + K(x - x_2 - b_2\varphi) = 0 \quad (3.21)$$

$$I_X\ddot{\varphi} + b_1 c(\dot{x} - \dot{x}_1 + b_1\dot{\varphi}) - b_2 c(\dot{x} - \dot{x}_2 - b_2\dot{\varphi}) + b_1 k(x - x_1 + b_1\varphi) - b_2 k(x - x_2 - b_2\varphi) + k_R\varphi = 0 \quad (3.22)$$

$$m_1\ddot{x}_1 - c(\dot{x} - \dot{x}_1 + b_1\dot{\varphi}) + k_t(x_1 - y_1) - k(x - x_1 + b_1\varphi) = 0 \quad (3.23)$$

$$m_2\ddot{x}_2 - c(\dot{x} - \dot{x}_2 - b_2\dot{\varphi}) + k_t(x_2 - y_2) - k(x - x_2 + b_2\varphi) = 0 \quad (3.24)$$

The half-car model may be different for the front half and rear half due to different suspensions and mass distribution besides, unique antiroll bars with various torsional solidness might be utilized in the front and back equal parts.

Figure shows a simpler vibrating model of the system. The body of the vehicle is assumed to be a rigid bar. This bar has a mass m, which is the front or rear half of the total body mass, and a longitudinal mass moment of inertia I_x, which is half of the total body mass moment of inertia. The left and right wheels have a mass m_1 and m_2, respectively, although they are usually equal. The tires' stiffnesses are described by k_t.

Damping of tires is much smaller than the damping of shock absorbers; therefore, we may ignore the tire damping for simpler calculations. The suspension of the car has stiffness k and damping c for the left and right wheels. It isn't unexpected to make the suspension of the left and right wheels reflect. So, the left and right stiffness and damping are equal. However, the half-car model may have different k, c, and k_t for front and rear. The vehicle may also have an antiroll bar with a torsional stiffness k_R in front and/or rear. Using a simple model, the antiroll bar provides us with a torque M_R proportional to the roll angle ϕ:

$$M_R = -k_R\varphi \quad (3.25)$$

However, a better model of the antiroll bar effect is

$$M_R = -k_R\left(\varphi - \frac{x_1 - x_2}{\omega}\right) \quad (3.26)$$

To find the equations of motion for the half car vibrating model, we use the Lagrange method. The kinetic and potential energies of the system are

$$k = \frac{1}{2}m\dot{x}^2 + \frac{1}{2}m_1\dot{x}_1^2 + \frac{1}{2}m_2\dot{x}_2^2 + \frac{1}{2}l_x\dot{\varphi}^2 \tag{3.27}$$

$$V = \frac{1}{2}k_t(x_1 - y_1)^2 + \frac{1}{2}k_t(x_2 - y_2)^2 + \frac{1}{2}k_R\varphi^2 + \frac{1}{2}k(x - x_1 - b_1\varphi)^2 + \frac{1}{2}k(x - x_2 + b_2\varphi)^2 \tag{3.28}$$

And the dissipation function is

$$D = \frac{1}{2}c(\dot{x} - \dot{x}_1 - b_1\dot{\varphi})^2 + \frac{1}{2}c(\dot{x} - \dot{x}_2 + b_2\dot{\varphi})^2 \tag{3.29}$$

Applying the Lagrange method

$$\frac{d}{dt}\left(\frac{\partial K}{\partial \dot{q}_r}\right) - \frac{\partial K}{\partial q_r} + \frac{\partial D}{\partial \dot{q}_r} + \frac{\partial V}{\partial q_r} = f_r \quad r = 1,2,\ldots,4 \tag{3.30}$$

Provides us with the equations of motion. The equations can be rearranged in matrix form,

$$[m]\ddot{x} + [c] + [k]x = F \tag{3.31}$$

Where, $x = \begin{bmatrix} x \\ \theta \\ x_1 \\ x_2 \end{bmatrix}$

$$[m] = \begin{bmatrix} m & 0 & 0 & 0 \\ 0 & l_x & 0 & 0 \\ 0 & 0 & m_1 & 0 \\ 0 & 0 & 0 & m_2 \end{bmatrix}$$

$$[C] = \begin{bmatrix} 2c & cb1 - cb2 & -c & -c \\ cb1 - cb2 & cb1^2 + cb2^2 & -cb1 & cb2 \\ -c & -cb1 & c & 0 \\ -c & cb2 & 0 & c \end{bmatrix}$$

$$[k] = \begin{bmatrix} 2k & kb1 - kb2 & -k & -k \\ cb1 - cb2 & kb1^2 + kb2^2 + k_R & -kb1 & kb2 \\ -K & -Kb1 & K + K_t & 0 \\ -K & Kb2 & 0 & K + K_t \end{bmatrix}$$

$$F = \begin{bmatrix} 0 \\ 0 \\ y1kt1 \\ y2kt2 \end{bmatrix}$$

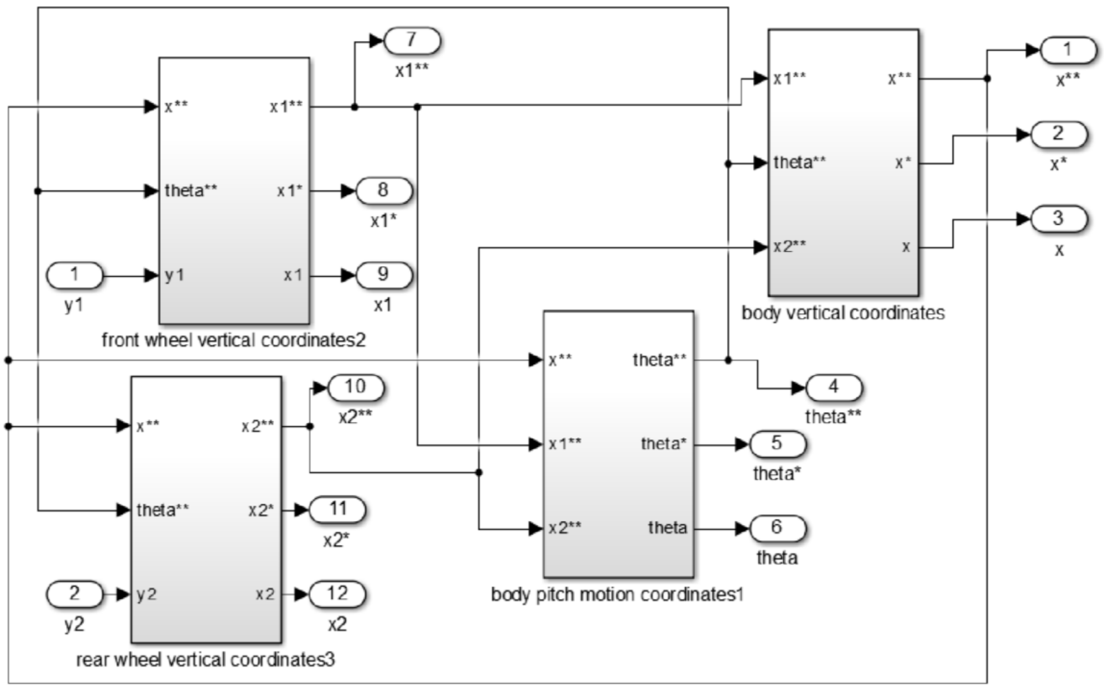

Figure 3.5 Simulink Model of HCM Implemented in MATLAB

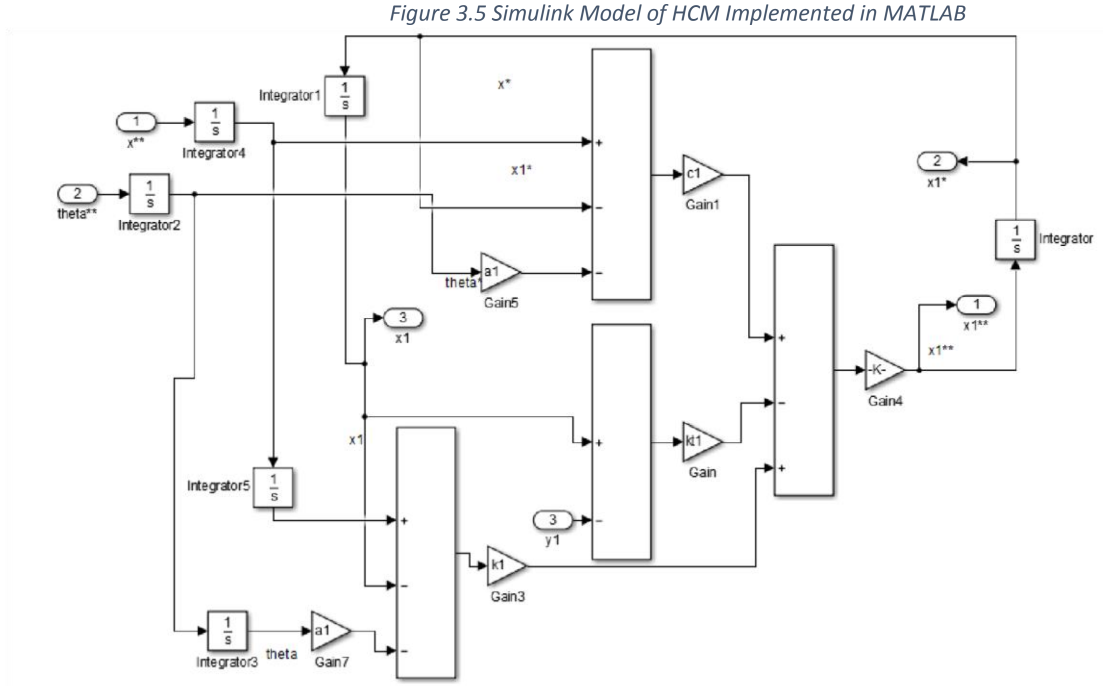

Figure 3.6 Front Wheel Coordinate Subsystem

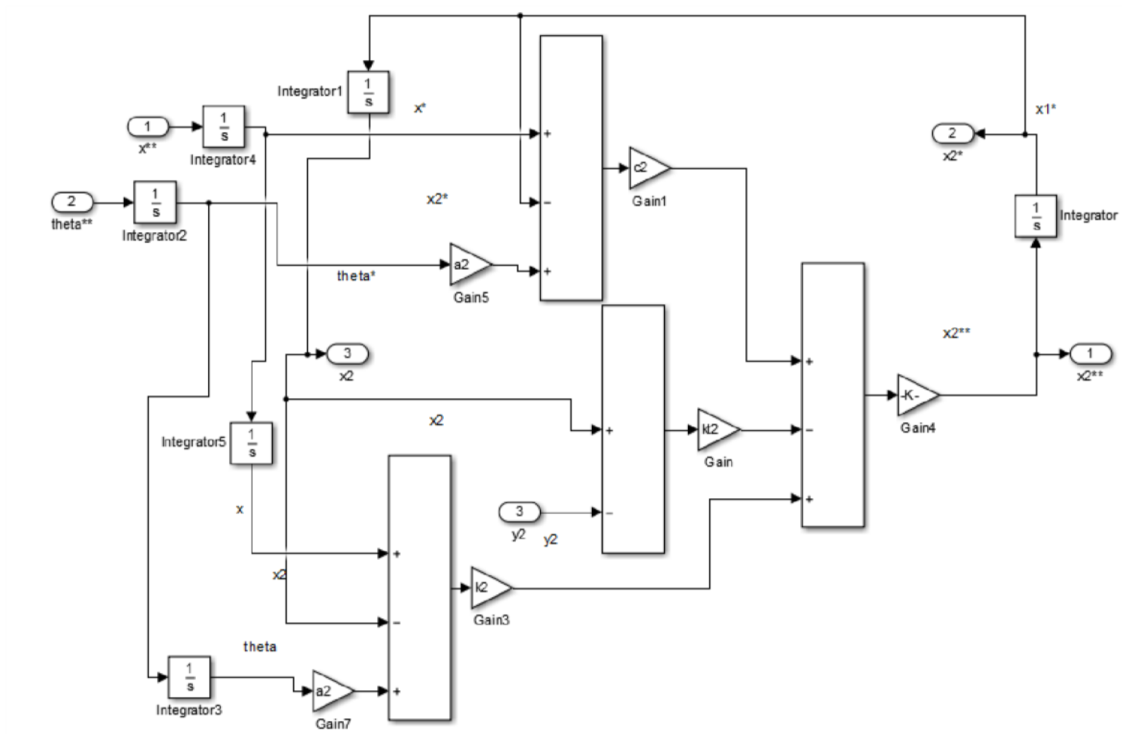

Figure 3.7 Rear Wheel Coordinate System

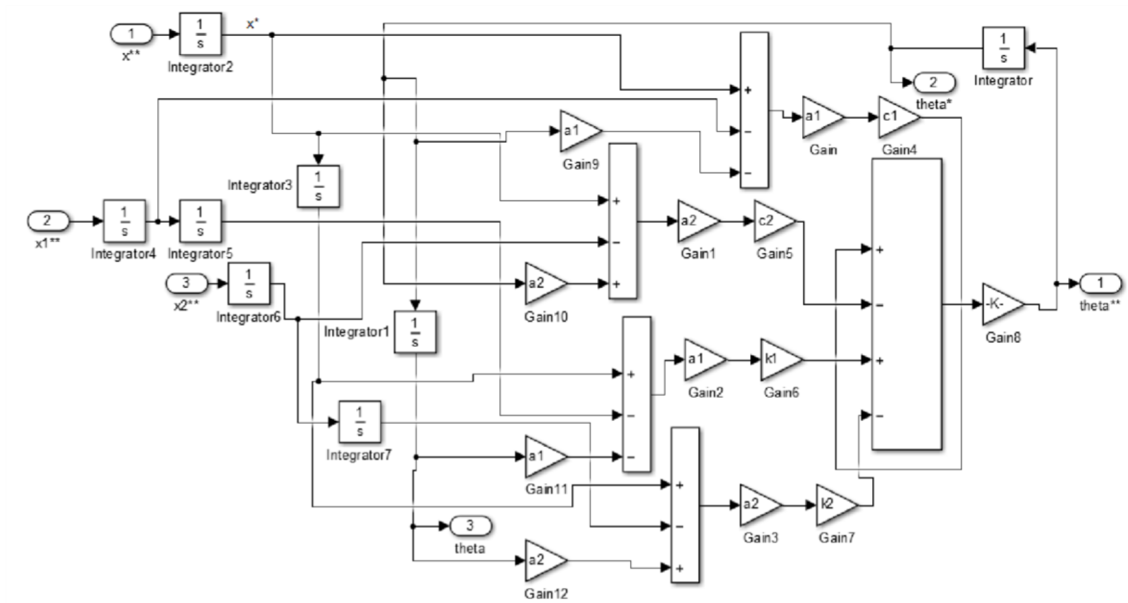

Figure 3.8 Body Pitch Motion Subsystem

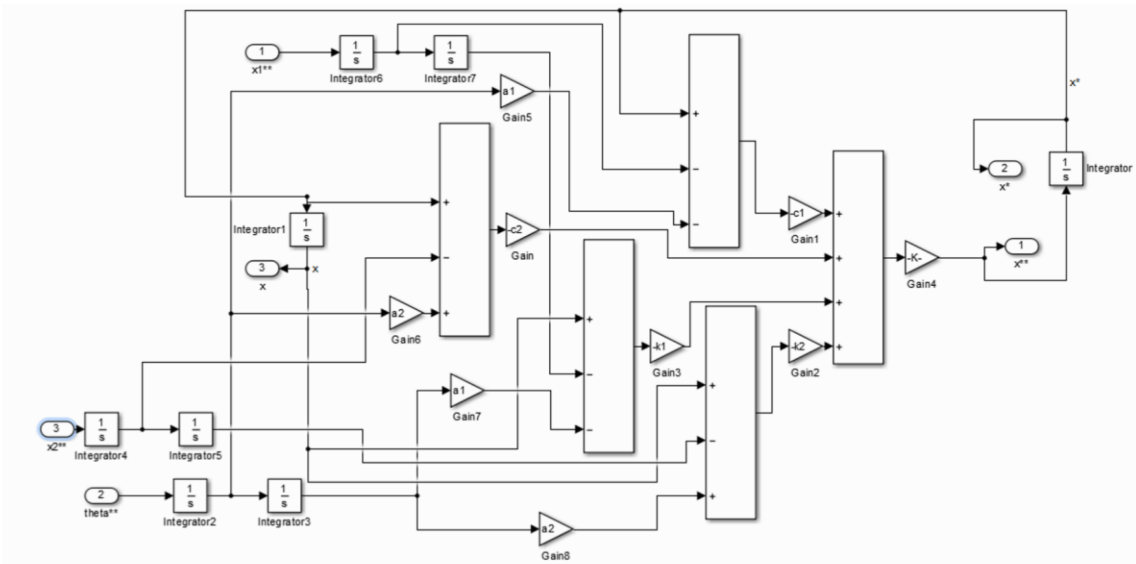

Figure 3.9 Body Vertical Motion Subsystem

3.3 Full Car Model (FCM)

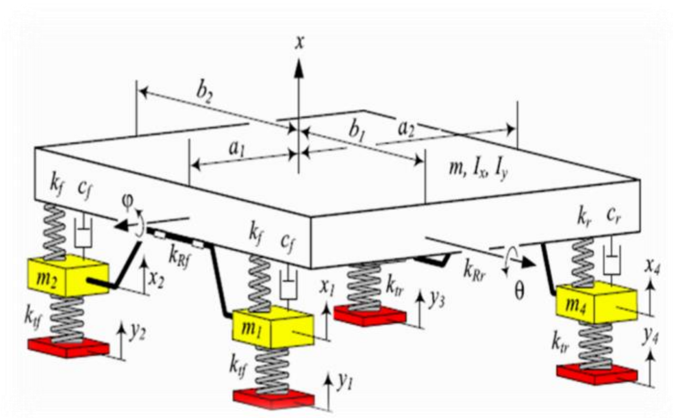

Figure 3.10 Full Car Model (FCM)

The general vibrating model of a vehicle is called the full car model. Such a model, shown in Fig. 3.10, includes the body bounce x, body roll ϕ, body pitch θ , wheels' hops x1, x2, x3, and x4 and independent road excitations y1, y2, y3, and y4. [12,2,6,7]

A full car vibrating model has seven DOF and a set of seven equations of motion:

$$m\ddot{x} + c_f\,(\dot{x} - \dot{x}_1 + b_{1\dot{\varphi}} - a_1\theta) + c_f\,(\dot{x} - \dot{x}_2 - b_{2\dot{\varphi}} - a_1\theta)$$

$$+ c_r\,(\dot{x} - \dot{x}_3 - b_{1\dot{\varphi}} + a_2\theta) + c_r\,(\dot{x} - \dot{x}_4 + b_{2\dot{\varphi}} + a_2\theta)$$

$$+ k_f\,(x - x_1 + b_{1\varphi} - a_1\theta) + k_f\,(x - x_2 - b_{2\varphi} - a_1\theta)$$

$$+ k_r\,(x - x_3 - b_{1\varphi} + a_2\theta) + k_f\,(x - x_4 + b_{2\varphi} + a_2\theta) = 0 \tag{3.32}$$

$$I_{x\ddot{\varphi}} + b_1 c_f\left(\dot{x} - \dot{x}_1 + b_{1\dot{\varphi}} - a_1\dot{\theta}\right) - b_2 c_f(\dot{x} - \dot{x}_2 - b_{2\dot{\varphi}} - a_1\dot{\theta})$$

$$-b_1\,c_r\,(\dot{x} - \dot{x}_3 - b_{1\dot{\varphi}} + a_2\theta) + b_2 c_r\,(\dot{x} - \dot{x}_4 + b_{2\dot{\varphi}} + a_2\theta)$$

$$+b_1\,c_r\,(x - x_1 + b_{1\varphi} - a_1\theta) - b_2 k_f\,(x - x_2 - b_{2\varphi} - a_1\theta)$$

$$-b_1\,k_f\,(x - x_3 - b_{1\varphi} + a_2\theta) + b_2 k_r\,(x - x_4 + b_{2\varphi} + a_2\theta)$$

$$+k_r\left(\varphi - \frac{x_1 - x_2}{\omega}\right) = 0 \tag{3.33}$$

$$I_{\,y}\ddot{\theta} - a_1(\dot{x} - \dot{x}_1 + b_{1\dot{\varphi}} - a_1\theta) - a_1 c_f(\dot{x} - \dot{x}_2 - b_{2\dot{\varphi}} - a_1\theta)$$

$$+a_2 c_r\left(\dot{x} - \dot{x}_3 - b_{1\dot{\varphi}} + a_2\dot{\theta}\right) + a_2 c_r(\dot{x} - \dot{x}_4 + b_{2\dot{\varphi}} + a_2\dot{\theta})$$

$$-a_1(x - x_1 + b_{1\varphi} - a_1\theta) - a_1 k_f(x - x_2 - b_{2\varphi} - a_1\theta)$$

$$+a_2(x - x_3 - b_{1\varphi} + a_2\theta) + a_2 k_r(x - x_4 + b_{2\varphi} + a_2\theta) = 0. \tag{3.34}$$

$$m_f\ddot{x}_1 - c_f\left(\dot{x} - \dot{x}_1 + b_1\dot{\varphi} - a_1\dot{\theta}\right) - k_f(x - x_1 + b_1\varphi - a_1\theta)$$

$$-k_R\,\frac{1}{\omega}\left(\varphi - \frac{x_1 - x_2}{\omega}\right) + k_{t_f}(x_1 - y_1) = 0 \tag{3.35}$$

$$m_f\ddot{x}_2 - c_f\left(\dot{x} - \dot{x}_2 - b_2\dot{\varphi} - a_1\dot{\theta}\right) - k_f(x - x_2 - b_2\varphi - a_1\theta)$$

$$+k_R\,\frac{1}{\omega}\left(\varphi - \frac{x_1 - x_2}{\omega}\right) + k_{t_f}(x_2 - y_2) = 0 \tag{3.36}$$

$$m_r\ddot{x}_3 - c_r(\dot{x} - \dot{x}_3 - b_1\dot{\varphi} + a_2\dot{\theta}) - k_r(x - x_3 - b_1\varphi + a_2\theta) + k_{tr}(x_3 - y_3) = 0 \quad (3.37)$$

$$m_r\ddot{x}_4 - c_r(\dot{x} - \dot{x}_4 + b_2\dot{\varphi} + a_2\theta)$$

$$-k_r(x - x_4 + b_2\varphi + a_2\theta) + k_{tr}(x_4 - y_4) = 0 \quad (3.38)$$

Figure 3.10 shows the vibrating model of the system. The body of the vehicle is assumed to be a rigid slab. This rigid body has a mass m, which is the total body mass of the car, a longitudinal mass moment Ix, and a lateral mass moment Iy. The mass moments are only the body mass moments and these are less than the vehicle's mass moments. The wheels have masses m1, m2, m3, and m4, respectively.

However, it is common to have the same wheels at left and right:

$m_1 = m_2 = m_f$ and $m_3 = m_4 = m_r$

The front and rear tire stiffnesses are indicated by ktf and ktr , respectively. Because the damping of tires is much smaller than the damping of shock absorbers, we may ignore the tires' damping for simpler calculations. The suspension of the car has stiffness kf and damping cf in the front and stiffness kr and damping cr in the rear It isn't unexpected to make the suspension of the left and right wheels reflect. Thus, their stiffness and damping are also equal. The vehicle may also have an antiroll bar in front and in the back, with a torsional stiffness kRf and kRr . Using a simple model, the antiroll bar provides us with a torque –MR proportional to the roll angle ϕ:

$$M_R = -(k_{Rf} + k_{Rr})\,\varphi = -k_R\varphi \quad (3.39)$$

However, a better model of the antiroll bar reaction is

$$M_R = -k_{R_f}\left(\varphi - \frac{x_1 - x_2}{\omega_f}\right) - k_{R_f}\left(\varphi - \frac{x_4 - x_3}{\omega_r}\right) \quad (3.40)$$

Most cars only have an antiroll bar in front because of softer springs in front. For these cars, the moment of the antiroll bar simplifies to

$$M_R = -k_R\left(\varphi - \frac{x_1 - x_2}{\omega}\right) \quad (3.41)$$

If we use $\omega_f \equiv \omega = b_1 + b_2$ and $k_{Rf} \equiv k_R$

To find the equations of motion of the full car vibrating model, we use the Lagrange method. The kinetic and potential energies of the system are

$$K = \frac{1}{2}m\dot{x}^2 + \frac{1}{2}I_x\dot{\varphi}^2 + \frac{1}{2}I_y\dot{\theta}^2 + \frac{1}{2}m_f(\dot{x}_1^2 + \dot{x}_2^2) + \frac{1}{2}m_r(\dot{x}_3^2 + \dot{x}_4^2) \quad (3.42)$$

$$V = \frac{1}{2}k_f(x - x_1 + b_{1\varphi} - a_1\theta)^2 + \frac{1}{2}k_f(x - x_2 - b_{2\varphi} - a_1\theta)^2$$

$$+\frac{1}{2}k_r\left(x-x_3-b_{1\varphi}-a_2\theta\right)^2+\frac{1}{2}k_r\left(x-x_4+b_{2\varphi}+a_2\theta\right)^2$$

$$+\frac{1}{2}k_R\left(\varphi-\frac{x_1-x_2}{\omega}\right)^2+\frac{1}{2}k_{tf}(x_1-y_1)^2+\frac{1}{2}k_{tf}(x_2-y_2)^2$$

$$+\frac{1}{2}k_{tr}(x_3-y_3)^2+\frac{1}{2}k_{tr}(x_4-y_4)^2 \tag{3.43}$$

and its dissipation function is

$$D=\frac{1}{2}c_f\left(\dot{x}-\dot{x}_1+b_{1\dot{\varphi}}-a_1\dot{\theta}\right)^2+\frac{1}{2}c_f\left(\dot{x}-\dot{x}_2-b_2\dot{\varphi}-a_1\dot{\theta}\right)^2$$

$$+\frac{1}{2}c_r\left(\dot{x}-\dot{x}_3-b_1\dot{\varphi}+a_2\dot{\theta}\right)^2+\frac{1}{2}c_r\left(\dot{x}-\dot{x}_4+b_2\dot{\varphi}+a_2\dot{\theta}\right)^2 \tag{3.43}$$

Applying the Lagrange method,

$$\frac{d}{dt}\left(\frac{\partial K}{\partial \dot{q}_r}\right)-\frac{\partial K}{\partial q_r}+\frac{\partial D}{\partial \dot{q}_r}+\frac{\partial V}{\partial q_r}=f_r \quad r=1,2,\dots,7$$

provides us with the equations of motion.

The set of equations of motion can be rearranged in matrix form,

$$[m]\ddot{x}+[c]\dot{x}+[k]x=F \tag{3.44}$$

Where,

$$[\mathrm{m}]=\begin{bmatrix} m & 0 & 0 & 0 & 0 & 0 & 0 \\ 0 & I_x & 0 & 0 & 0 & 0 & 0 \\ 0 & 0 & I_y & 0 & 0 & 0 & 0 \\ 0 & 0 & 0 & m_f & 0 & 0 & 0 \\ 0 & 0 & 0 & 0 & m_f & 0 & 0 \\ 0 & 0 & 0 & 0 & 0 & m_r & 0 \\ 0 & 0 & 0 & 0 & 0 & 0 & m_r \end{bmatrix}$$

$$[\mathrm{c}]=\begin{bmatrix} c_{11} & c_{12} & c_{13} & -c_f & -c_f & -c_r & -c_r \\ c_{13} & c_{13} & c_{13} & -b_1c_f & -b_1c_f & -b_1c_f & -b_1c_f \\ c_{13} & c_{13} & c_{13} & a_1c_f & a_1c_f & a_1c_f & a_1c_f \\ -c_f & -b_1c_f & a_1c_f & c_f & 0 & 0 & 0 \\ -c_f & -b_1c_f & a_1c_f & 0 & c_f & 0 & 0 \\ -c_r & -b_1c_f & -a_1c_f & 0 & 0 & c_r & 0 \\ -c_r & -b_1c_f & -a_1c_f & 0 & 0 & 0 & c_r \end{bmatrix}$$

$$c_{21}=c_{12}=b_1c_f-b_2c_f-b_1c_r+b_2c_r$$
$$c_{31}=c_{13}=2a_2c_r-2a_1c_f$$

$$c_{22}=b_{12}c_f+b_{22}c_f+b_{12}c_r+b_{22}c_r$$

$$c_{32}=c_{23}=a_1b_2c_f-a_1b_1c_f-a_2b_1c_r+a_2b_2c_r$$

$$c_{33}=2c_fa_1^2+2c_ra_2^2$$

$$[\mathrm{k}] = \begin{bmatrix} k_{11} & k_{12} & k_{13} & -k_f & -k_f & -k_r & -k_r \\ k_{21} & k_{22} & k_{23} & k_{24} & k_{25} & b_1 k_r & -b_2 k_r \\ k_{31} & k_{32} & k_{33} & a_1 c_f & a_1 k_f & a_1 k_f & -a_1 k_r \\ -k_f & k_{42} & a_1 k_f & k_{44} & -\frac{k_r}{\omega^2} & 0 & 0 \\ -k_f & k_{52} & a_1 k_f & -\frac{k_r}{\omega^2} & k_{55} & 0 & 0 \\ -k_r & -b_1 k_r & -a_2 k_r & 0 & 0 & k_r + k_{tr} & 0 \\ -k_r & -b_2 k_r & -a_2 k_r & 0 & 0 & 0 & k_r + k_{tr} \end{bmatrix}$$

$$k_{11} = 2k_f + 2k_r$$

$$k_{21} = k_{12} = b_1 k_f - b_2 k_f - b_1 k_r + b_2 k_r$$

$$k_{31} = k_{13} = 2a_2 k_r - 2a_1 k_f$$

$$k_{22} = k_R + b_{12} k_f + b_{22} k_f + b_{12} k_r + b_{22} k_r$$

$$k_{32} = k_{23} = a_1 b_2 k_f - a_1 b_1 k_f - a_2 b_1 k_r + a_2 b_2 k_r$$

$$k_{42} = k_{24} = -b_1 k_f - \frac{1}{\omega} k_R$$

$$k_{52} = k_{25} = b_2 k_f + \frac{1}{\omega} k_R$$

$$k_{33} = 2k_f a_1^2 + 2k_r a_2^2$$

$$k_{44} = k_f + k_{t_f} + \frac{1}{\omega^2} k_R$$

$$k_{55} = k_f + k_{t_f} + \frac{1}{\omega^2} k_R$$

$$\mathrm{X} = \begin{bmatrix} x \\ \varphi \\ \theta \\ x_1 \\ x_2 \\ x_3 \\ x_4 \end{bmatrix}$$

$$\mathrm{F} = \begin{bmatrix} 0 \\ 0 \\ 0 \\ y_1 k_{tf} \\ y_2 k_{tf} \\ y_3 k_{tr} \\ y_4 k_{tr} \end{bmatrix}$$

The Simulink Model of Full Car Model developed in Matlab is shown in figures below:

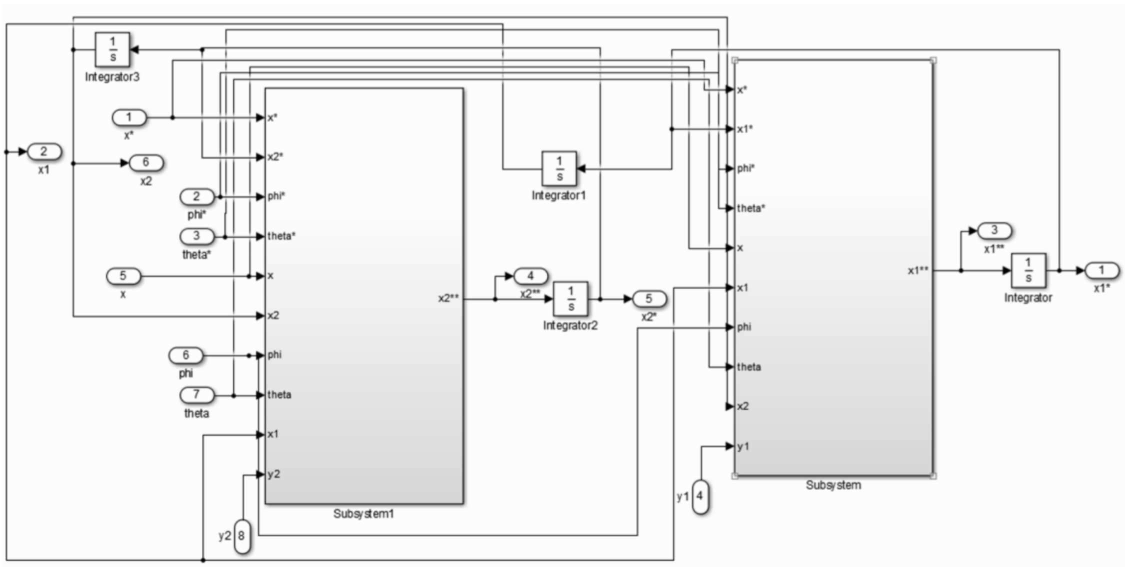

Figure 3.11 Simulink Model of FCM Implemented in MATLAB

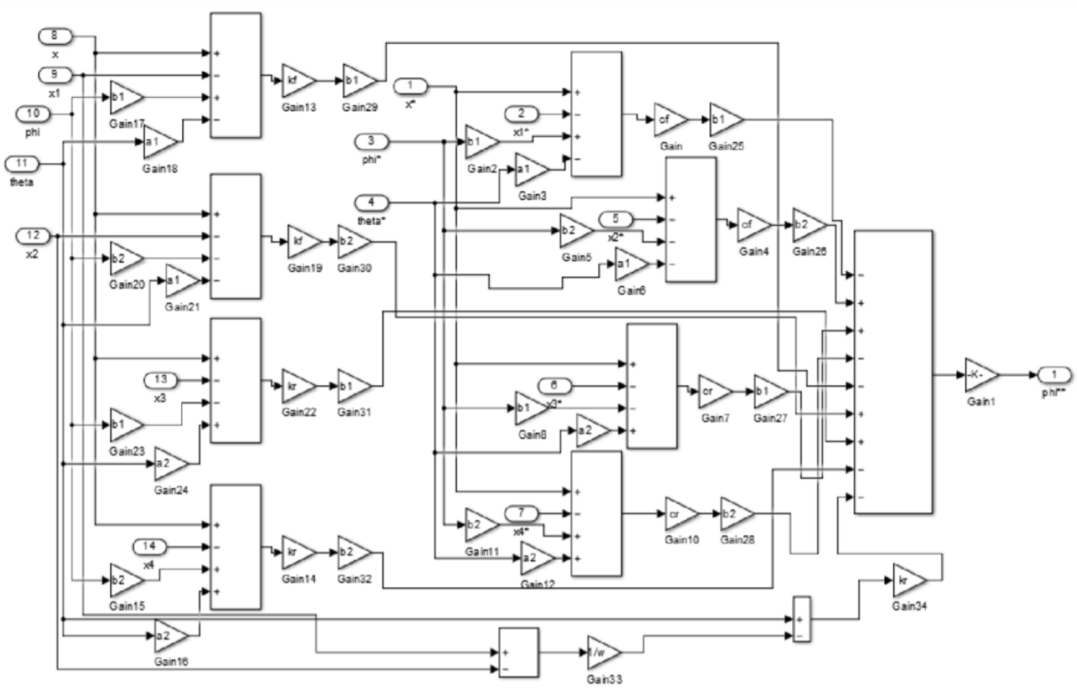

Figure 3.12 Body Roll model subsystem

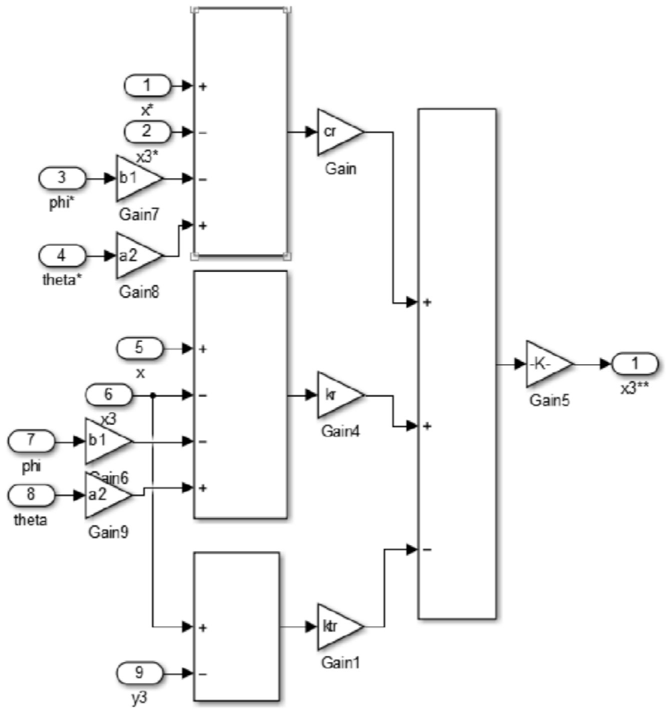

Figure 3.13 Wheel Motion Subsystem, the other wheel motion models are similar

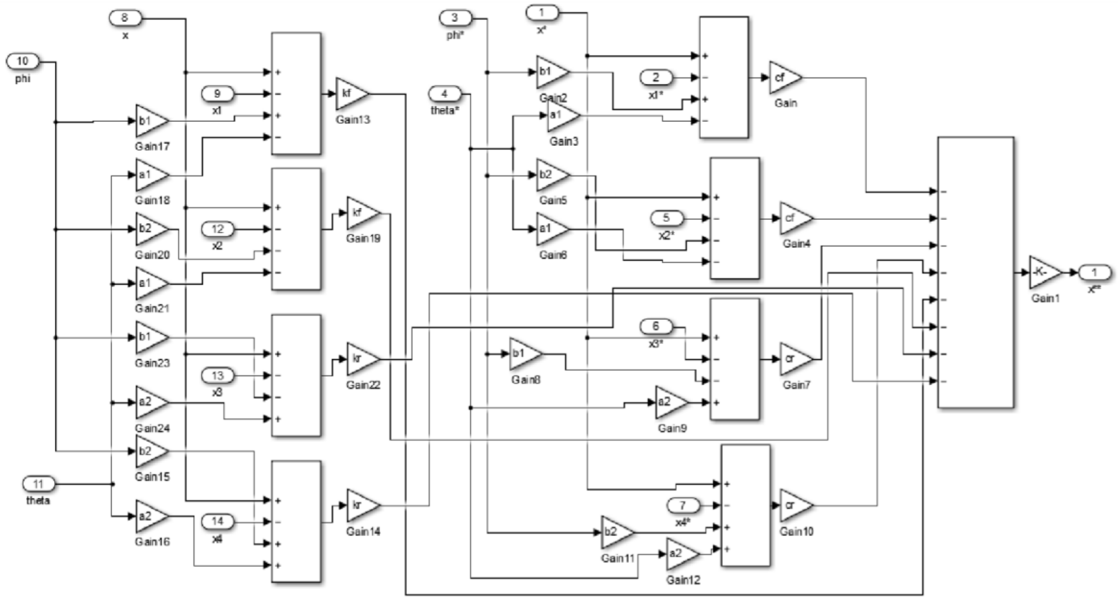

Figure 3.14 Body Vertical Motion Subsystem

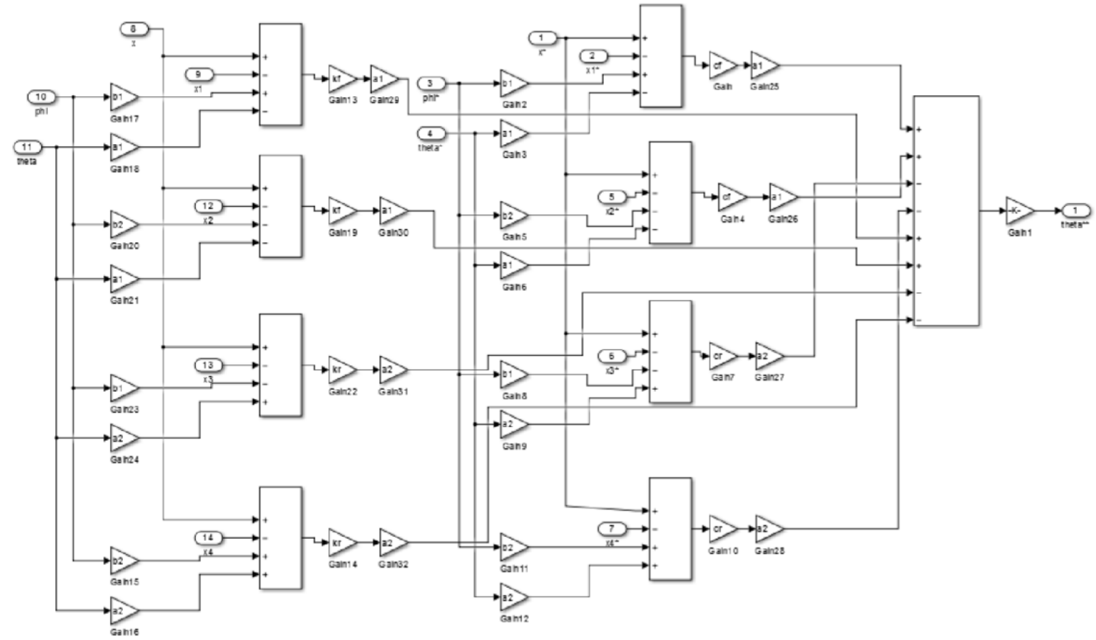

Figure 3.15 Body Pitch angle Motion Subsystem

CHAPTER 4. Road Input Profiles

4.1. Road

Sophisticated road models provide the road height z_R and the local friction coefficient μ_L at each point x, y, Figure 4.1.

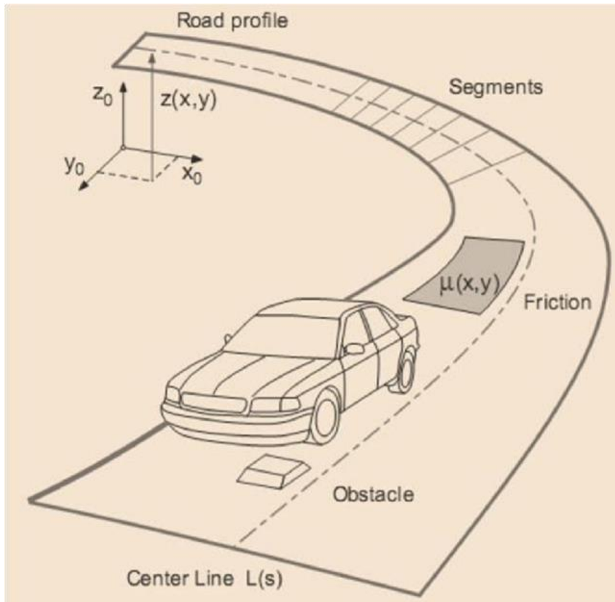

Figure 4. 1 Sophisticated road model

The wheel model is then responsible to calculate the local road inclination, by isolating the flat course depiction from the vertical format and the surface properties of the roadway practically subjective street designs are conceivable. Other than single deterrents or track grooves the abnormalities of a street are of stochastic nature. A vehicle driving over an arbitrary street profile essentially performs center, pitch and move movements. The local inclination of the road profile also induces longitudinal and lateral motions as well as yaw motions. On normal roads the lateral motions have less influence on ride comfort and ride safety. To restrict the exertion of the stochastic depiction generally more straightforward street models are utilized.

If the vehicle drives along a given path its momentary position can be described by the path variable x = x(t). Henceforth, a completely two-dimensional street model can be diminished to a parallel track model, Figure 4.2.

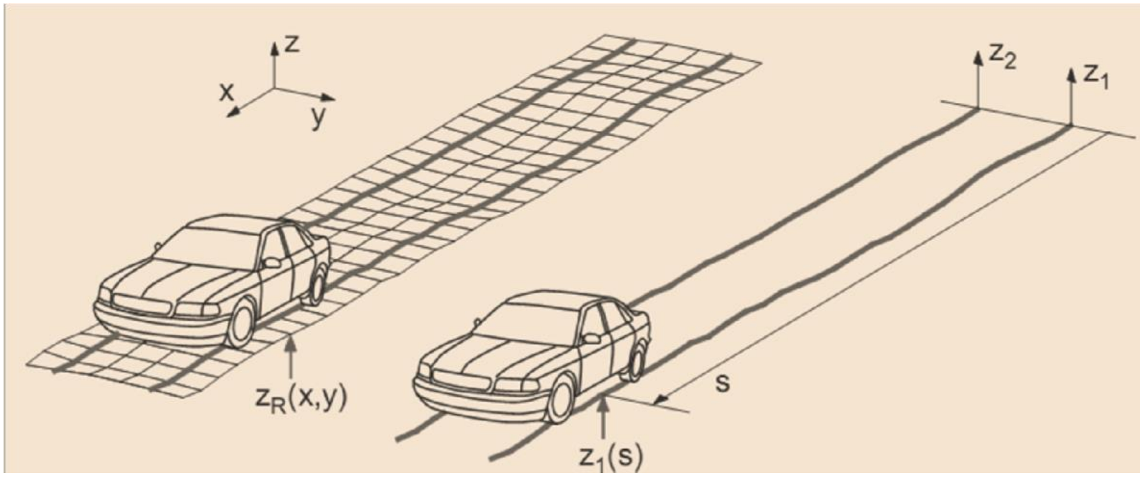

Figure 4. 2 Parallel track road model

Now, the road heights on the left and right track are provided by two one-dimensional functions $z_1 = z_1(x)$ and $z_2 = z_2(x)$. Inside the parallel track model no data about the nearby sidelong street tendency is accessible. In the event that this data isn't given by extra capacities the effect of a nearby parallel street tendency to vehicle movements isn't considered. For basic studies the irregularities at the left and the right track can considered to be approximately the same, $z_1(x) \sim z_2(x)$. Then, a single track road model with $(x) = 1(x) = z_2(x)$ can be used. Now, the move excitation of the vehicle is dismissed as well.

4.2. Deterministic Profiles:

4.2.1. Bumps and Potholes

Bumps and Potholes on the road are single obstacles of nearly arbitrary shape. Already with simple rectangular cleats the dynamic reaction of a vehicle or a single tyre to a sudden impact can be investigated. In the event that the state of the deterrent is approximated by a smooth capacity, similar to a cosine wave, then, discontinuities will be avoided [13, 9].

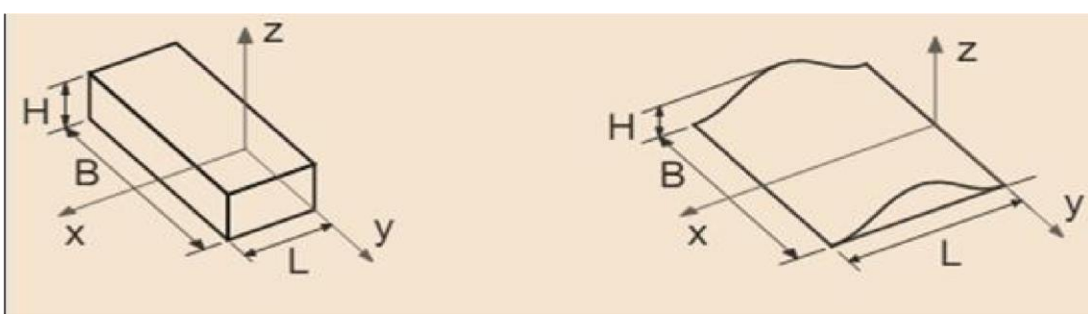

Figure 4. 3 Rectangular and Sine Bump

Usually the obstacles are described in local reference frames, Figure 4.3.

Then, the rectangular cleat is simply defined by

$$z(x,y) = \begin{cases} H & if\ 0 < x < L \\ 0 & else \end{cases} \tag{4.1}$$

And cosine bump is given by:

$$z(x,y) = \begin{cases} (1 - \mathrm{a} * \cos(8\pi t)) & if\ 0 < x < L \\ 0 & else \end{cases} \tag{4.2}$$

where H, B and L denote height, width and length of the obstacle. Potholes are obtained if negative values for the height (H < 0) are used.

4.2.2. Different type of Bump Profiles:

Indian Roads Congress (IRC) has given some guidelines for construction of bumps. But all bumps are not of same profiles and many of them are constructed randomly. According to IRC the length of the bump should be 3.7 m and maximum height should be 0.1 m at preferred crossing speed 25 km/h (6.94 m/s). Here, in addition to standard bump profile equations for half sine wave, harmonic and cycloidal profiles are presented and bumps generated by Matlab/Simulink are shown in Figures A.1 – A.3.

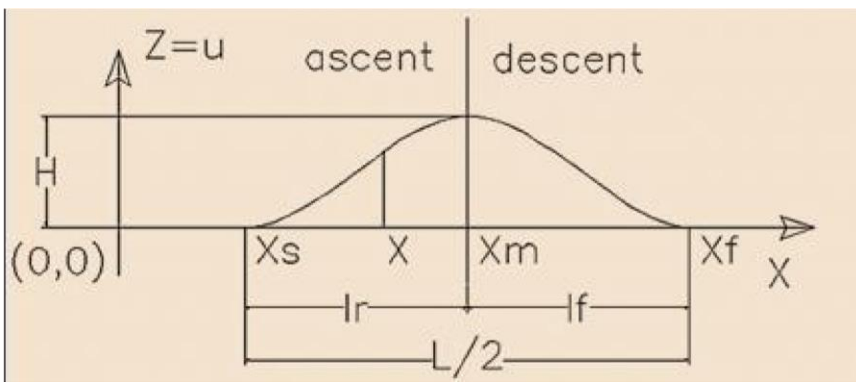

Figure 4. 4 Sine Bump

L = Length of Bump, (m)

H = Maximum bump height, (m) = Profile length/2

l_r = length of bump at assent side profile, (m) l_f = length of bump at decent side profile, (m)

x = distance of vehicle at time t sec from base point (t=0), (m) = $v_0 . t$ u = Vertical displacement of tyre (unsprung mass) = z, (m)

x_s = distance of vehicle at starting of bump from base point(t=0), (m)

x_f = distance of vehicle at ending of bump from base point(t=0), (m)

4.3. Random Profiles:

4.3.1. Classification of Random Road Profiles

Road elevation profiles can be measured point by point or by high-speed profilometers. The power spectral densities of roads show a characteristic drop in magnitude with the wave number, refer reference [1]. This basically mirrors the way that the abnormalities of the street may add up to a few meters over the length of many meters, though those deliberate over the length of one meter are ordinarily just some cm. in amplitude.

4.3.2 The classification of road profiles according to the ISO 8608

Basic detail of this standard is provided in Chapter 1 of this Thesis under the Section 1.8. More details regarding its implementation is described in this section.

The ISO 8608 describes the methodologies to be used for the generation of the road surface profile, by implementing two different procedures from data measured on site [1,4]. The first provides a description of the road roughness profile through the calculation of the PSD (Power Spectral Density) of vertical displacements G_d, both as a function of spatial frequency n ($n = \frac{\Omega}{2\pi}$ cycles/m) and of angular spatial frequency Ω. In practice, on ordinate both (n) and (Ω) are plotted in function of n and Ω with log-log scale.

The second procedure provides the calculation of the PSD of the accelerations (n) and (Ω) of the profile in terms of slope variation of the road surface per unit of covered distance. The passage from the first to the second method is immediate, because the PSD of vertical displacements G_d and the PSD of accelerations G_a are linked by the following equations:

$$G_a(n) = (2\pi n)^4 \cdot G_d(n)$$
$$G_a(\Omega) = \Omega^4 \cdot G_d(\Omega) \qquad (4.3)$$

The ISO 8608, in order to facilitate the comparison of the different road roughness profiles, proposes a classification which is based, as already stated, on their PSD, calculated in correspondence of conventional values of spatial frequency n0=0.1 cycles/m and angular spatial frequency $\Omega_0 = 1\,\frac{rad}{m}$.

Assuming for (n_0) and (Ω_0) the values established in ISO 8608 (see Figure 4.5), eight classes of roads are identified: from class A to class H. By comparing the Power Spectral Density associated with the various classes, we can deduce that class A include roads that have a minor degree of roughness and, therefore, for the purposes of the production of vibrations can be defined of the best quality. Conversely, in class H are included all roads that have a high degree of roughness and can therefore be regarded as very poor.

Road class	$G_d(n_0)$ (10^{-6} m^3)		$G_d(\Omega_0)$ (10^{-6} m^3)	
	Lower limit	Upper limit	Lower limit	Upper limit
A	—	32	—	2
B	32	128	2	8
C	128	512	8	32
D	512	2048	32	128
E	2048	8192	128	512
F	8192	32768	512	2048
G	32768	131072	2048	8192
H	131072	—	8192	—
	n_0=0.1 cycles/m		Ω_0=1 rad/m	

Figure 4. 5 ISO Road Classification

The identification of the class of a real roughness profile measured on site is assessed by calculating the Power Spectral Density of the real profile in correspondence of n0 and Ω0, and then comparing it with those appearing in ISO Standard for the various classes.

In simulations, the ISO 8608 provides that the roughness profile of the road surface can be defined using the equations provided in [1]. The Matlab code and Simulink models of road profile inputs are provided in appendix section for further reference.

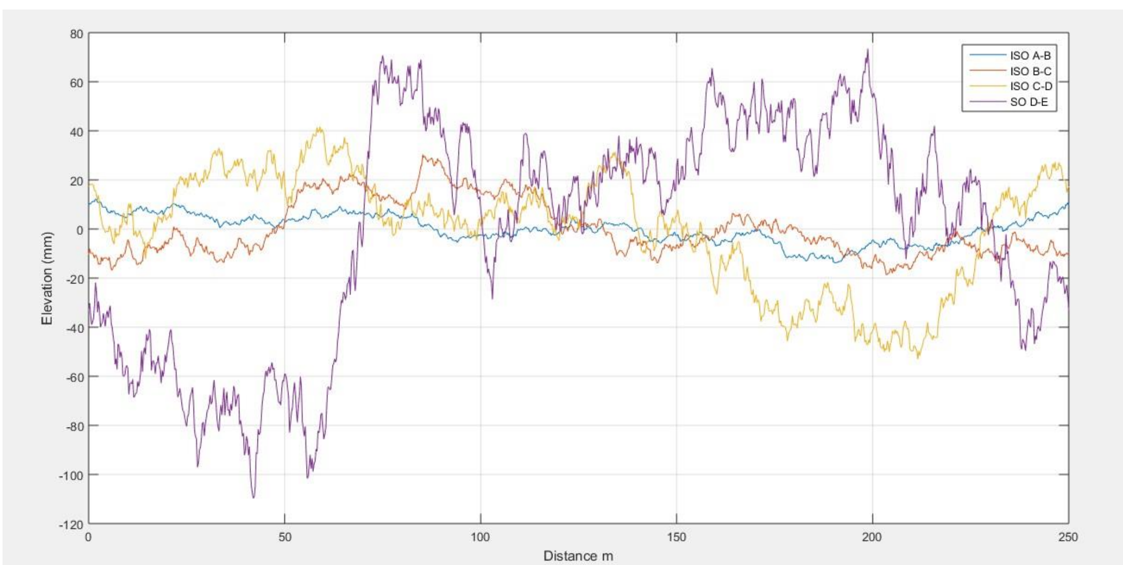

Figure 4. 6 ISO Road Profile implemented in MATLAB

4.3. Simulation of Road Profiles:

Besides considering ISO 8608 road Profile other profiles like, rectangular clit, sudden step disturbances and potholes and random road are considered [1,2,3,4,6]. The Simulink of the above described road profiles are provided below in the following figures.

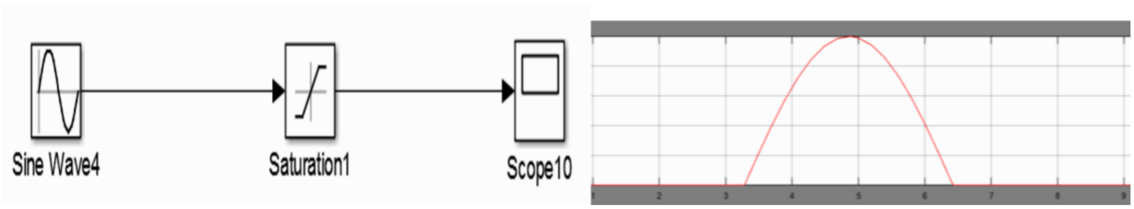

Figure A. 1 Half Sine Road Input

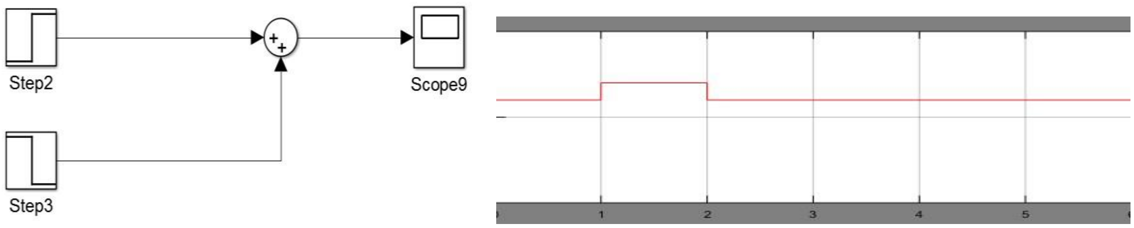

Figure A. 2 Simulink Model for Rectangular Clit

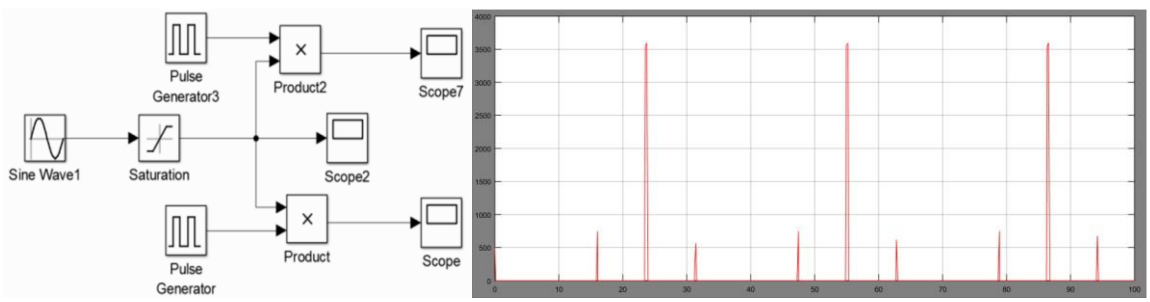

Figure A. 3 Simulink Model for different Pulse Profile

CHAPTER 5: RESULT ANALYSIS

5.1 RESULT ANALYSIS OF QCM

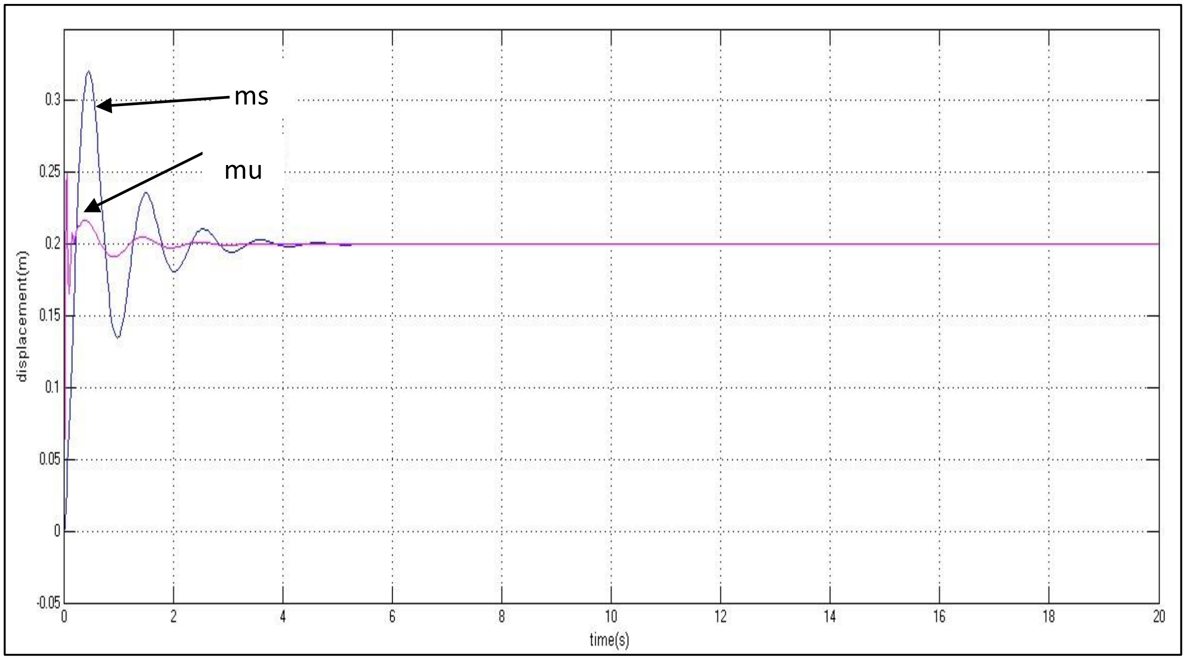

Figure 5. 1 Sprung, Unsprung mass displacement for step response, ms = 400, mu = 40

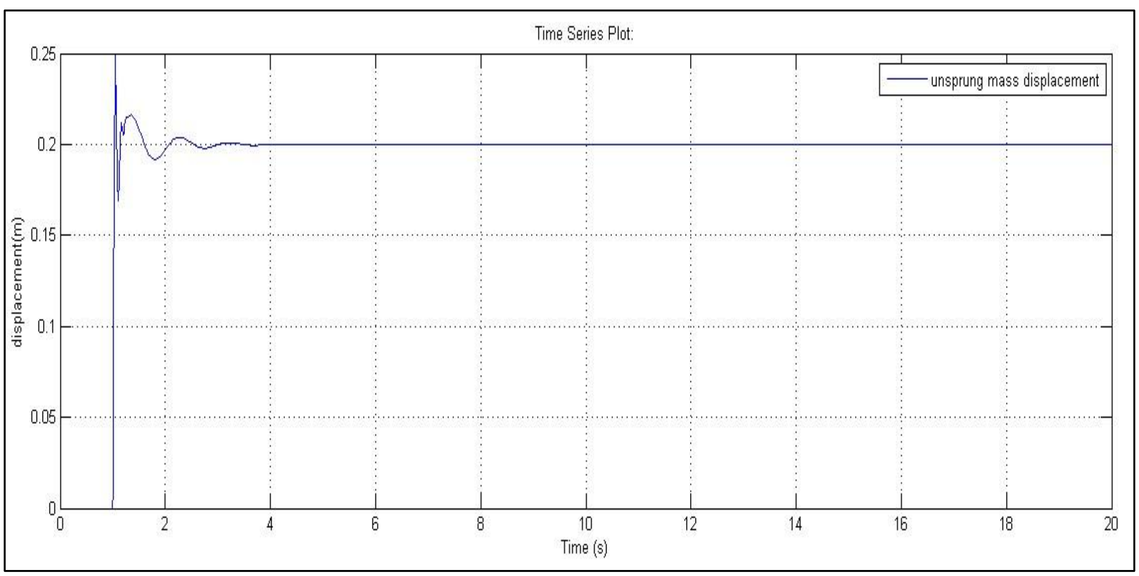

Figure 5. 2 Unsprung mass displacement for step response, ms = 400, mu = 40

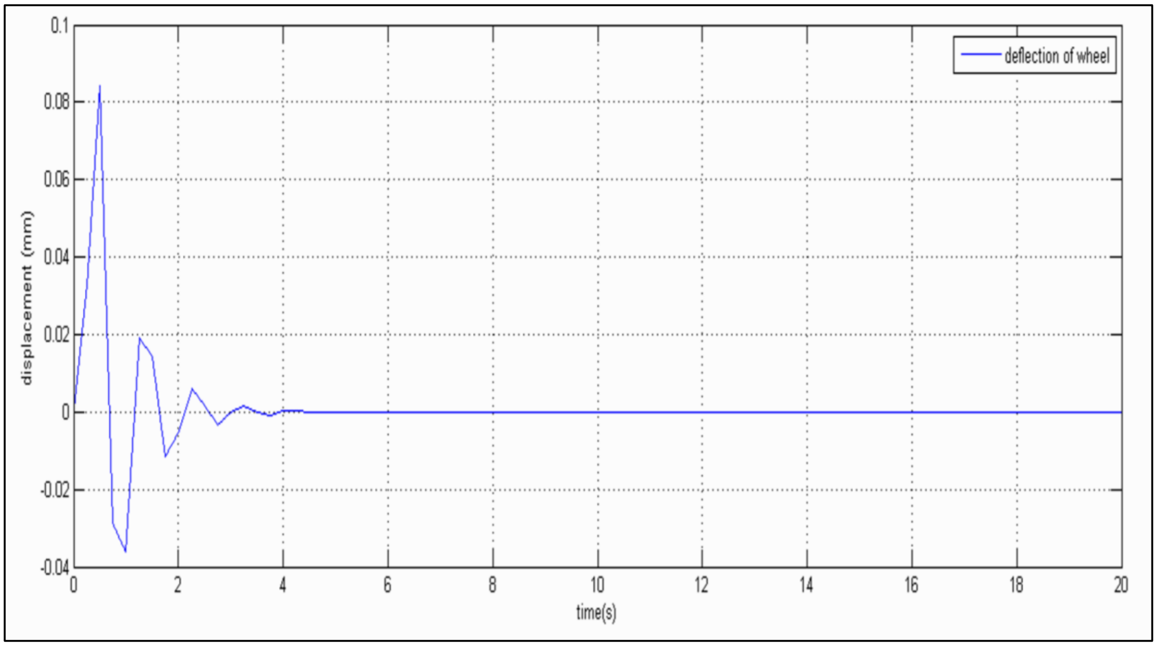

Figure 5. 3 Tire deflection of QCM

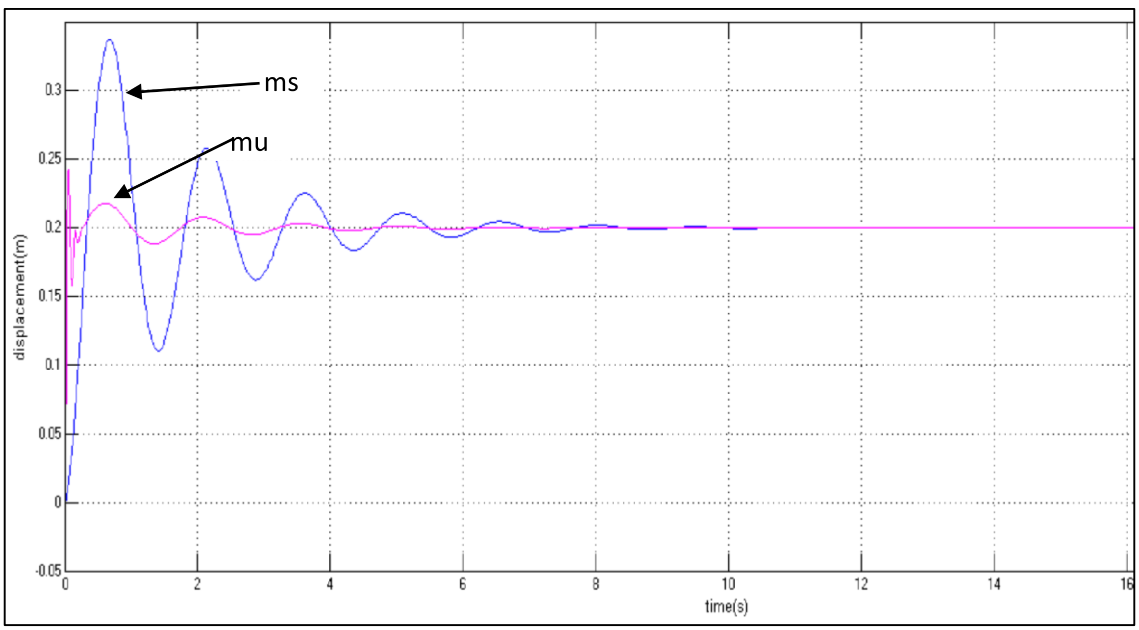

Figure 5. 4 Sprung, Unsprung mass displacement for step response, ms = 1000, mu = 40

The following results were obtained from the simulation and the state space model. Both the results were identical as expected. The input excitation is step type of amplitude 0.2. As expected the number of oscillation increases as mass increases. Also the displacement get stabilized after some time as expected and as per the theory.

Sr. No.	Sprung Mass (kg)	Unsprung Mass (kg)	Parameters		
			Rise Time (s)	Overshoot	Settling Time (s)
1	500	50	0.1597	60.4291	3.2045
2	700	50	0.1965	64.5816	4.4189
3	900	50	0.2273	67.5546	5.7023
4	1000	50	0.2411	68.7621	6.6670
5	500	150	0.1460	61.4221	3.2145
6	700	150	0.1854	66.1022	4.4280
7	900	150	0.2146	68.3433	5.7114
8	1000	150	0.2275	69.6006	6.6815
9	500	250	0.1257	66.3845	3.2244
10	700	250	0.1677	66.0639	4.4369
11	900	250	0.2066	69.6230	5.7205
12	1000	250	0.2222	71.1023	6.6953
13	500	350	0.1217	66.5714	3.2340
14	700	350	0.1522	71.0963	4.8830
15	900	350	0.1877	70.0105	6.2435
16	1000	350	0.2058	69.9822	6.7085

Table 5. 1 Sprung mass displacement for different m_s and m_u

The avoidance between the haggle suspensions is significant for the investigation of traveler comfort. The Figure 5.3 shows the redirection results and it is obvious from that there is a hop when excitation is given, this is expectable.

Additionally it has been seen that the inactive parameters are for the most part fix and can't be changed aside from the mass (sprung). By changing the mass we observed that the oscillations are increased for both sprung and unsprung. It is also observed, from Table 5.2, and also from Figure 5.1 – 5.4 that the peak for sprung mass displacement is reduced and that for unsprung mass is increased, for different sprung mass and unsprung mass.

Sr. No.	Sprung Mass (kg)	Unsprung Mass (kg)	Parameters		
			Rise Time (s)	Overshoot	Settling Time (s)
1	500	50	0.0248	29.4586	1.5403
2	700	50	0.0248	28.5050	1.8958
3	900	50	0.0249	27.9474	2.7757
4	1000	50	0.0249	27.7473	2.9635
5	500	150	0.0396	47.2459	1.5517
6	700	150	0.0398	44.6549	1.9025
7	900	150	0.0400	44.3503	2.7890
8	1000	150	0.0401	44.2196	2.9735
9	500	250	0.0479	55.4942	1.6014
10	700	250	0.0480	53.6533	1.9050
11	900	250	0.0480	52.6015	2.7995
12	1000	250	0.0481	52.2282	2.9829
13	500	350	0.0557	59.8806	2.0305
14	700	350	0.0558	57.8479	2.3821
15	900	350	0.0559	56.6769	2.8195
16	1000	350	0.0559	56.2594	2.9829

Table 5. 2 Unsprung mass displacement for different ms and mu

The parameters in Table 5.1 and 5.2 [2] are calculated considering the important terms in control i.e. Peak, Settling time, overshoot and Rise time. On the basis of this calculation the conclusion is obtained.

Note here that sprung mass will always be greater than unsprung mass i.e; mass of vehicle will always be greater than mass of wheel. But as mass of wheel increases at constant sprung mass the rise time decreases, while overshoot and settling time decreases. Also with the increase in sprung mass rise time, settling time and peak of the deflection increases.

The displacement of unsprung mass i.e. of wheel is of more importance as there is a sudden and major increase in the parameter which is passed to the suspension and gets degraded afterwards.

Thus suspension rejects the vibration created because of the disturbance from road, but in selective way.

It should be noted that the vibration is more affected by changes in unsprung mass i.e. wheel than that of sprung mass i.e. body.

Analysis Based on Suspension Parameters

Sr. No.	Sprung Mass (kg)	Unsprung Mass (kg)	Ks (N/m)	Parameters		
				Rise Time (s)	Overshoot	Settling Time (s)
1	500	50	20000	0.16310424	59.43196862	3.248920143
2	500	50	21000	0.159746126	60.42913305	3.204481606
3	500	50	22000	0.156611752	61.37592007	3.157652126
4	500	50	30000	0.13763623	3.622061796	3.622061796

Table 5. 3 Sprung mass displacement for different ks

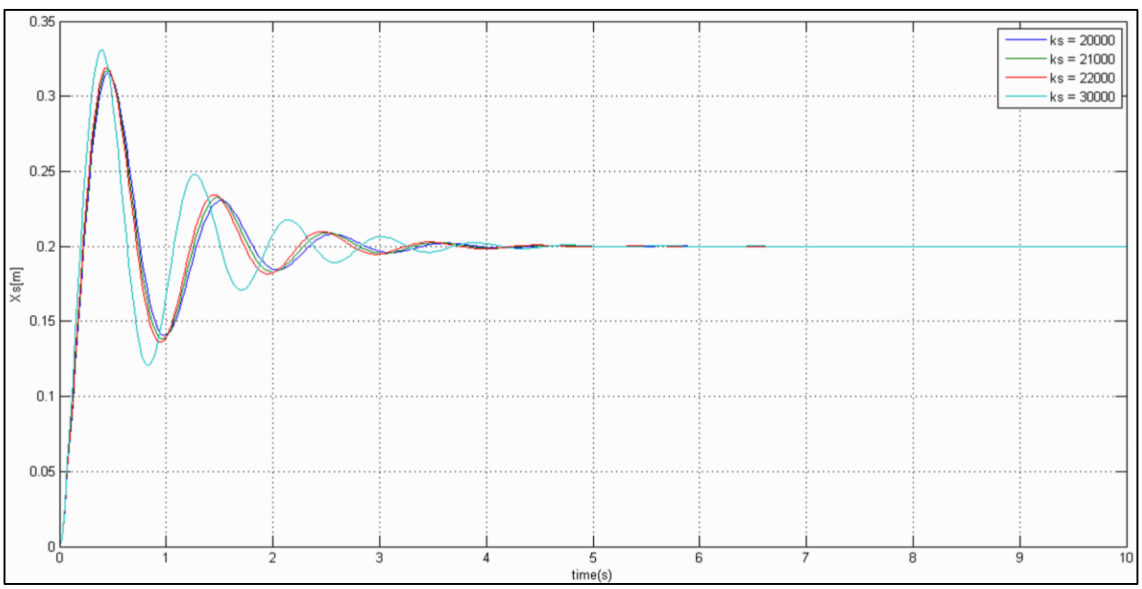

Figure 5. 5 Sprung mass displacement for different ks

From table 5.3 and Figure 5.5 it can be concluded that as spring constant ks increases vibration at body level increases. There is an increase in number of oscillation and settling time along with the magnitude

Sr. No.	Sprung Mass (kg)	Unsprung Mass (kg)	Ks (N/m)	Parameters		
				Rise Time (s)	Overshoot	Settling Time (s)
1	500	50	20000	0.024709808	30.0942986	1.540449241
2	500	50	21000	0.0248	29.4586	1.5403
3	500	50	22000	0.024805508	28.88454211	1.532331733
4	500	50	30000	0.025198111	24.45226183	1.821214911

Table 5. 4 Unsprung mass displacement for different ks

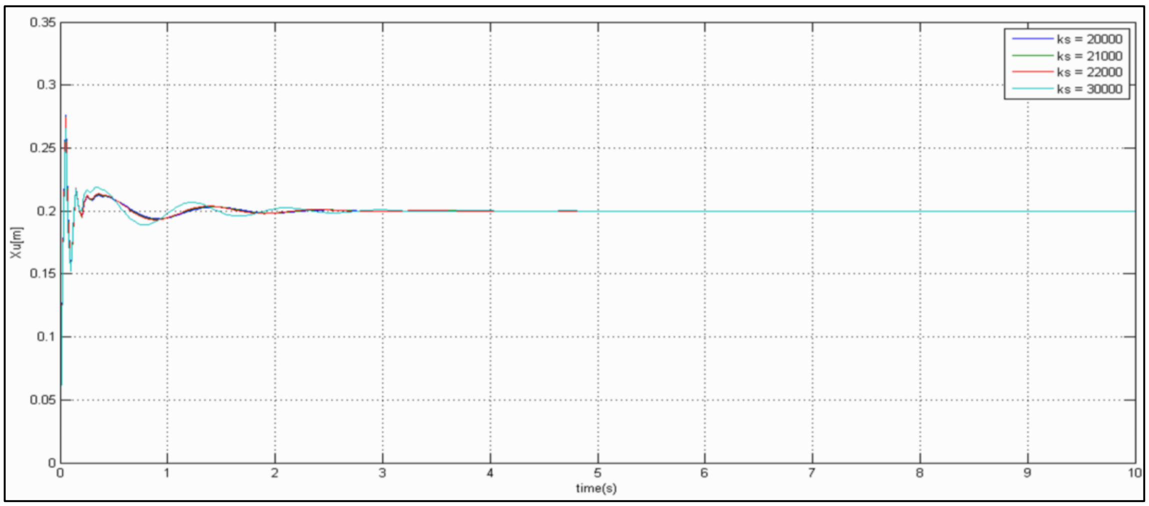

Figure 5. 6 Unsprung mass displacement for different ks

From table 5.4 and Figure 5.6 it can be concluded that as spring constant ks increases vibration at unsprung (wheel) level decrease. There is an increase in number of oscillation and settling time along with decrease in the magnitude.

Sr. No.	Sprung Mass (kg)	Unsprung Mass (kg)	Cs (Ns/m)	Parameters		
				Rise Time (s)	Overshoot	Settling Time (s)
1	500	50	1500	0.159746126	60.42913305	3.204481606
2	500	50	1600	0.158495516	58.67856362	3.143943368
3	500	50	2000	0.152896781	52.47168354	2.211180648
4	500	50	2100	0.151471254	51.09095927	2.190926488

Table 5. 5 Sprung mass displacement for different Cs

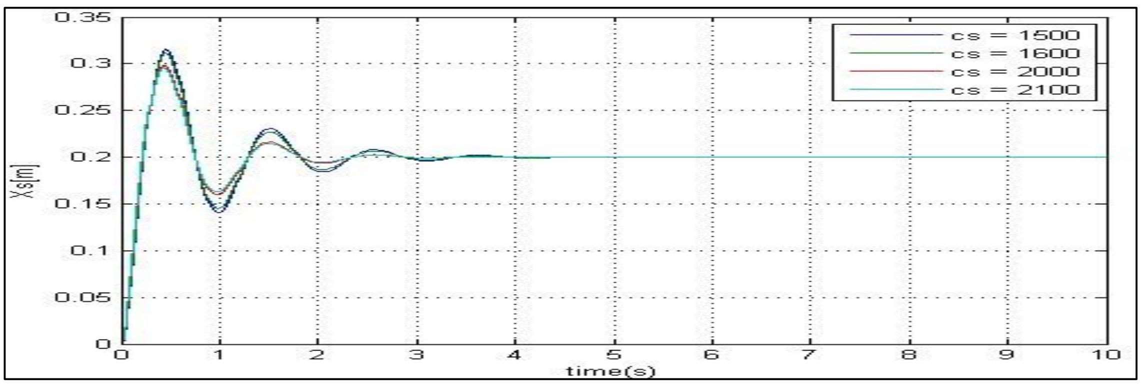

Figure 5. 7 Sprung mass displacement for different Cs

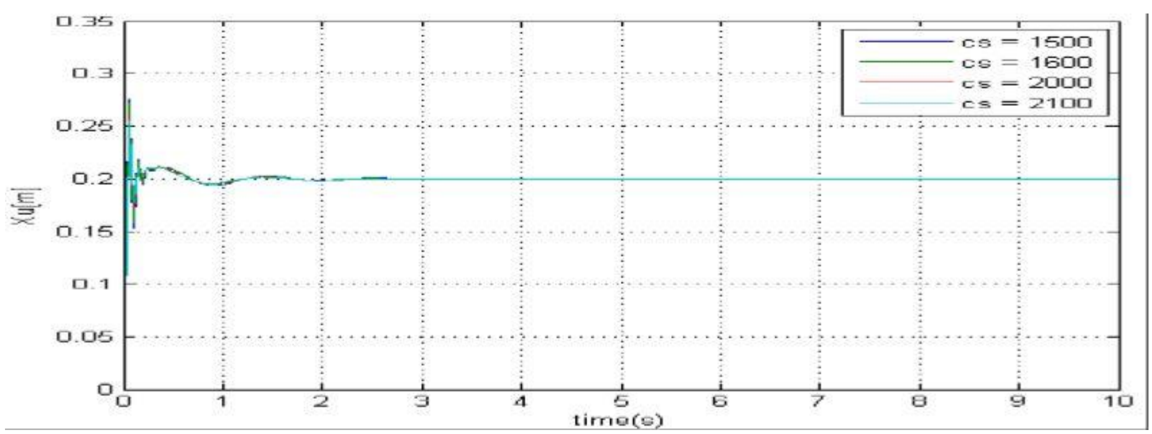

Figure 5. 8 Unsprung mass displacement for different Cs

Sr. No.	Sprung Mass (kg)	Unsprung Mass (kg)	Cs (Ns/m)	Parameters		
				Rise Time (s)	Overshoot	Settling Time (s)
1	500	50	1500	0.0248	29.4586	1.5403
2	500	50	1600	0.025065483	28.10311326	1.50185628
3	500	50	2000	0.026606577	21.87914582	1.04209403
4	500	50	2100	0.027065749	20.61171998	1.02674579

Table 5. 6 Unsprung mass displacement for different Cs

From table 5.5 and 5.6 and Figure 5.7 and 5.8, it can be concluded that as damping coefficient Cs increases vibration at any level decreases for both sprung and unsprung mass i.e for both wheel and vehicle body. There is a decrease in number of oscillation and settling time along with the magnitude

Sr. No.	Sprung Mass (kg)	Unsprung Mass (kg)	Kt (N/m)	Parameters		
				Rise Time (s)	Overshoot	Settling Time (s)
1	500	50	150000	0.159746126	60.42913305	3.204481606
2	500	50	170000	0.159669165	59.6032283	3.168306761
3	500	50	130000	0.160327379	61.47034915	3.248161319
4	500	50	200000	0.159942287	58.66313628	3.122849128

Table 5. 7 Sprung mass displacement for different kt

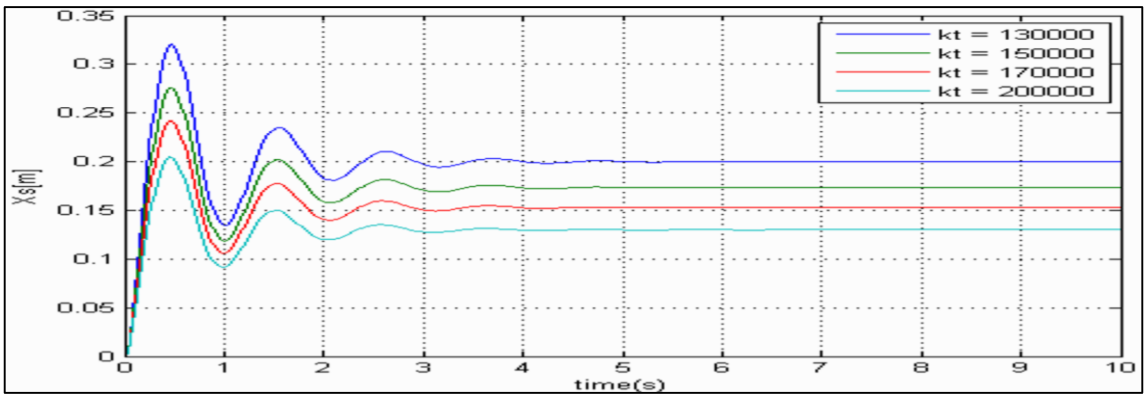

Figure 5. 9 Sprung mass displacement for different Kt

From table 5.7 and Figure 5.9 it can be concluded that as wheel spring constant kt increases vibration at body level shows a decrease in amplitude. There is minor decrease in number of oscillation and settling time along with the magnitude, thus we can say that the vibration pattern is similar only the magnitude decreases.

Sr. No.	Sprung Mass (kg)	Unsprung Mass (kg)	Kt (N/m)	Parameters		
				Rise Time (s)	Overshoot	Settling Time (s)
1	500	50	150000	0.0248	29.4586	1.5403
2	500	50	170000	0.022691576	33.31152453	1.475084847
3	500	50	200000	0.020485894	37.41418473	1.055235626
4	500	50	130000	0.02711253	25.98494718	1.592574126

Table 5. 8 Unsprung mass displacement for different kt

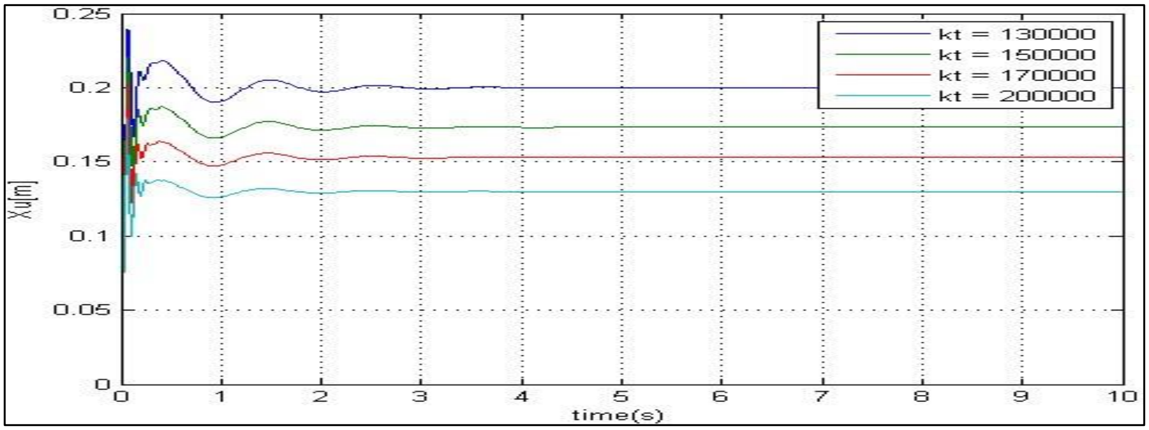

Figure 5.10 Unsprung mass displacement for different kt

From table 5.8 and Figure 5.10 it can be concluded that as wheel spring constant kt increases vibration at wheel level shows an increase in amplitude. There is minor decrease in number of oscillation and settling time along with the magnitude, thus we can say that the vibration pattern is similar only the magnitude increases.

When sine bump, rectangular or random disturbances is applied to the model, the output is obtained as follows:

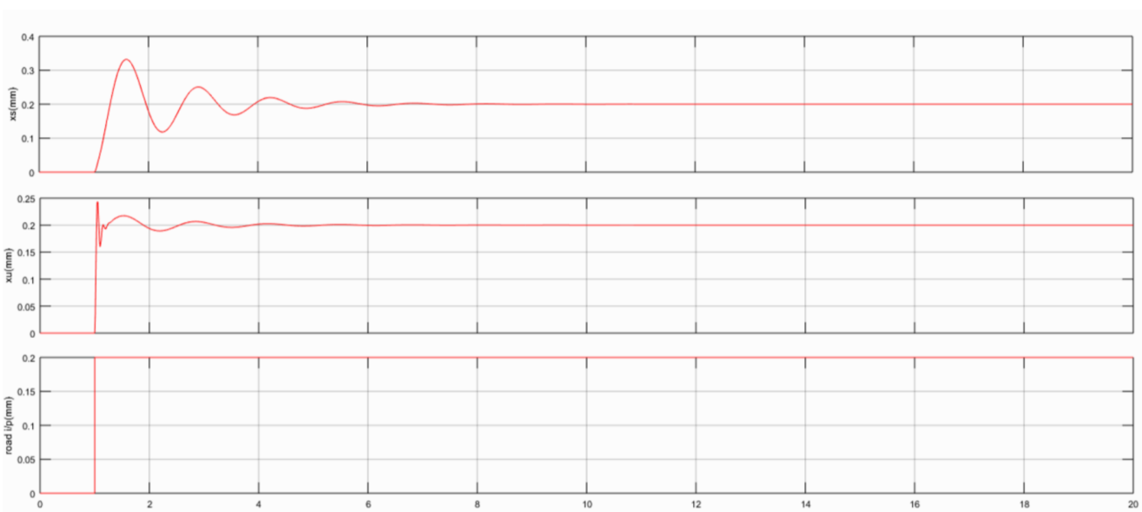

Figure 5. 11 Step Input Response of Quarter Car

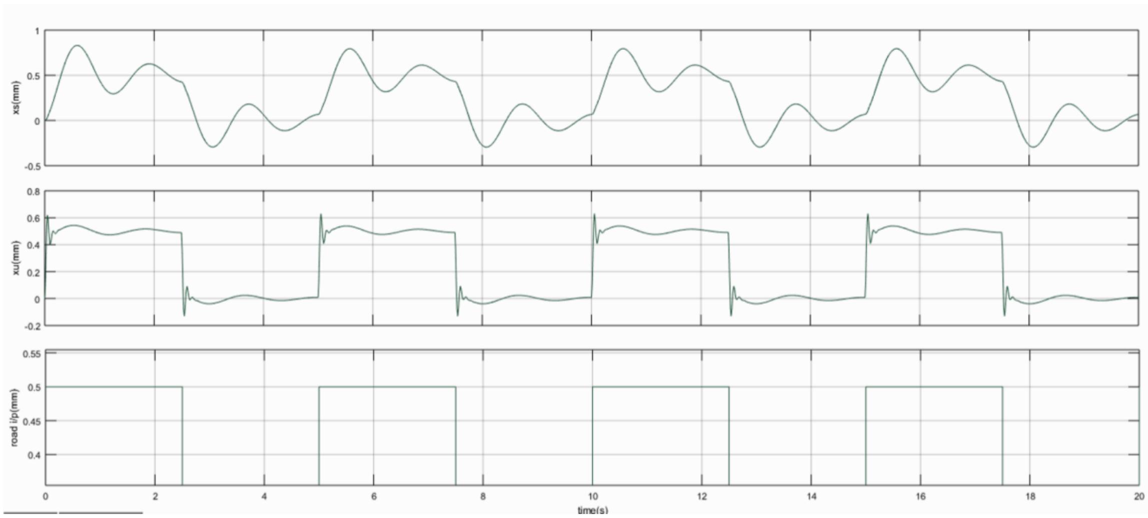

Figure 5. 12 Pulse Input Response of Quarter Car

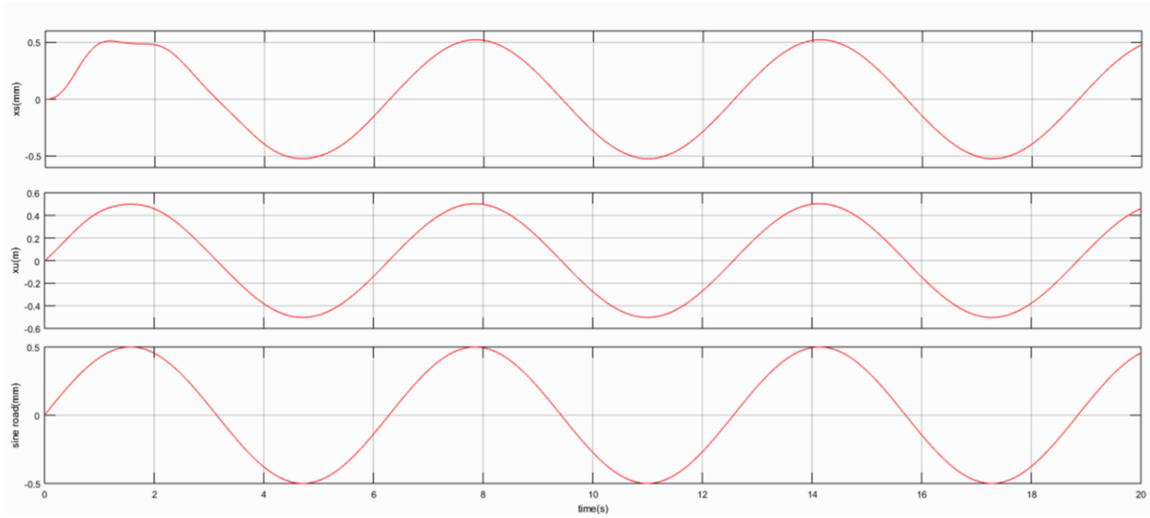

Figure 5. 13 Sine Input Response of Quarter Car

Figure 5. 14 Random Input Response of Quarter Car

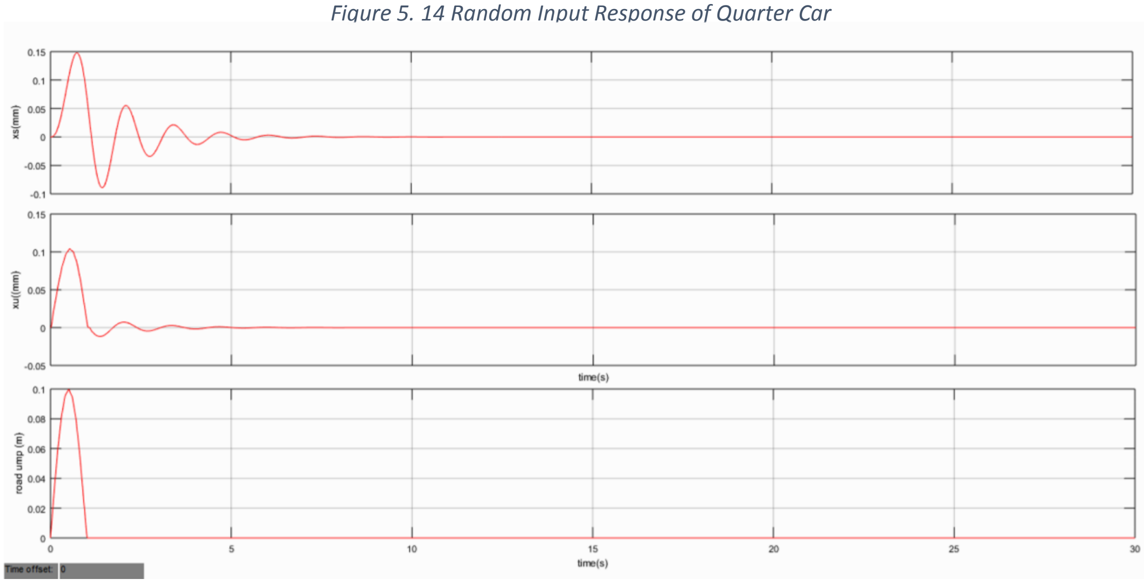

Figure 5. 15 Response of QCM for Single Bump

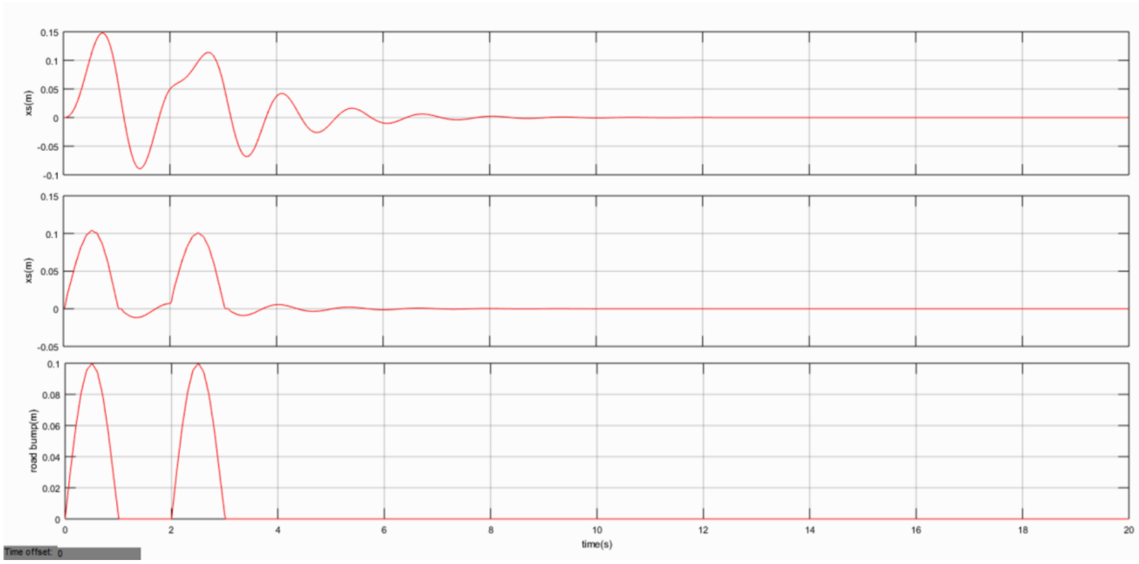

Figure 5. 16 Response of QCM for 2 Bump

From Figure 5.11 – 5.16, it is observed that after passing through suspension system the vibration decreases. Also it must be noted that if any external excitation is provided to the vehicle before the vibration is dead, within certain interval, the effect on driver is significant and would create an impact on the driver.

5.2: RESULT ANALYSIS OF BCM

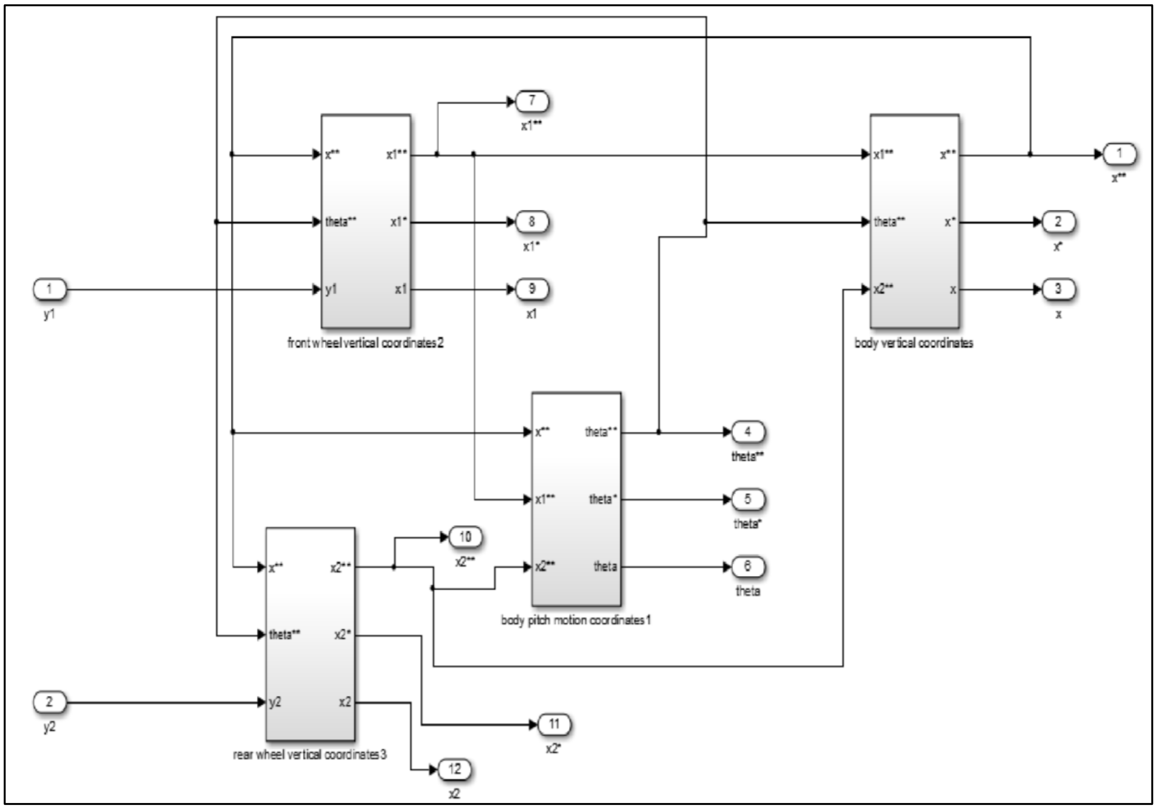

Figure 5. 17 Simulink Model of Bicycle Model

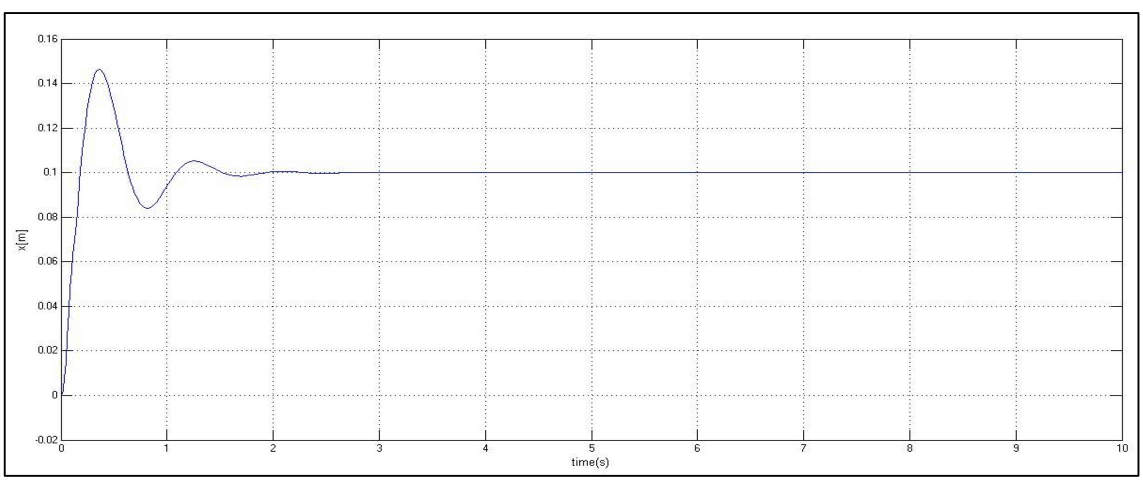

Figure 5. 18 Sprung mass displacement for symmetrical step response to BCM

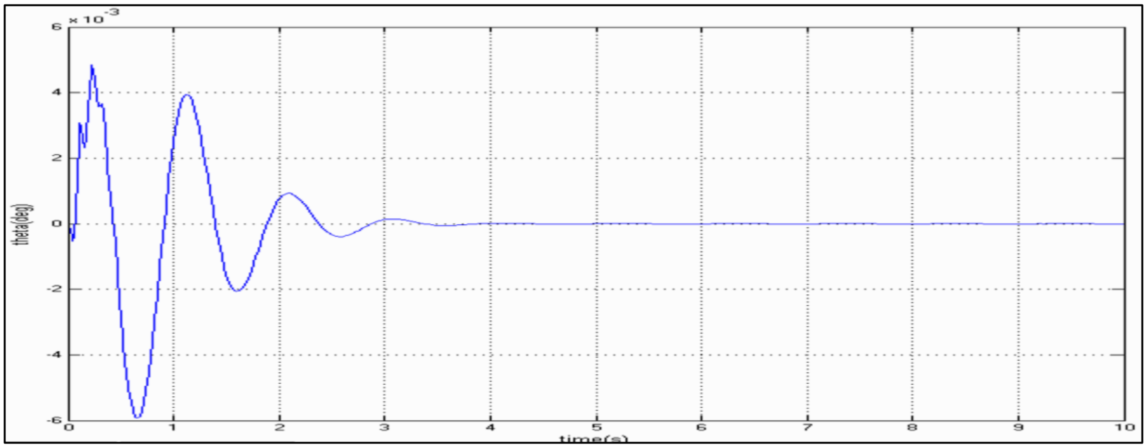

Figure 5. 19 Body Pitch motion for symmetrical step on BCM

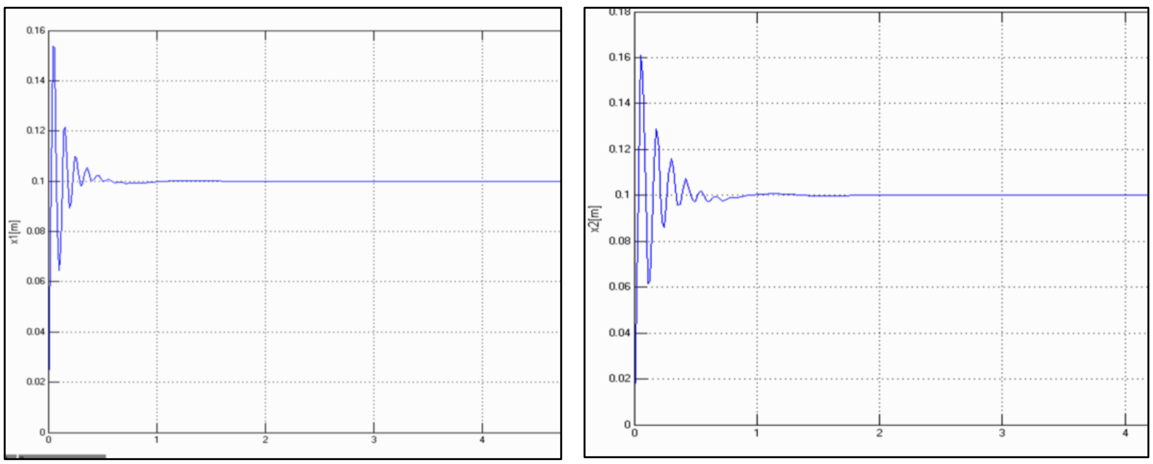

Figure 5. 20 Front and rear wheel displacement for symmetrical step response on BCM

The following results were obtained from the simulation and the state space model. Both the results were identical as expected. The input excitation is step type of amplitude 0.1. As expected the number of oscillation increases as mass increases. Also the displacement get stabilized after some time as expected and as per the theory. It must be noted that the response of both the wheels front and rear are identical to each other which gets clear from Figure 5.20.

Sr no.	m sprung mass (kg)	m1 front wheel mass (kg)	m2 rear wheel mass (kg)	rise time (s)	settling time (s)	peak	peak time (s)
1	400	50	80	0.0235	1.2404	1.6301	0.0614
2	400	50	100	0.0260	1.2323	1.6608	0.0687

3	400	50	120	0.0282	1.2790	1.6845	0.0752
4	400	100	80	0.0235	1.2413	1.6277	0.0614
5	400	100	100	0.0260	1.2342	1.6583	0.0687
6	400	100	120	0.0282	1.2798	1.6822	0.0752
7	400	150	80	0.0235	1.2412	1.6263	0.0614
8	400	150	100	0.0260	1.2324	1.6567	0.0687
9	400	150	120	0.0282	1.2808	1.6804	0.0752
10	500	50	80	0.0235	1.3724	1.6199	0.0614
11	500	50	100	0.0260	1.3701	1.6497	0.0686
12	500	50	120	0.0282	1.3573	1.6726	0.0752
13	500	100	80	0.0235	1.3731	1.6190	0.0614
14	500	100	100	0.0260	1.3707	1.6487	0.0686
15	500	100	120	0.0282	1.3579	1.6716	0.0752
16	500	150	80	0.0235	1.3736	1.6186	0.0614
17	500	150	100	0.0260	1.3711	1.6481	0.0686
18	500	150	120	0.0282	1.3587	1.6710	0.0752
19	1000	50	80	0.0236	1.7175	1.5988	0.0612
20	1000	50	100	0.0261	1.7228	1.6263	0.0685
21	1000	50	120	0.0283	1.7330	1.6476	0.0750
22	1000	100	80	0.0236	1.7199	1.6012	0.0612
23	1000	100	100	0.0261	1.7254	1.6286	0.0684
24	1000	100	120	0.0283	1.7347	1.6495	0.0750
25	1000	150	80	0.0236	1.7228	1.6027	0.0612
26	1000	150	100	0.0261	1.7278	1.6302	0.0685
27	1000	150	120	0.0283	1.7376	1.6512	0.0750

Table 5. 9 Body Vertical Displacement for different sprung and unsprung mass

It has been seen that the latent parameters are by and large fix and can't be changed with the exception of the mass (sprung).It is additionally watched, from Table 5.9[3], that the top for sprung mass uprooting is diminished and that for unsprung mass is expanded, for various sprung mass and unsprung mass.

It is observed that as as unsprung mass increase settling time shows increase/decrease pattern when mass of front wheel is less than rear wheel and decrease when mass front wheel is greater than rear wheel

Likewise top increments when mass of front wheel is not exactly raise haggle when mass of front wheel is more prominent than back wheel

The pinnacle time shows an expansion when front wheel mass is not exactly raise haggle when front wheel mass is more noteworthy than back wheel yet as contrast builds it increments And rise time increases with increase in mass but rear wheel has more effect compared to front wheel.

It is clear from the table 2 that rear wheel have more effect on vehicle vibration than that of front wheel, so for a small change in mass of rear wheel a significant change is noticed.

Also it should be noted that as sprung mass increases, settling time and rise time increases while peak time decreases and peak magnitude point decreases.

The parameters of an aloof suspension framework are commonly fixed, being picked to accomplish a specific degree of bargain between street holding, load conveying and solace.

Sr. No	k1 (N/m)	k2 (N/m)	kt1 (N/m)	kt2 (N/m)	c1 (Ns/m)	c2 (Ns/m)	rise time (s)	settling time (s)	peak	peak time (s)
1	10000	10000	100000	100000	1000	1000	0.0337	1.4876	1.5127	0.0927
2	10000	10000	100000	100000	1000	2000	0.0378	0.8442	1.4444	0.1001
3	10000	10000	100000	100000	2000	1000	0.0336	1.9138	1.5194	0.0927
4	10000	10000	100000	100000	3000	1000	0.0336	1.9426	1.5237	0.0927
5	10000	10000	100000	100000	1000	1000	0.0337	1.4876	1.5127	0.0927
6	10000	10000	100000	200000	1000	1000	0.0227	0.9256	1.6365	0.0603
7	10000	10000	100000	300000	1000	1000	0.0181	0.8224	1.6956	0.0495
8	10000	10000	300000	100000	1000	1000	0.0336	1.4929	1.5175	0.0928
9	10000	10000	300000	200000	1000	1000	0.0226	0.9246	1.6403	0.0603
10	10000	10000	300000	300000	1000	1000	0.0181	0.8226	1.6980	0.0495
11	10000	10000	100000	100000	1000	1000	0.0337	1.4876	1.5127	0.0927
12	10000	20000	100000	100000	1000	1000	0.0364	39.418	1.4373	0.2535
13	20000	10000	100000	100000	1000	1000	0.0319	23.548	1.5135	0.0926

[	30000	20000	100000	100000	1000	1000	0.0318	9.9193	1.4268	0.0885
15	10000	10000	100000	200000	1000	2000	0.0246	0.3874	1.5016	0.0652
16	10000	10000	100000	200000	2000	1000	0.0226	0.9138	1.6386	0.0603
17	10000	10000	100000	200000	3000	1000	0.0226	0.9123	1.6400	0.0603
18	10000	10000	300000	200000	1000	2000	0.0246	0.3848	1.5095	0.0651
19	10000	10000	300000	200000	2000	1000	0.0226	0.9133	1.6447	0.0603
20	10000	10000	300000	200000	3000	1000	0.0226	0.9114	1.6479	0.0603
21	10000	20000	100000	100000	1000	2000	0.0419	2.2883	1.3872	0.1014
22	10000	20000	100000	100000	2000	1000	0.0363	9.1992	1.4511	0.2535
23	10000	20000	100000	100000	3000	1000	0.0363	7.3940	1.4606	0.2535
24	20000	10000	100000	100000	1000	2000	0.0351	3.5525	1.4447	0.0997
25	20000	10000	100000	100000	2000	1000	0.0318	5.2760	1.5189	0.0926
26	20000	10000	100000	100000	3000	1000	0.0318	4.2058	1.5224	0.0926

Table 5. 10 Suspension parameter changes and its effect on Body Vertical Coordinate Displacement

From table 5.10 we observe that when damping coefficient of front wheel is less than rear wheel the vibration decreases in magnitude and oscillation, while when damping coefficient of front wheel is more than rear wheel vibration increases in magnitude and oscillation.

From table 5.10 we observe that when wheel spring constant of front wheel is less than rear wheel the vibration increases in magnitude but its effect ends earlier, while when wheel spring constant front wheel is more than rear wheel vibration shows same effect as it has before.

From table 5.10 we observe that when spring constant of front wheel is less than rear wheel the vibration shows slight decrease in magnitude with increase in oscillation but its effect last longer, while when spring constant of front wheel is more than rear wheel vibration shows same effect as it has before but compared to the previous case it shows a decrease.

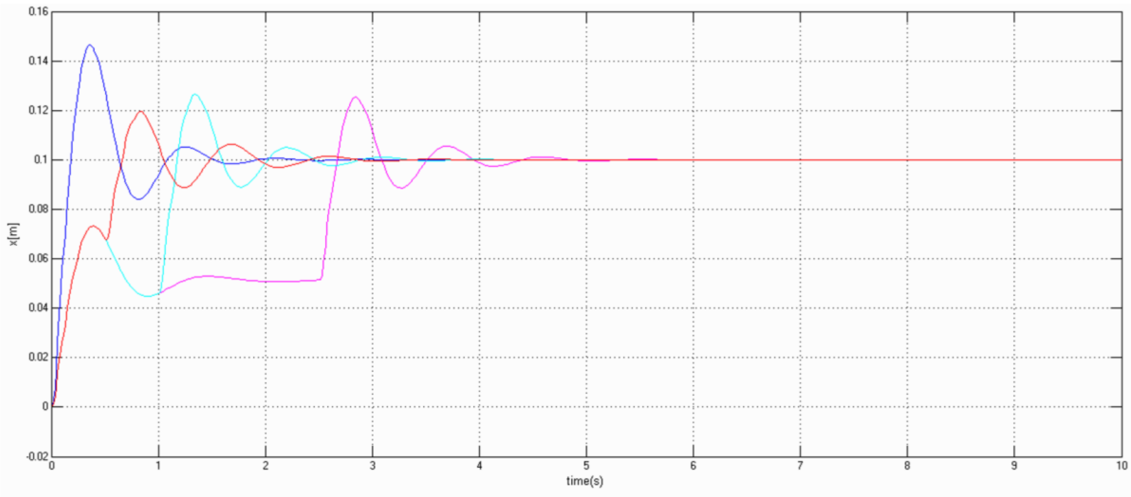

Figure 5. 21 Displacement of car body at different velocities for BCM

The above figure 5.21 shows the response of BCM for different velocity, it is clear that when velocity decreases the effect of both the wheel is seen clearly but when the speed increases the peak increases and the difference cannot be seen in front and rear wheel vibration.

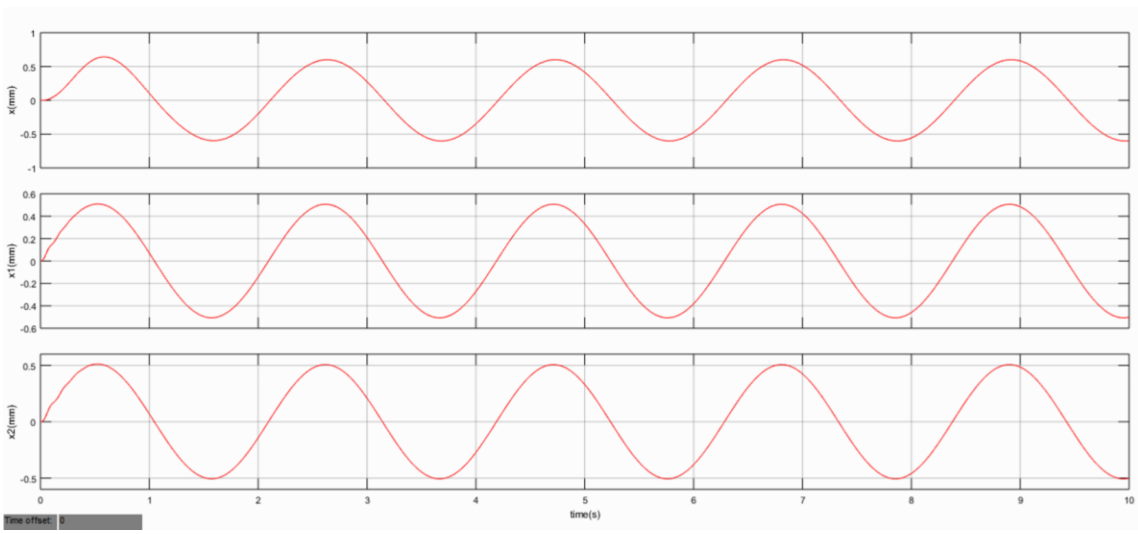

Figure 5. 22 Body displacement for a BCM for Sine Road Profile

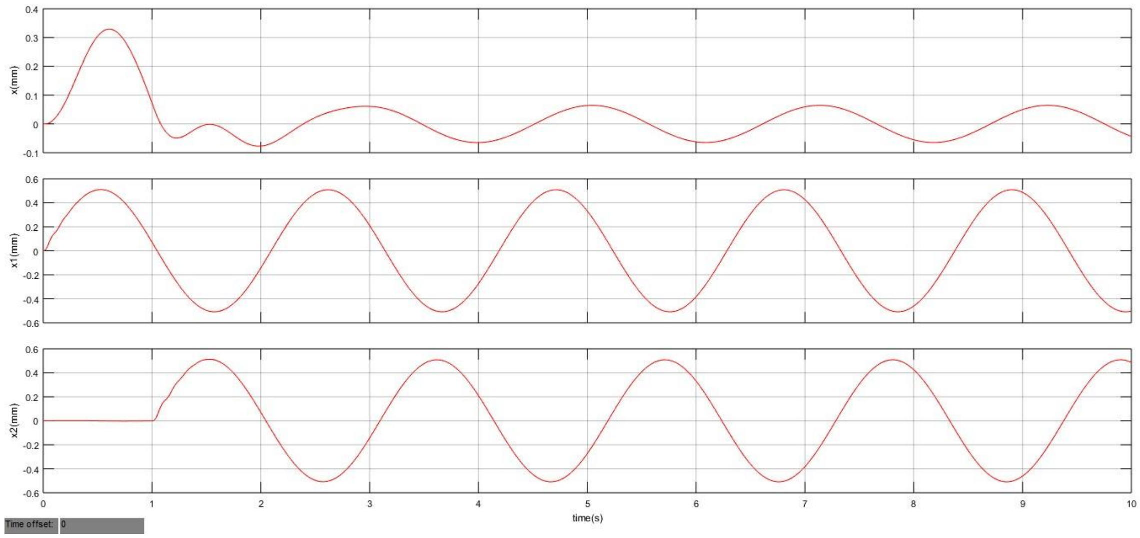

Figure 5. 23 Body displacement for BCM for different Sine Road Profile with time shift between each signal.

From figure 5.22 and 5.23 we observe that when continuously same disturbance is given to the vehicle the output of the vehicle body vertical motion shows the same pattern of disturbance but when the disturbance is obtained with a time shift than the effect on the body motion shows the difference of the vibration of that of the unsprung mass vibration.

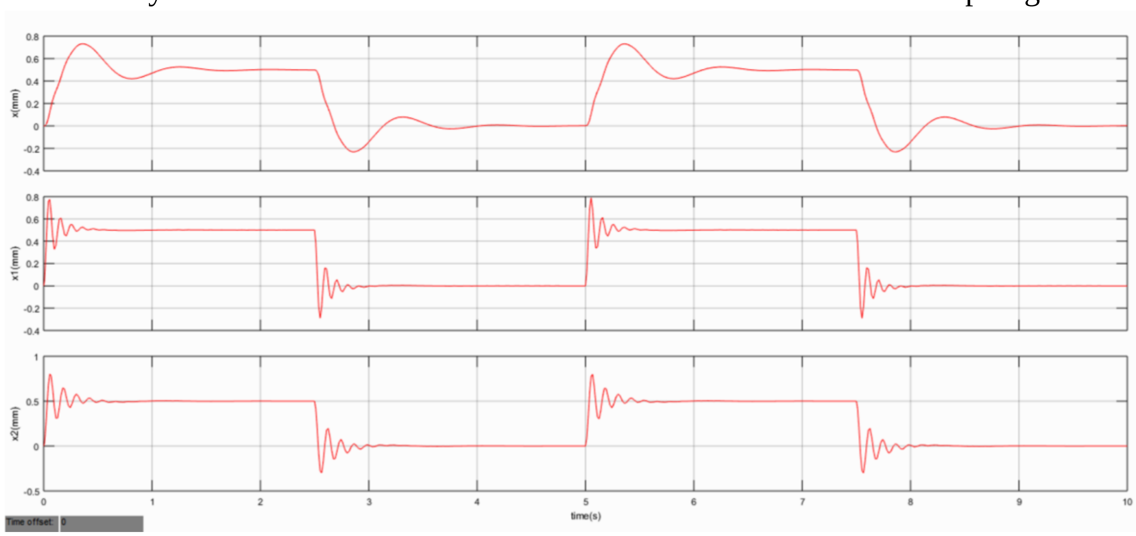

Figure 5. 24 Body displacement for BCM for Pulse Input

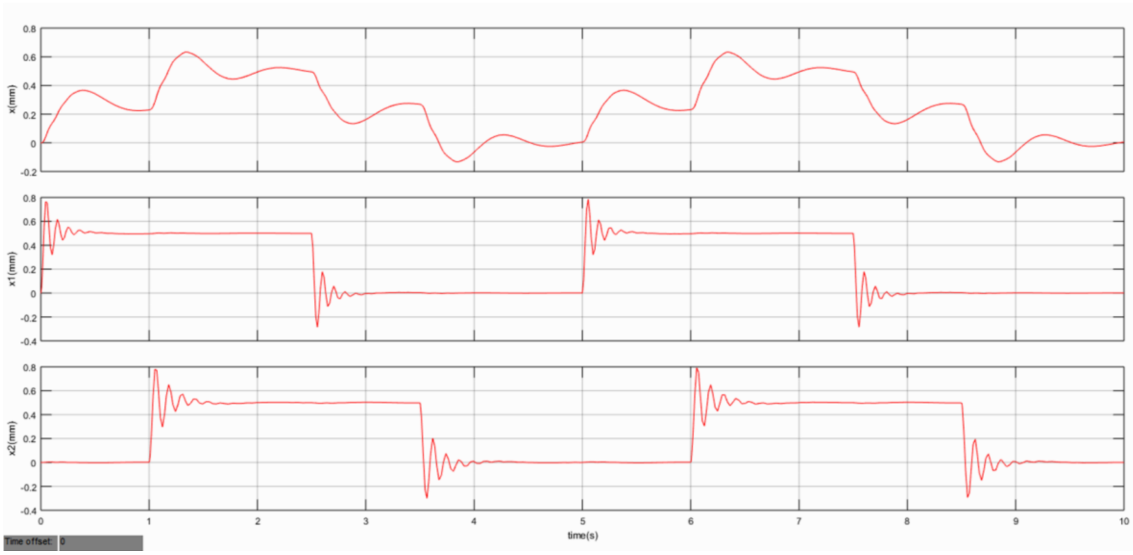

Figure 5. 25 Body displacement for BCM for different Pulse at front and Rear wheel

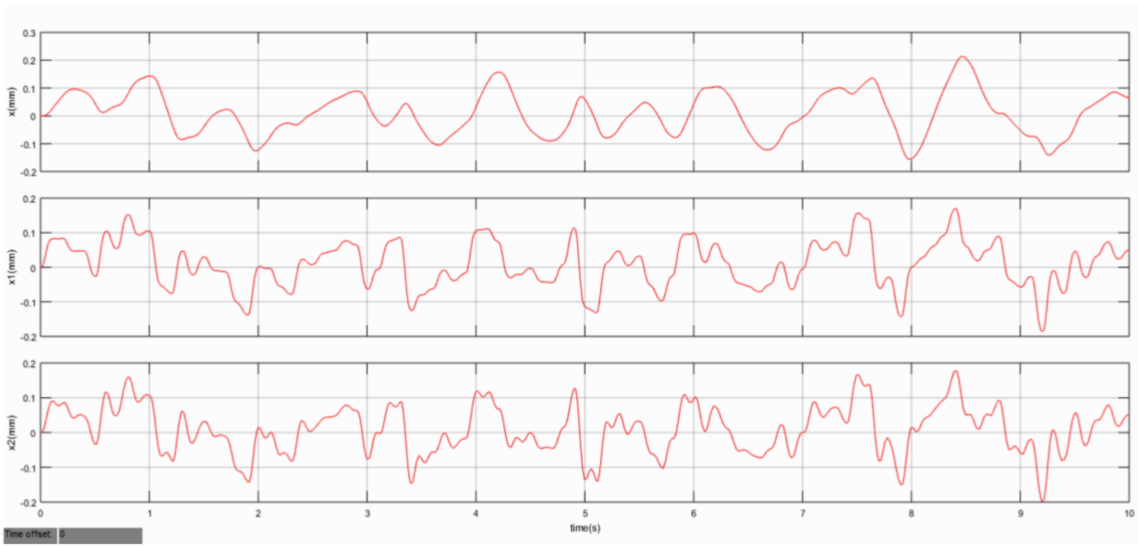

Figure 5. 26 Body Response BCM for Random Road Profile

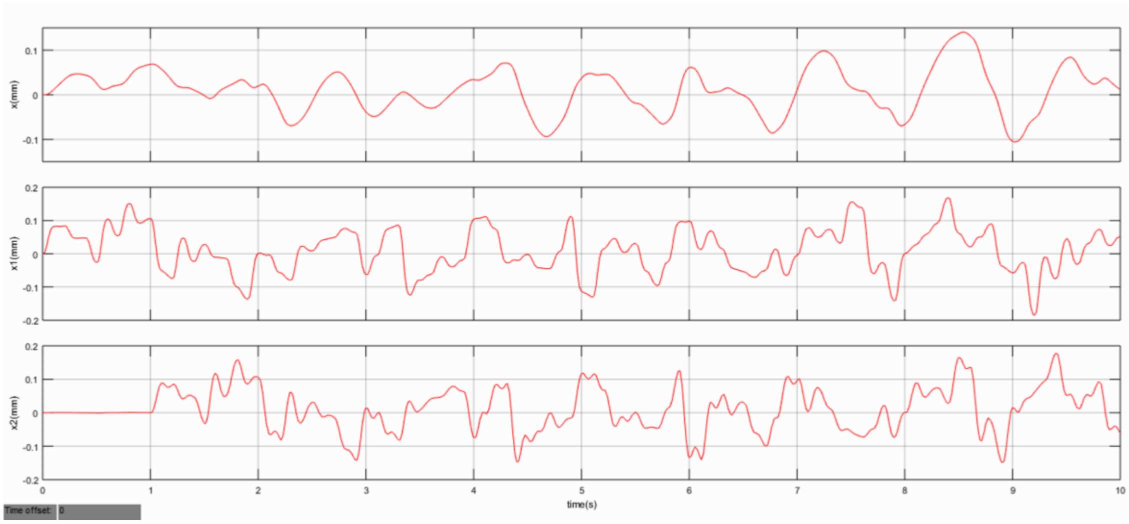

Figure 5. 27 Body displacement for BCM for different Random Inputs on both wheels

It is observed from the Figure 5.24 – 5.27 that the effect of vibration decreases after passing through the suspension system of the vehicle. It is clearly seen the effect of vibration is reduced.

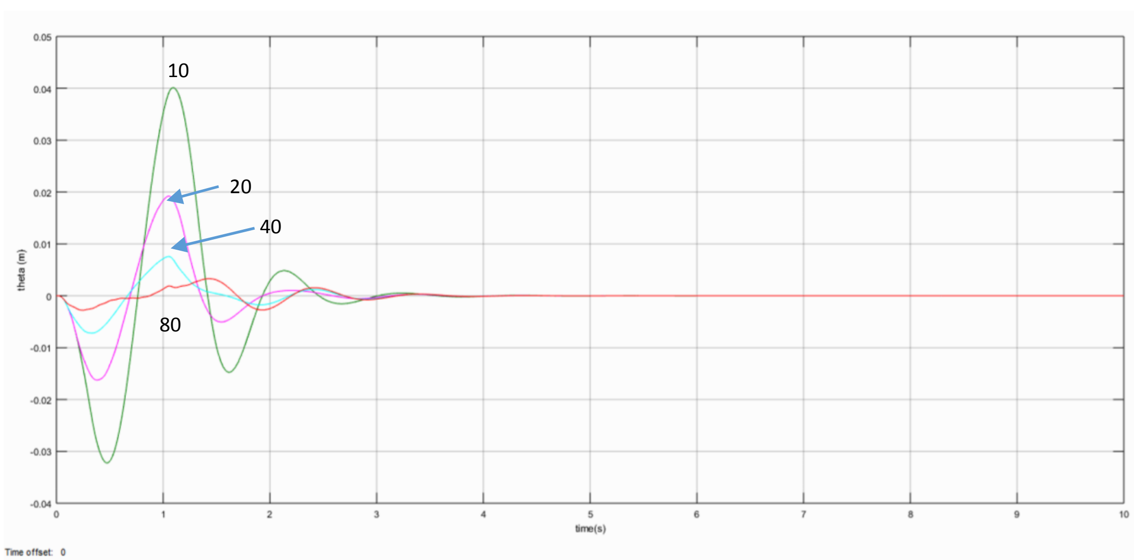

Figure 5. 28 Response of BCM body pitch motion for different velocity

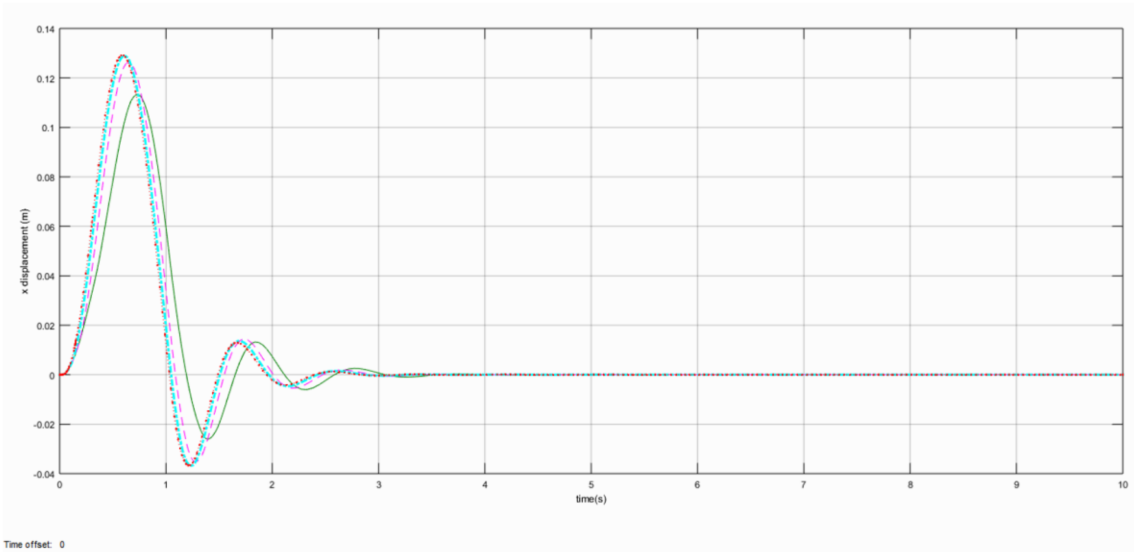

Figure 5. 29 Response of BCM body vertical motion for different velocity

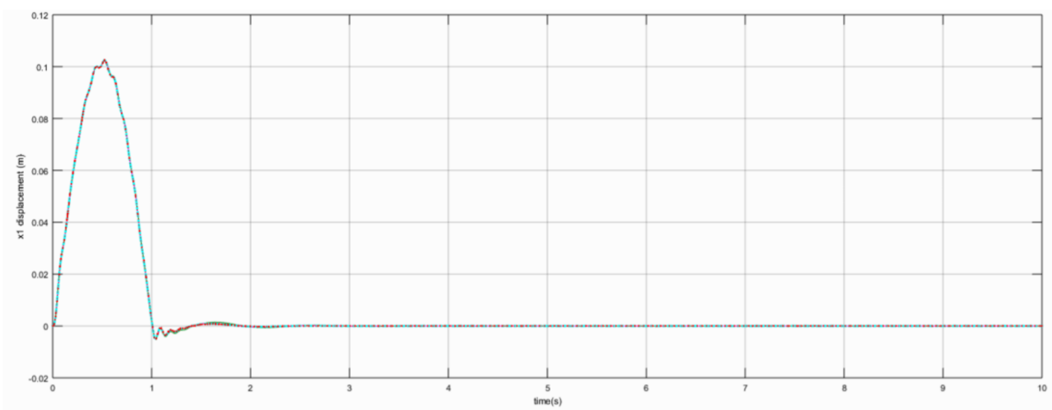

Figure 5. 30 Response of BCM front wheel motion for different velocity

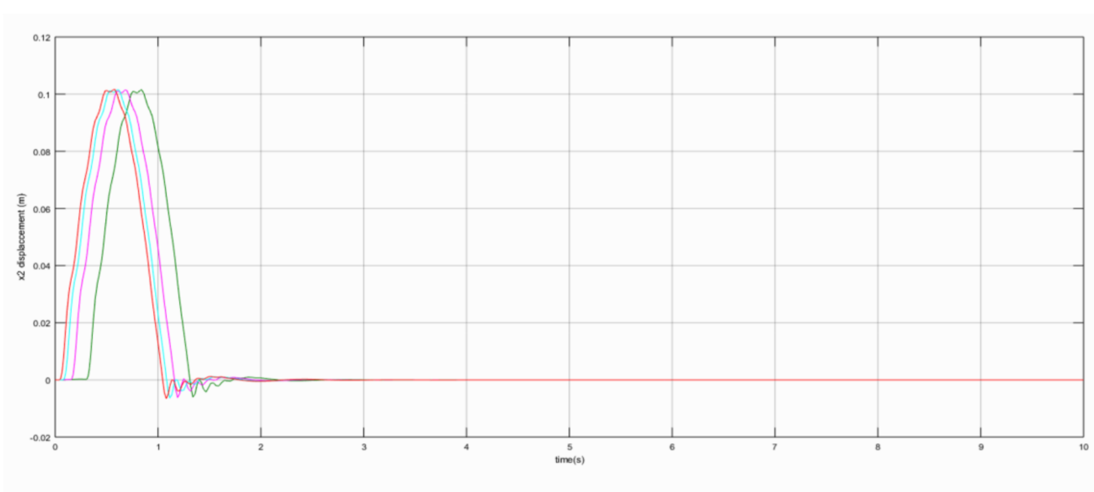

Figure 5. 31 Body displacement for BCM rear wheel motion for different velocity

It is observed in Figure 5.28 – 5.31 shows the response of Bicycle Car Model (BCM) at Different velocity for a bump on the road of amplitude 0.1. The effect is same as experienced earlier in other cases.

5.3: RESULT ANALYSIS OF HCM

Only the body pitch motion equation changes in half car model, rest of the equations are same and so do the response of the model.

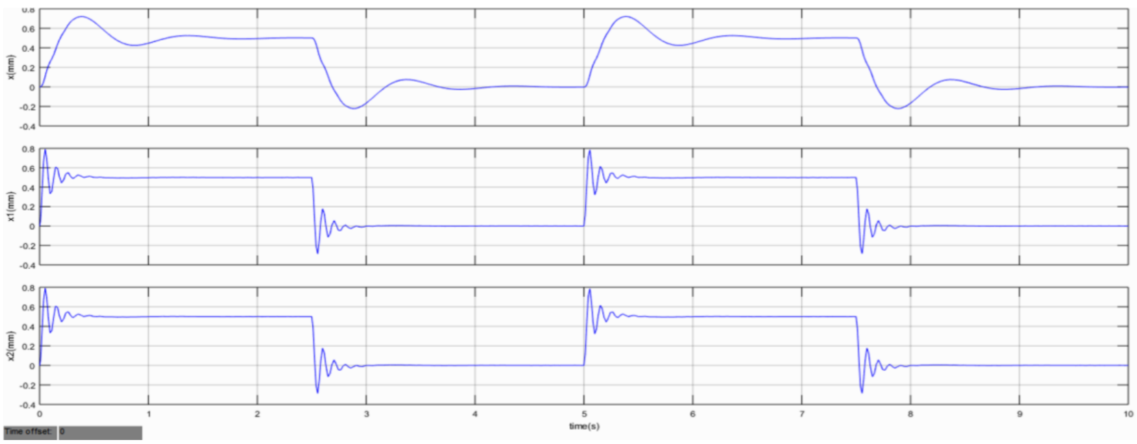

Figure 5. 32 Body displacement for HCM for Pulse Input

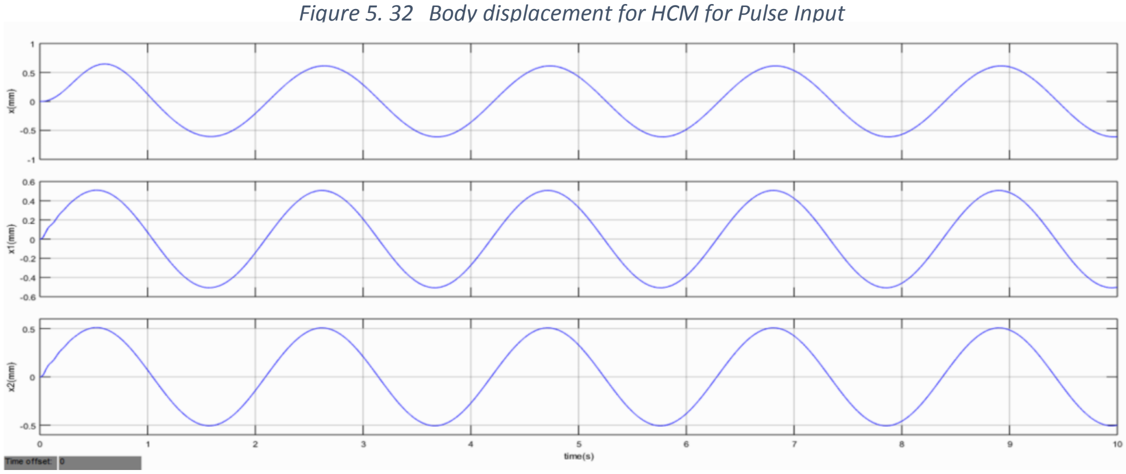

Figure 5. 33 Body displacement for HCM for Sine Inputs on wheel

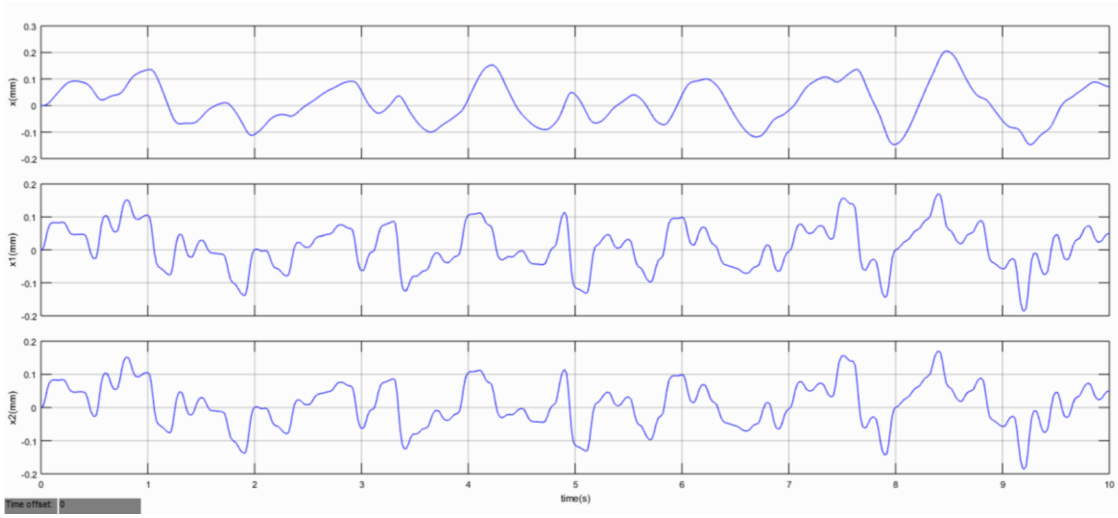

Figure 5. 34 Body displacement for HCM for Random Road Inputs on wheel

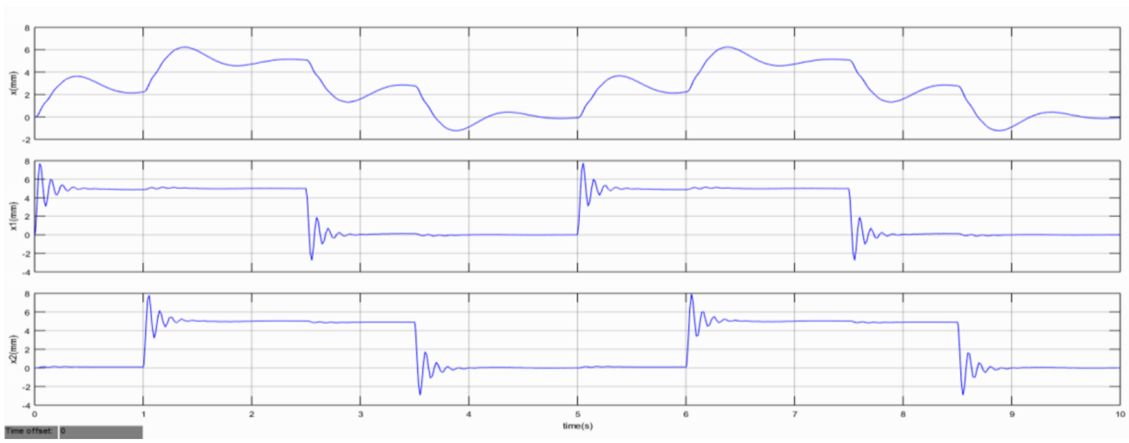

Figure 5. 35 Body displacement for HCM for different Pulse Inputs on wheel

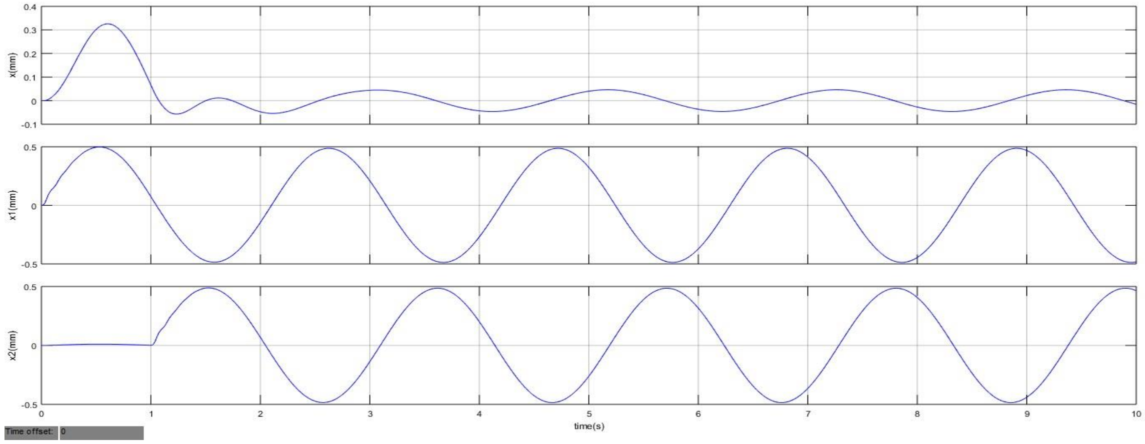

Figure 5. 36 Response of HCM for different Sine Inputs on wheel

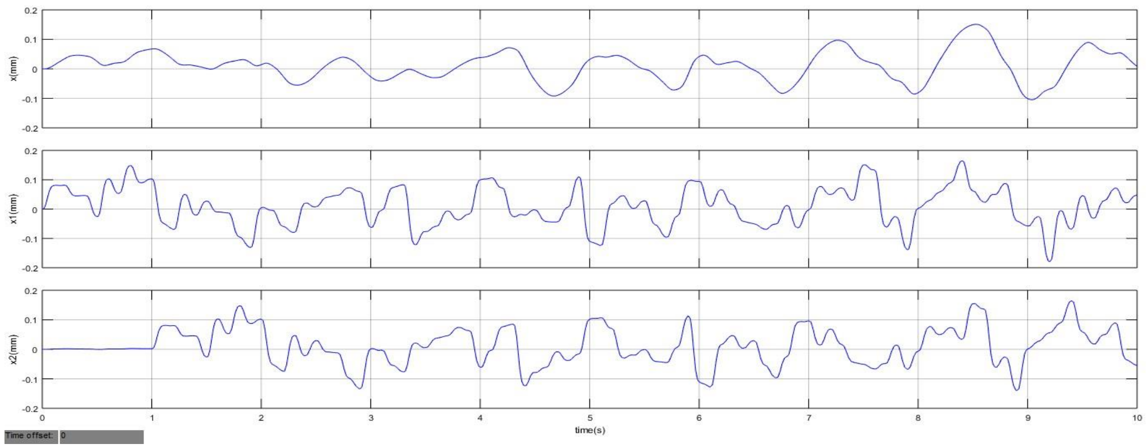

Figure 5. 37 Response of HCM for different Random Inputs on wheel

The Figures 5.32 – 5.37 shows the same effect as in BCM. Thus we can say that there is no major difference in BCM and HCM.

5.4: RESULT ANALYSIS OF FCM

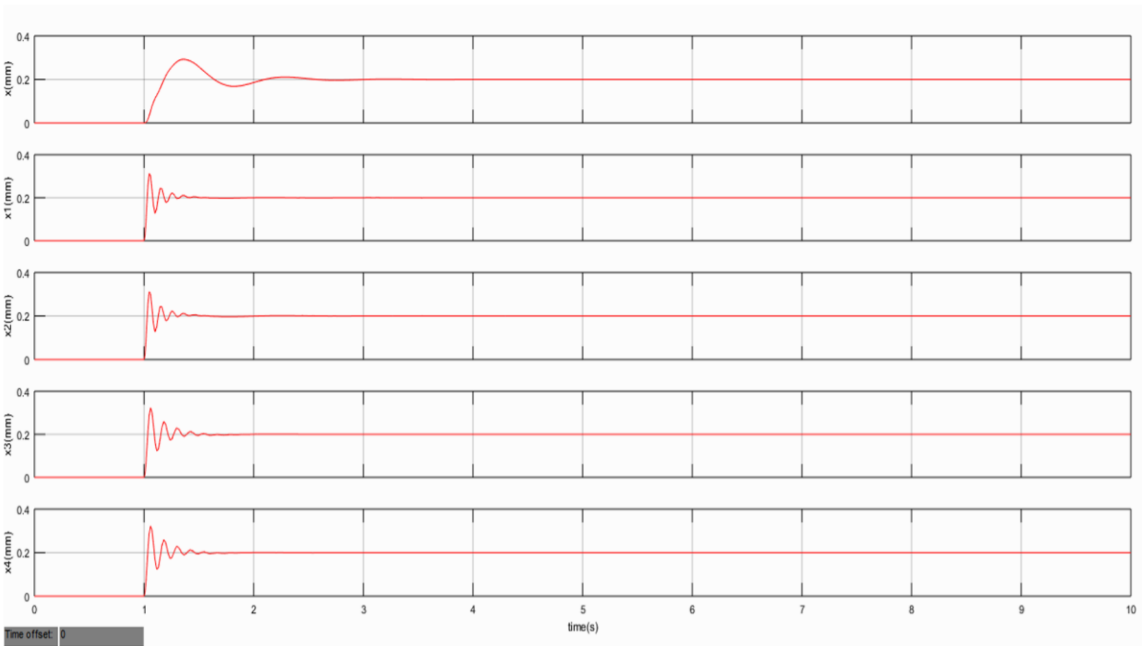

Figure 5. 38 Body displacement for FCM for Symmetrical Step Inputs on wheel

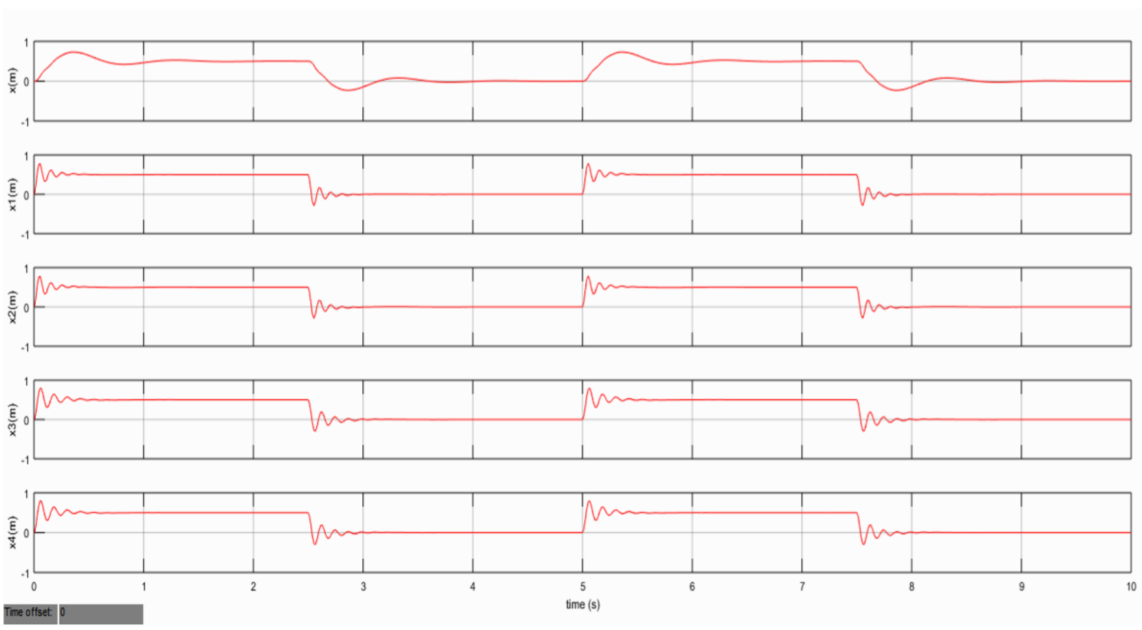

Figure 5. 39 Body displacement for FCM for Symmetrical Pulse Inputs on wheel

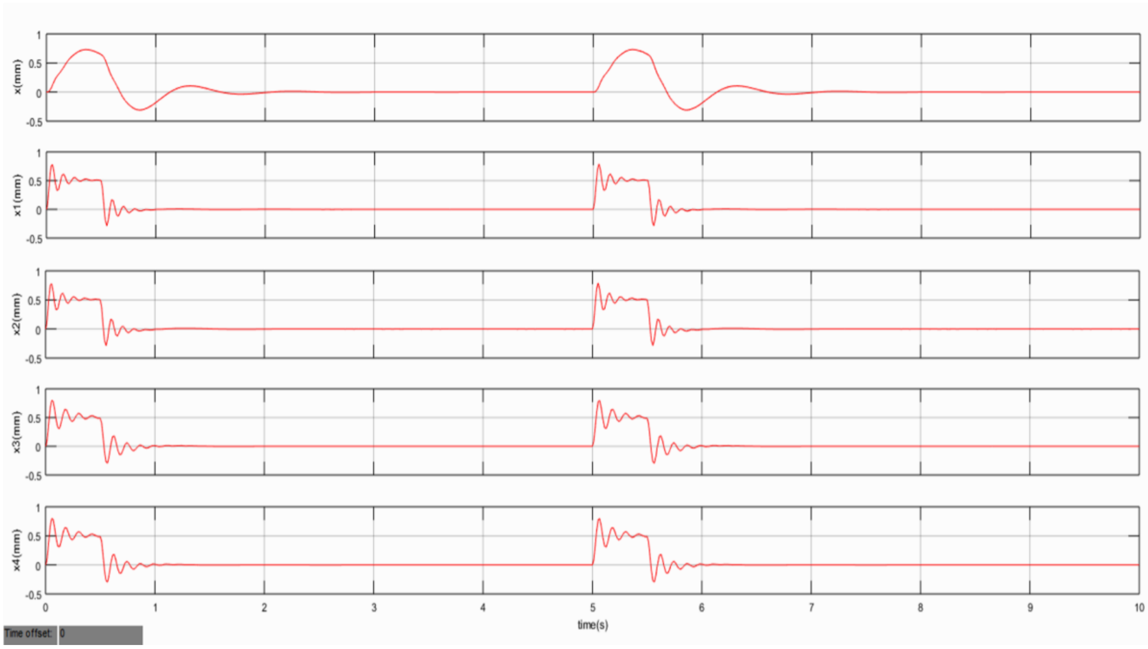

Figure 5. 40 Body displacement for FCM for Symmetrical Pulse Inputs on wheel of small width

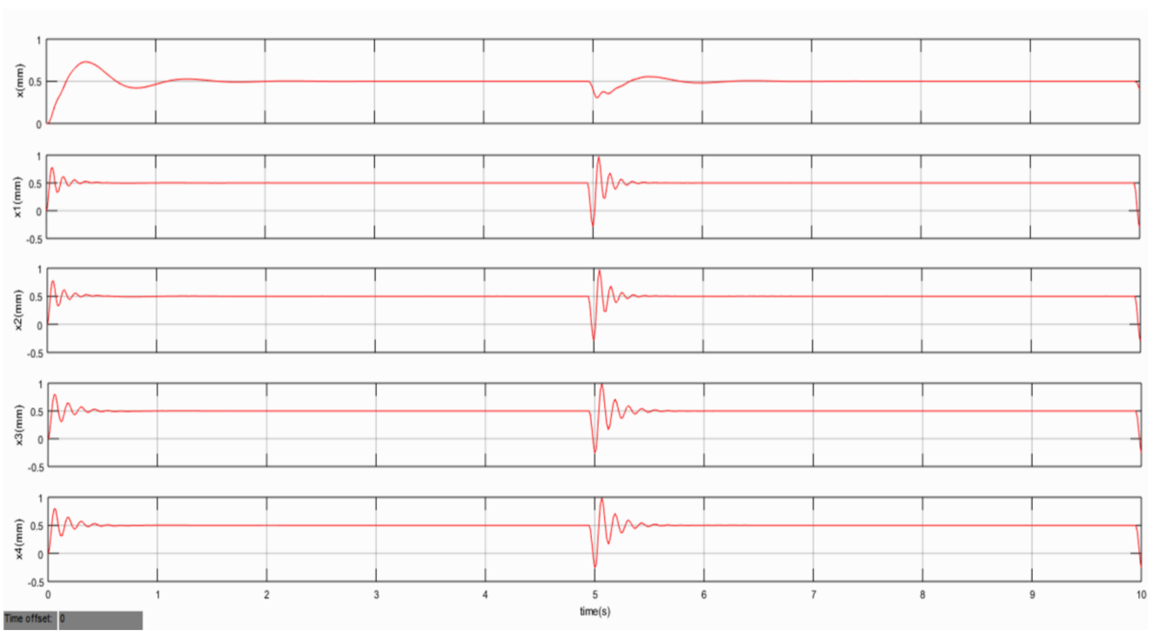

Figure 5. 41 Body displacement for FCM for Symmetrical Step Inputs on wheel at different time

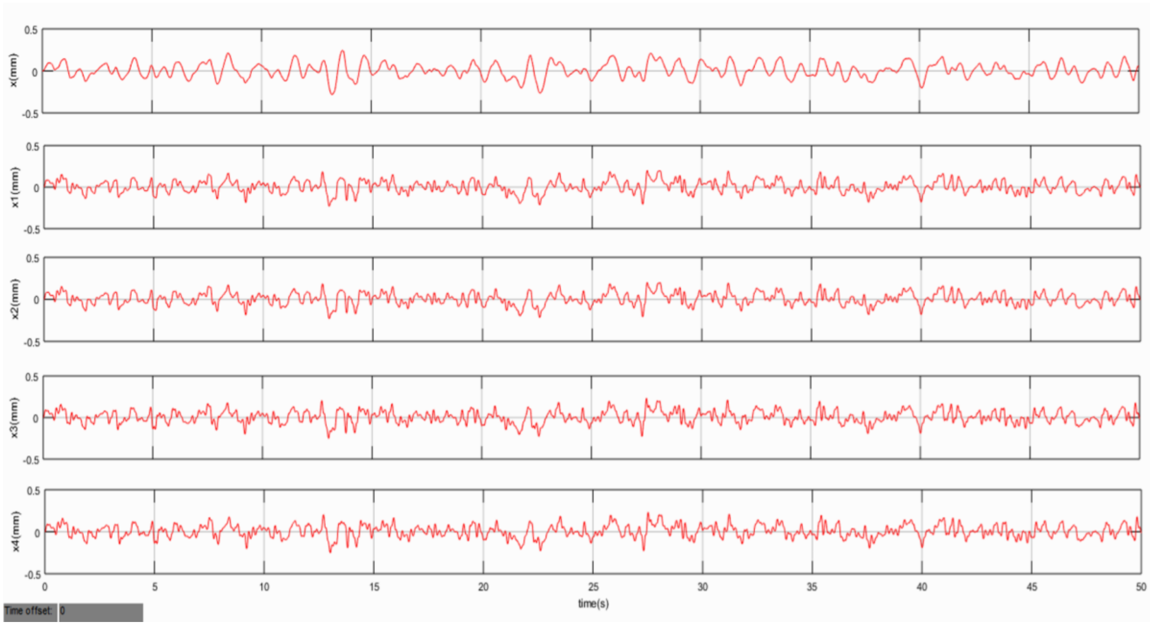

Figure 5. 42 Body displacement for FCM for Symmetrical Random Road Inputs on wheel

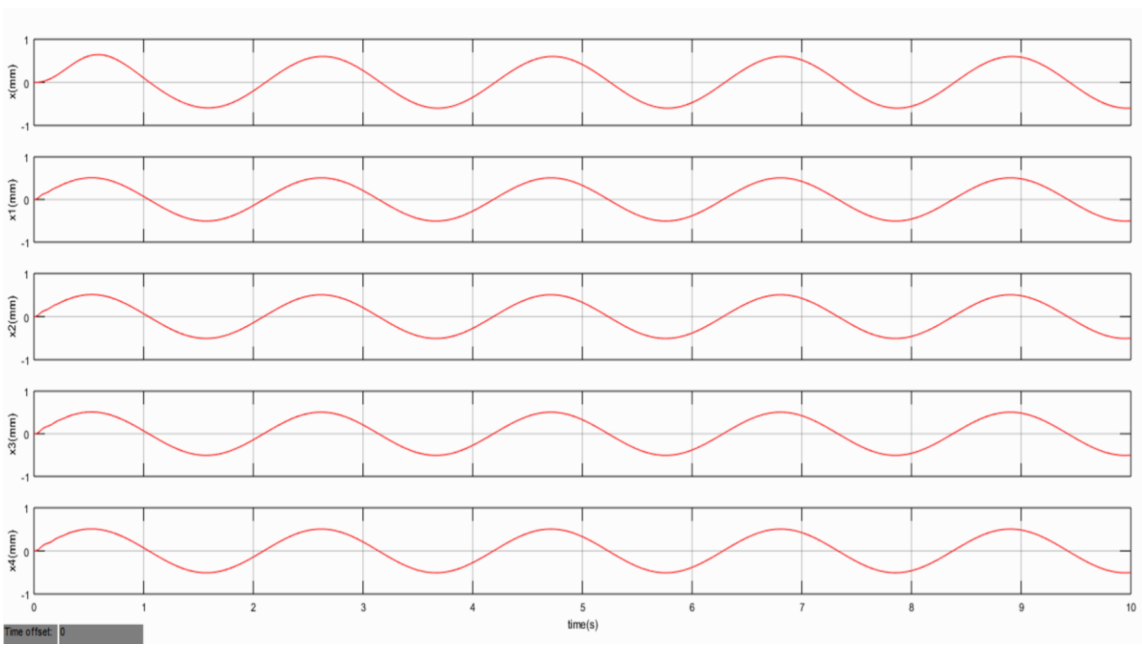

Figure 5. 43 Body displacement for FCM for Symmetrical sine Inputs on wheel

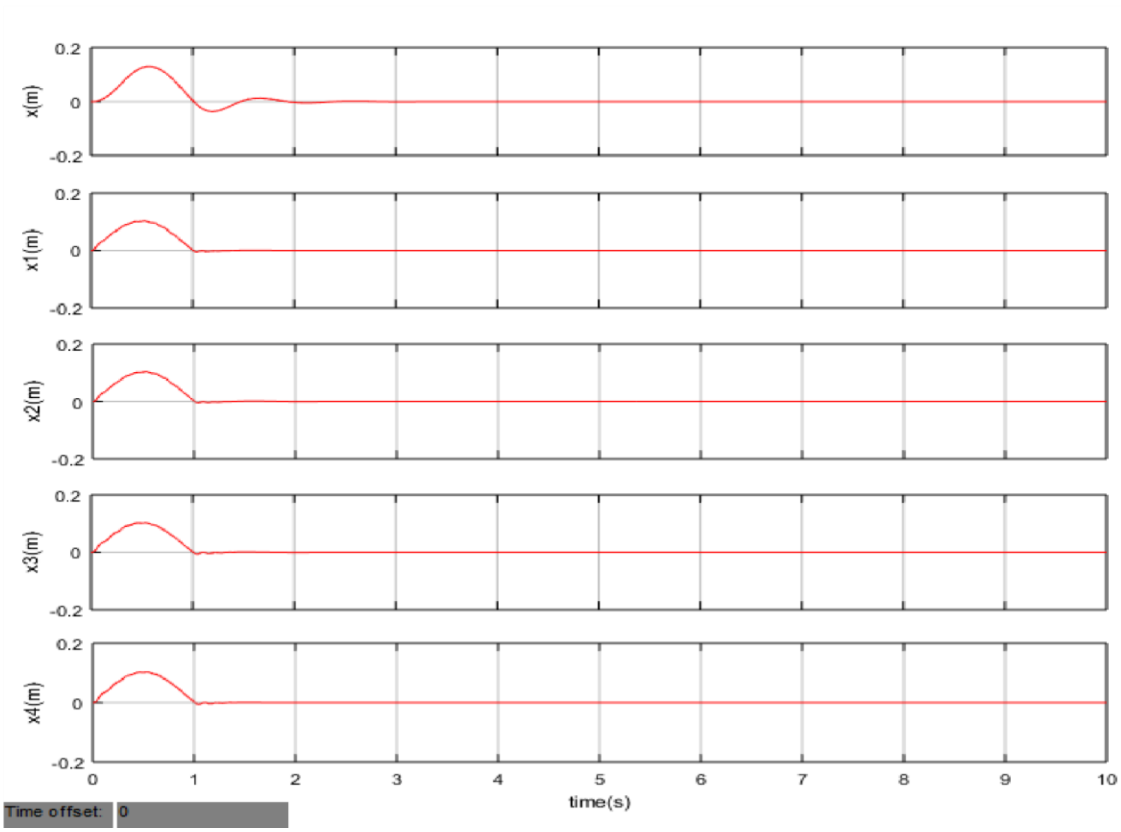

Figure 5. 44 Body displacement for FCM for Symmetrical Bump Inputs on wheel

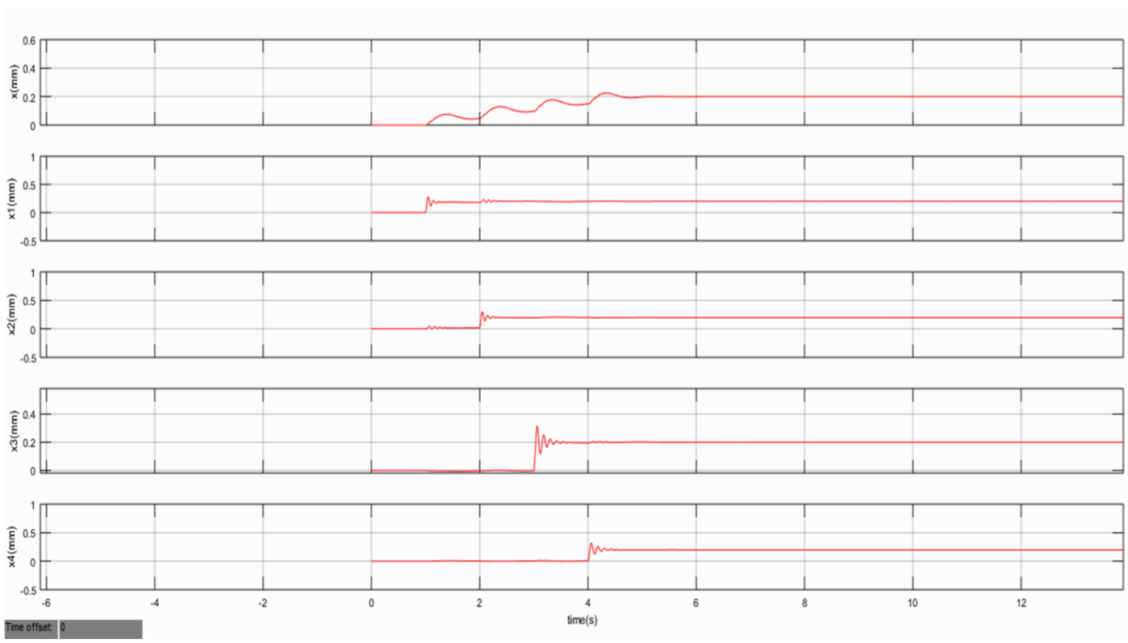

Figure 5. 45 Body displacement for FCM for Step Inputs on wheel at different time

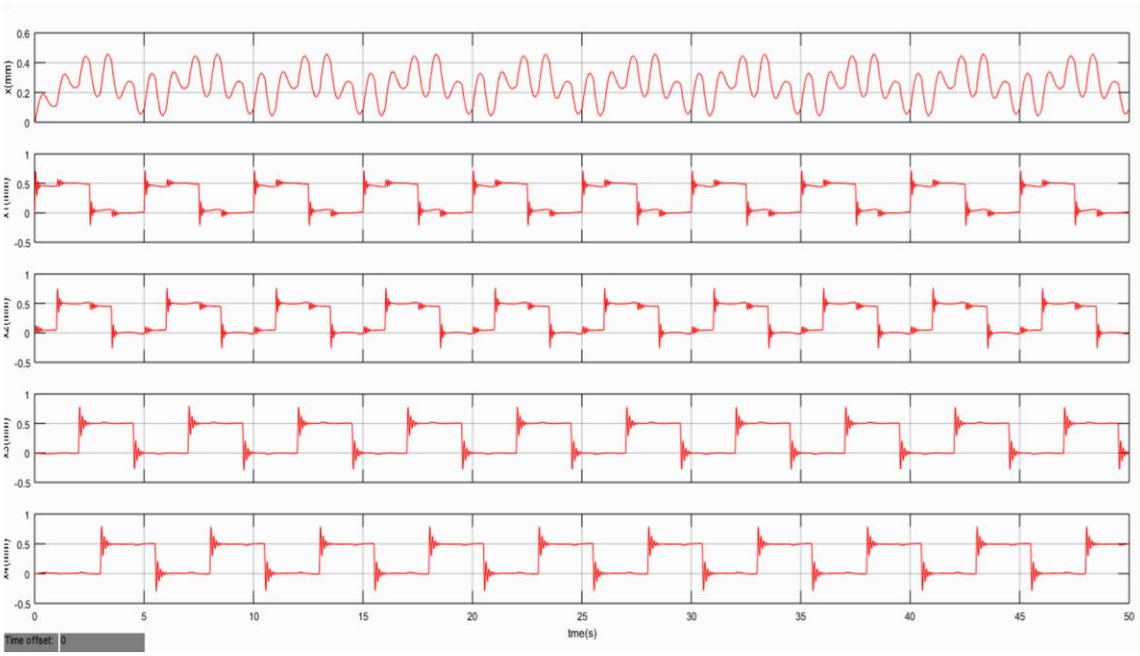

Figure 5. 46 *Body displacement for* FCM for Pulse Inputs on wheel at different time

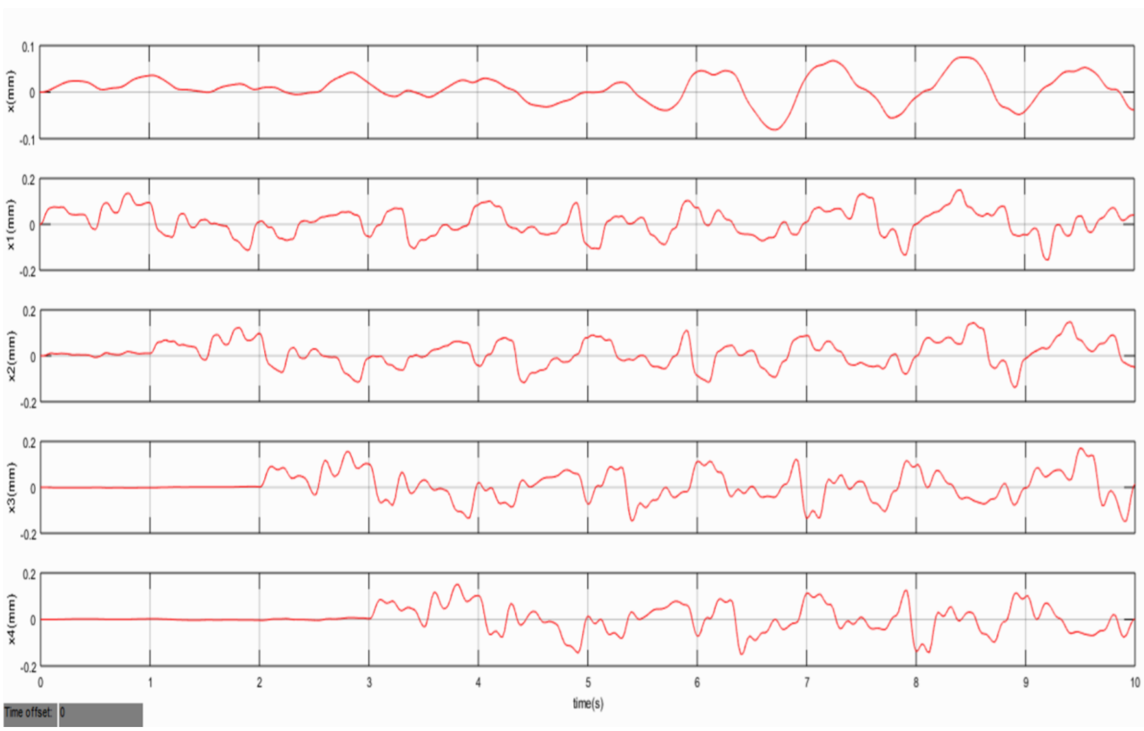

Figure 5. 47 *Body displacement for* FCM for Random Road Inputs on wheel at different time

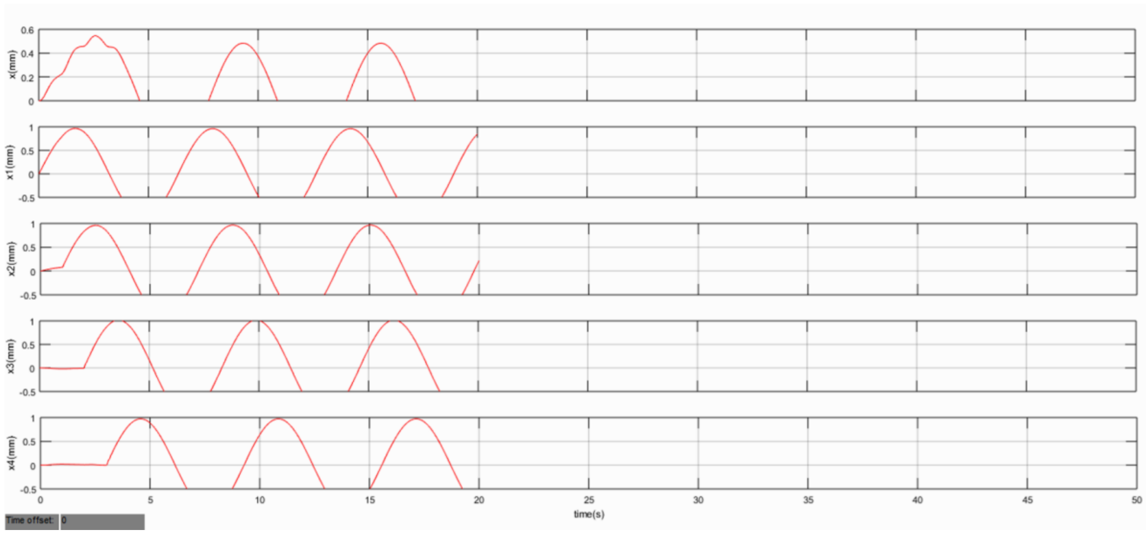

Figure 5. 48 Body displacement for FCM for Bump Inputs on wheel at different time

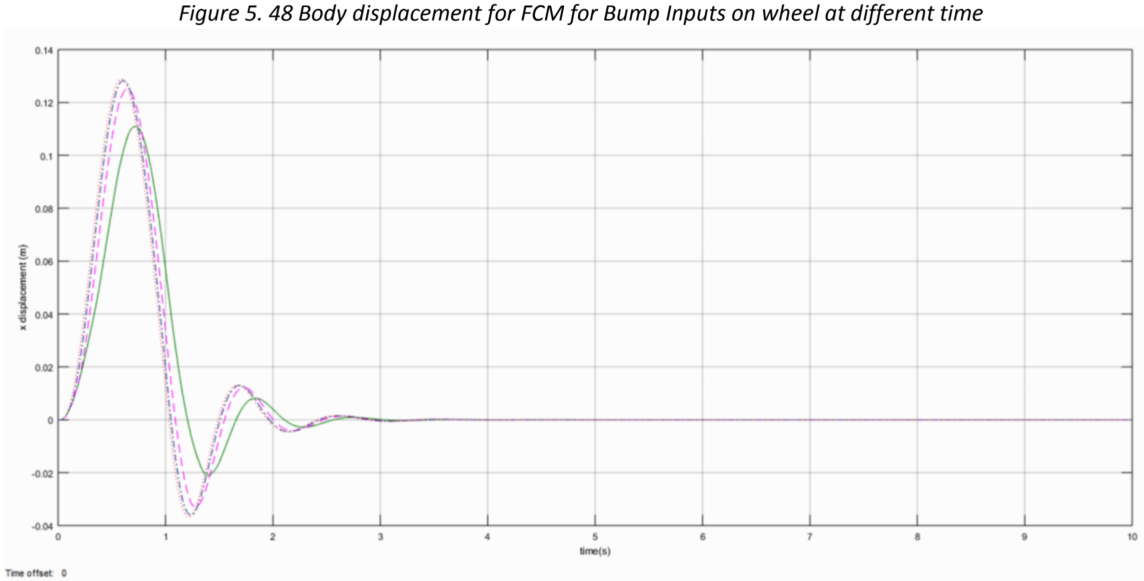

Figure 5. 49 Body displacement for FCM body vertical motion for Single Bump Inputs on wheel at different velocity

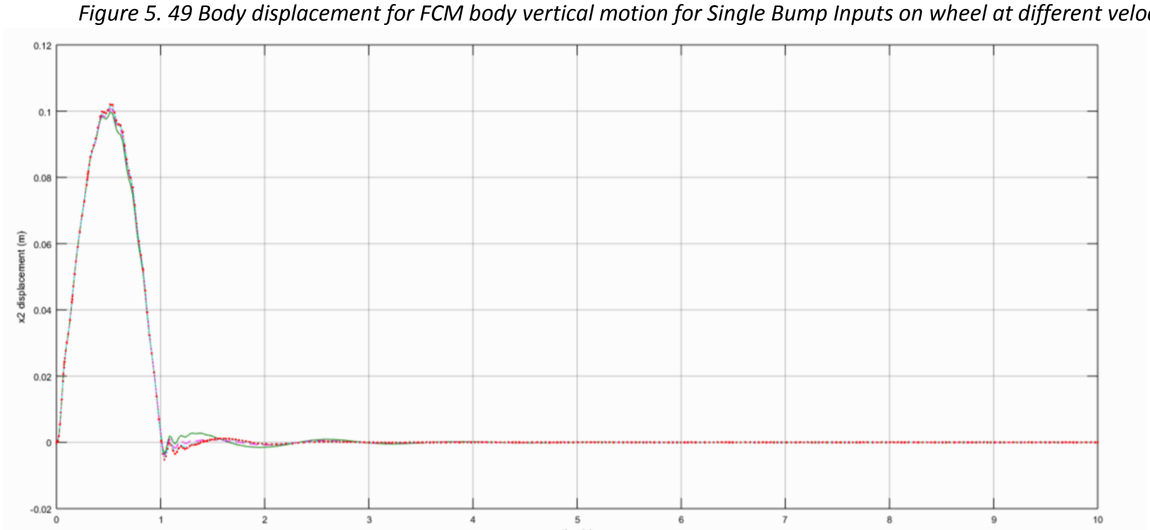

Figure 5. 50 Body displacement for FCM front right wheel for Single Bump Inputs on wheel at different velocity

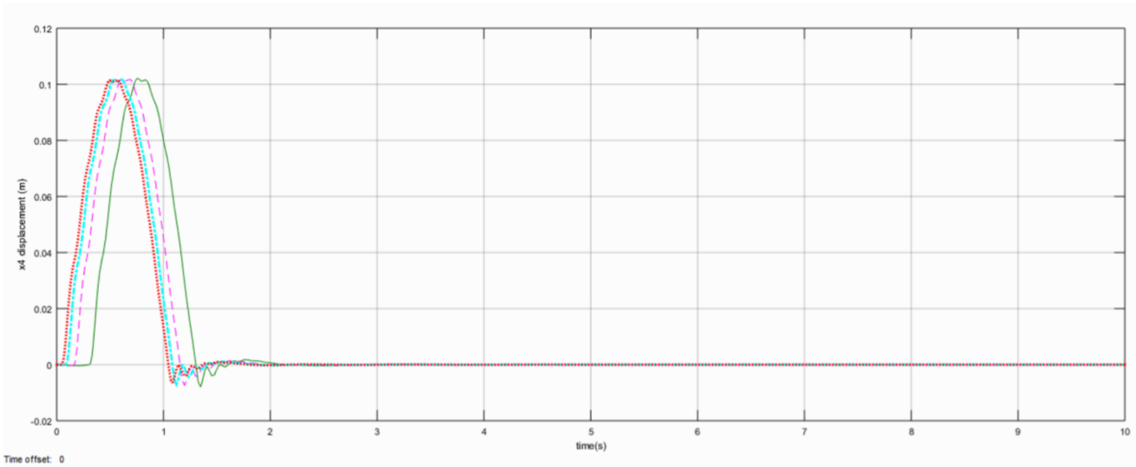

Figure 5. 51 Body displacement for FCM rear right wheel for Single Bump on wheel at different velocity

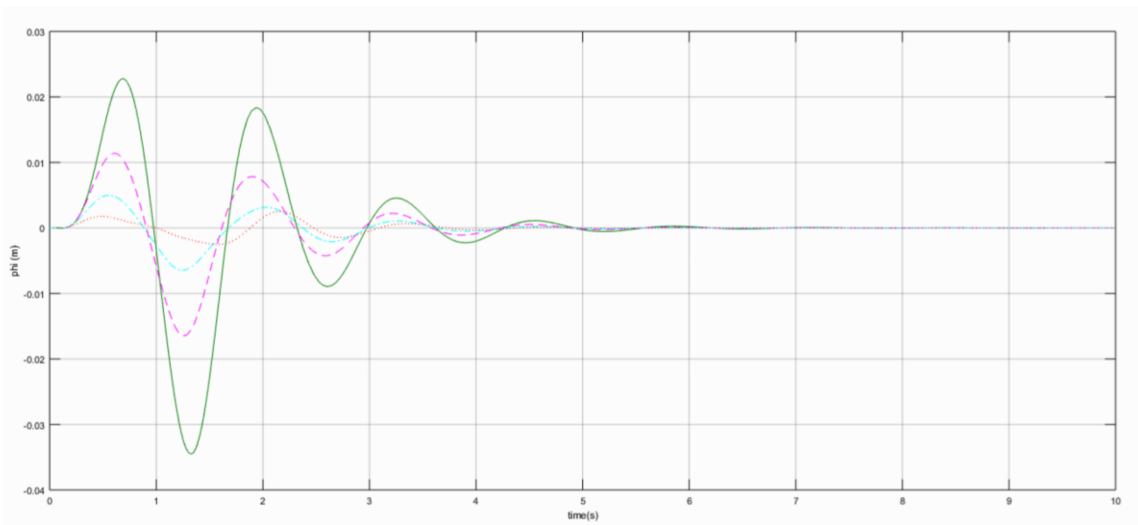

Figure 5. 52 Body displacement for FCM body roll motion for Single Bump on wheel at different velocity

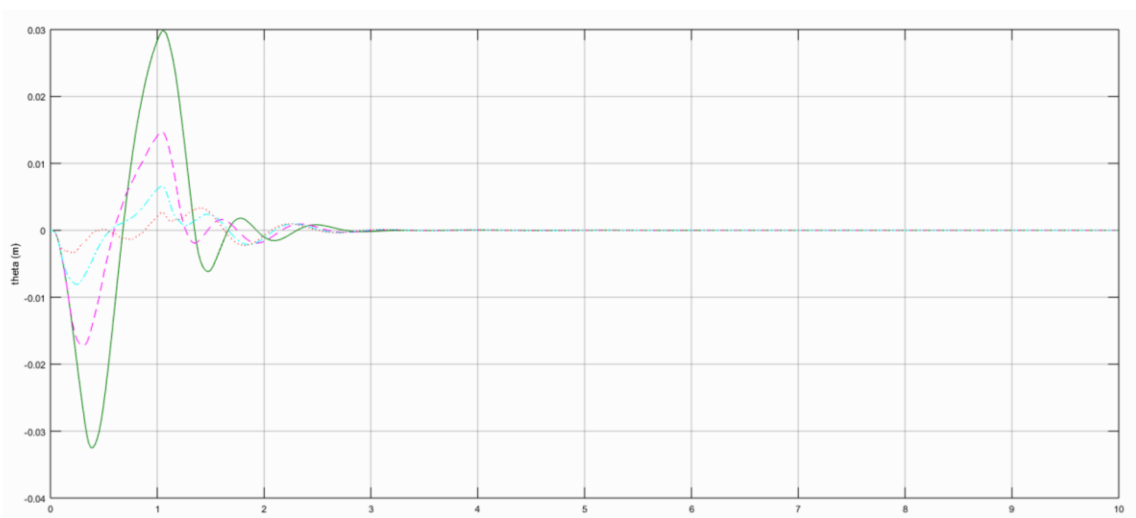

Figure 5. 53 Body displacement for FCM body pitch motion for Single Bump Inputs on wheel at different velocity

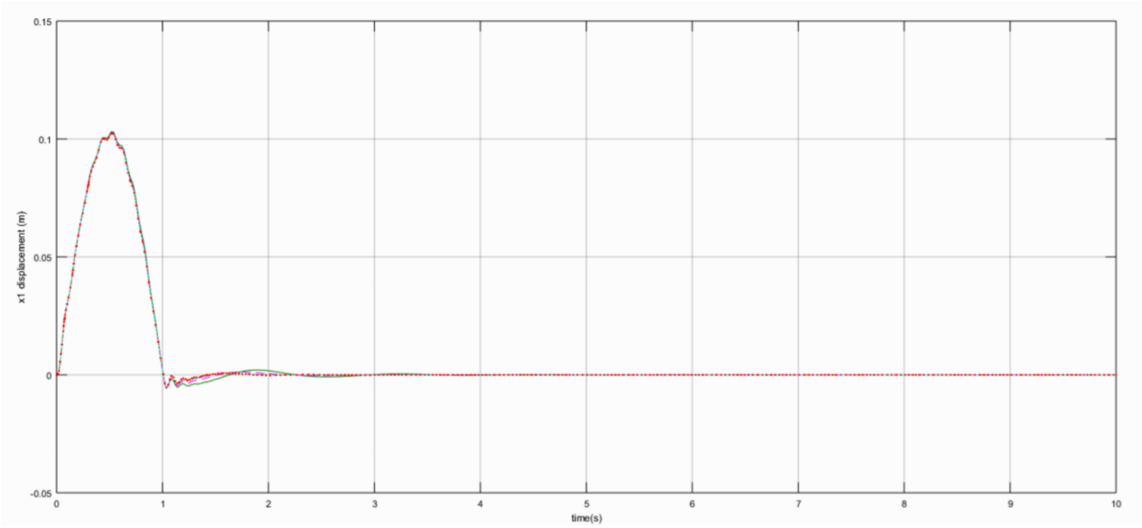

Figure 5. 54 Body displacement for FCM front left wheel for Single Bump Inputs on wheel at different velocity

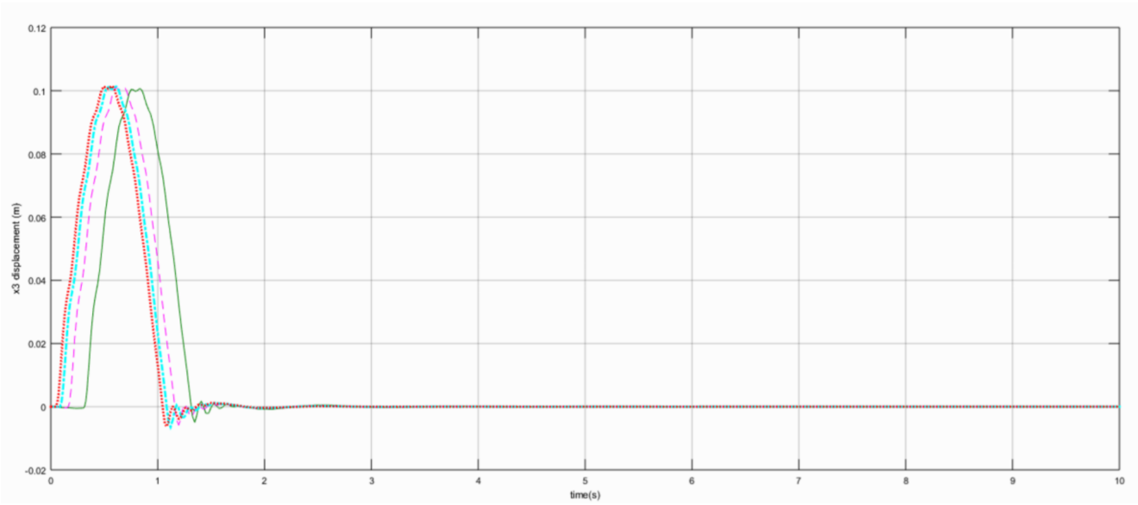

Figure 5. 55 Body displacement for FCM rear left wheel for Single Bump Inputs on wheel at different velocity

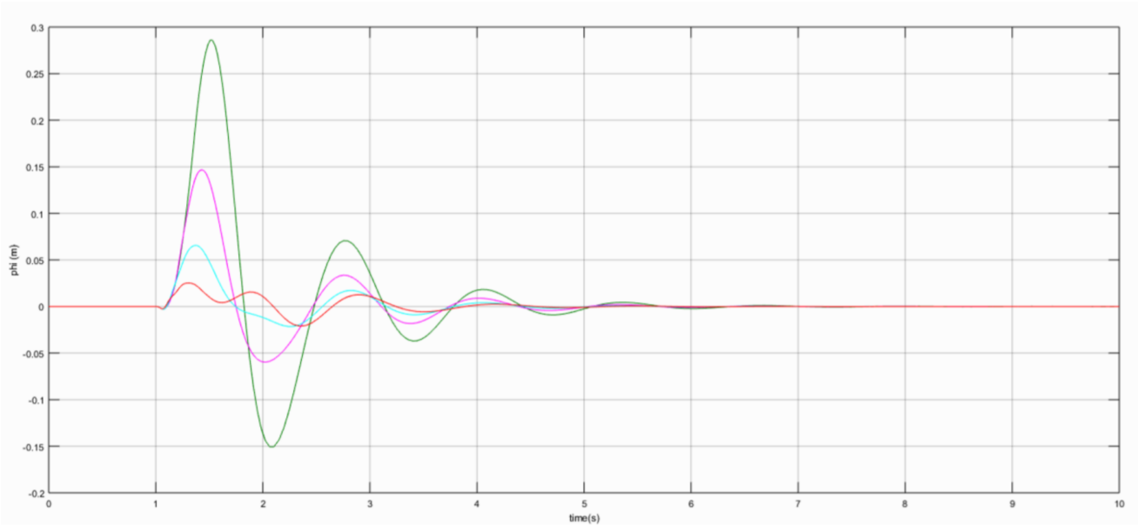

Figure 5. 56 Body roll angle displacement for FCM for Single Step Inputs on wheel at different velocity

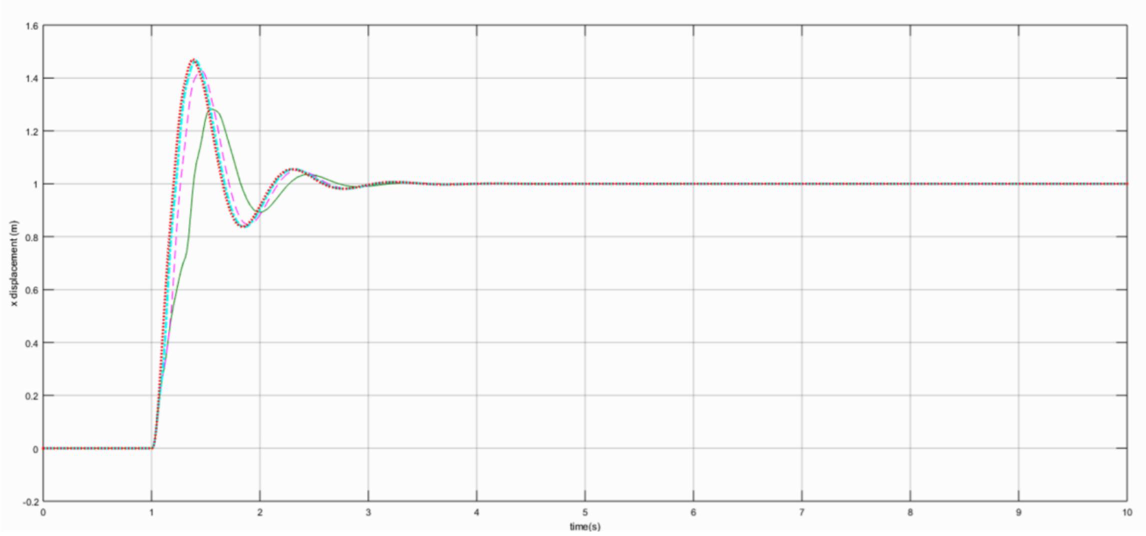

Figure 5. 57 Vertical Body displacement for FCM for Single step Input on wheel at different velocity

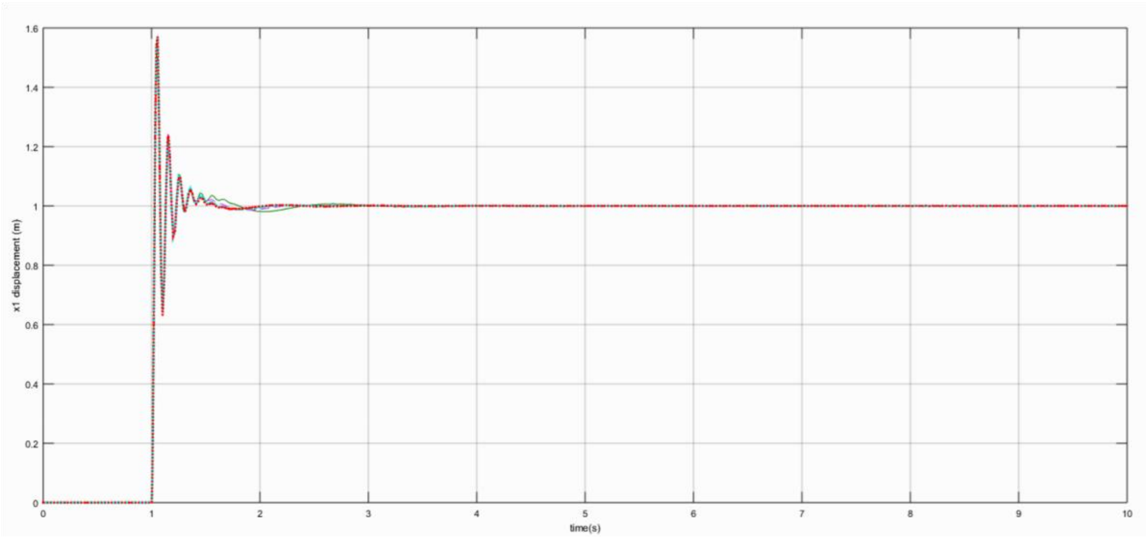

Figure 5. 58 Displacement for FCM of the front right wheel for Single Step Inputs on wheel at different velocity

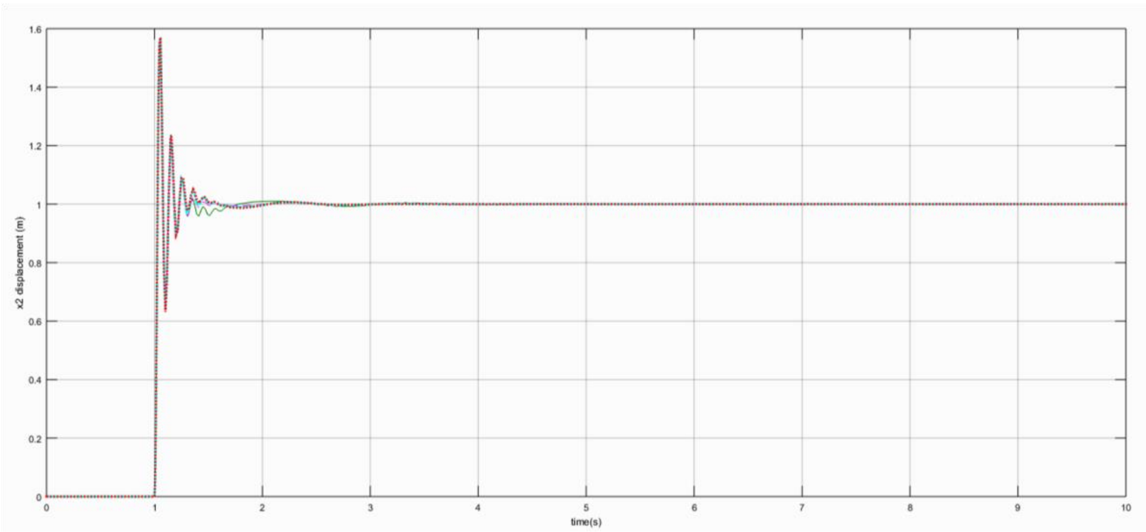

Figure 5. 59 Displacement for FCM of the front right wheel for Single Step Inputs on wheel at different velocity

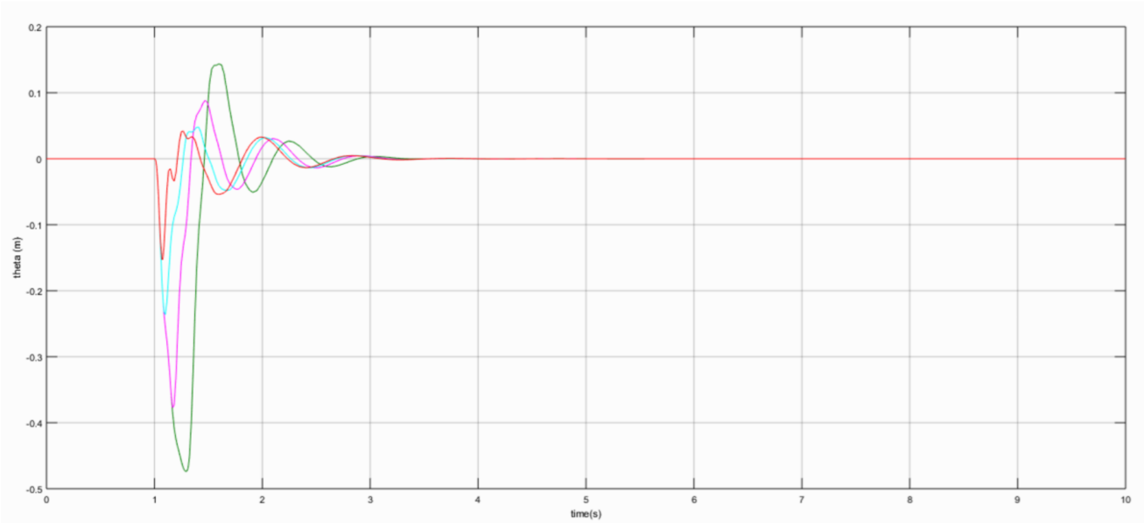

Figure 5. 60 Displacement of FCM of front left wheel for Single Bump Inputs on wheel at different velocity

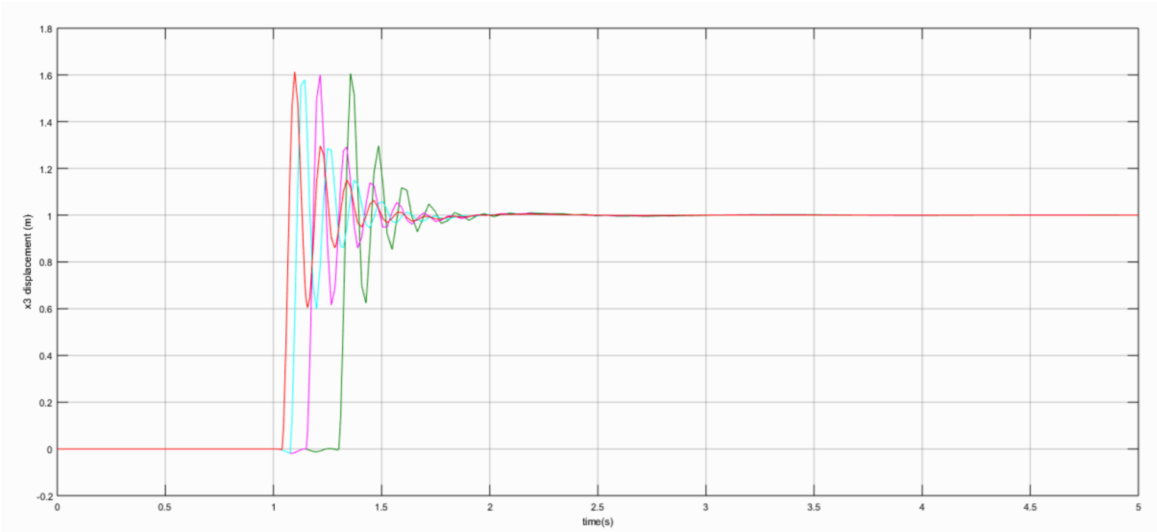

Figure 5. 61 Displacement of FCM of rear right wheel for Single Bump Inputs on wheel at different velocity

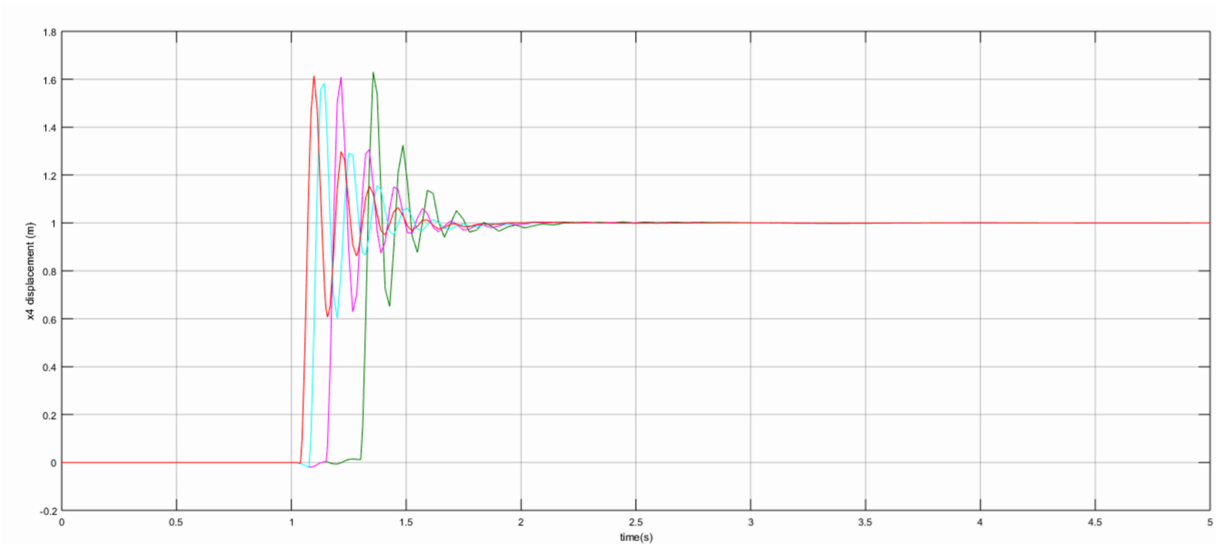

Figure 5. 62 Displacement of FCM of rear left wheel for Single Bump Inputs on wheel at different velocity

Table 5. 11 Body Vertical Displacement for different sprung and unsprung masses for FCM

Sr. No	m (kg)	mfl (kg)	mfr (kg)	mrl (kg)	mrr (kg)	Rise time (s)	Sett. Time (s)	Peak	Peak time (s)
1	500	50	50	50	50	0.0921	2.0005	0.1392	1.2790
2	500	50	50	70	70	0.0864	2.0046	0.1383	1.2712
3	500	50	50	150	150	0.0775	2.0204	0.1419	1.2798
4	500	70	70	50	50	0.0864	2.0056	0.1382	1.2699
5	500	150	150	50	50	0.0774	2.0259	0.1420	1.2936
6	500	50	50	50	90	0.0864	2.0042	0.1396	1.2680
7	500	50	50	90	50	0.0864	2.0043	0.1396	1.2684
8	500	50	90	50	50	0.0859	2.0059	0.1393	1.2499
9	500	90	50	50	50	0.0859	2.0059	0.1393	1.2495
10	600	50	50	50	50	0.1050	2.1889	0.1414	1.3000
11	1200	50	50	50	50	0.1619	3.2771	0.1508	1.4477

It is observed from the above Table 5.11 that as Rear wheels mass increases number of oscillation increases with increase in amplitude. Rise time, Settling Time, Peak Increases but Peak Time shows a decrease for some time and then increases.

As Front wheels mass increases number of oscillation increases with increase in amplitude. Rise time Decreases, Settling Time, Peak Increases but Peak Time Shows a decrease for some time and then increases.

As Body mass increases number of oscillation increases with increase in amplitude. Rise time, Settling Time, Peak and Peak Time Increases.

When considering Front and Rear wheels if right wheel mass is greater than left wheel mass then vibration increases as seen from the increase in peak, Oscillations increases as there is an increase in settling time. If right wheel mass is less than left wheel mass the effect remains the same with increase in vibration and oscillation.

It is also observed that the effect of rear wheels is more than that of the front wheels.

CHAPTER 6: Conclusion
6.1 Conclusion

Vibration in vehicle occurs mainly due to road surface irregularities. The increase in speed don't have significant change in the behavior of vehicle. The vibration behavior depends on the type of road profile.

Study shows that as sprung mass increase there is increases in sprung mass displacement and that of unsprung mass displacement decreases, as suspension spring constant increases, settling time and overshoot increases while rise time decreases. As damping coefficient increases rise time, settling time and overshoot decreases, as tire stiffness increases rise time, settling time and overshoot decreases.

Each wheel has its effect on the other which increases the vibration, but could also cancel it out. This is clearly seen in the FCM. At high speed the effect of both wheel is symmetric which can be differentiated at low speed. This effect is seen in HCM and BCM.

QCM is not better for considering the overall dynamic effect of the vehicle road interaction, but the responses are quite significant. The repetition and magnitude of vibration is important which create impact on the driver and the speed of vehicle. When considering the vehicle repetition of same type of input makes the system oscillatory till it is applied.

Road roughness, bumps, curves and slopes effects the vehicle on road. Study of these effects on vehicle is considered. It shows that the suspension works as a low pass filter in a selective way.

CHAPTER 7:References

[1] M. Agostinacchio, D. Ciampa, S. Olita (2014),"The vibrations induced by surface irregularities in road pavements – a Matlab® approach," European Transport, Springer, 2014

[2] Hassaan, G. A, Mohammed, N.A, "Frequency Response of 10 Degrees of Freedom Full-Car Model For Ride Comfort", International Journal of Scientific Research Engineering & Technology (IJSRET), Volume 4, Issue 1, January 2015

[3] C. B. Patel, P. P. Gohil, B. Borhade, "Modelling And Vibration Analysis Of A Road Profile Measuring System", International Journal of Automotive and Mechanical Engineering (IJAME), Volume 1, pp. 13-28, January-June 2010

[4] Tyan F., Hong Y., et al, "Generation of Random Road Profiles", Journal of Advance Engineering, Jan, 2009.

[5] Robichaud J. M., P. Eng, "Reference Standards for Vibration Monitoring and Analysis", Bretech Engg., 2009

[6] R. Darus, Y. Md. Sam, "Modeling and Control Active Suspension System for a Full Car Model", 5th IEEE International Colloquium on Signal Processing & Its Applications (CSPA), 2009

[7] Setiawan J. D., Mochamad S., Singh A., "Modeling, Simulation and Validation of 14 DOF Full Vehicle Model", International Conference on Instrumentation, Communications, Information Technology, and Biomedical Engineering (ICICI BME), Nov., 2009

[8] Guo L., Zhang L., "Vehicle Vibration Analysis in Changeable Speeds Solved by Pseudoexcitation Method", Mathematical Problems in Engineering, Hindawi Publishing Corporation, Article ID 802720, Aug., 2010

BOOKS

[9] Rao, S.S., Mechanical Vibrations, 5th ed., Prentice Hall, 2011

[10] Dukkipati, R. V., Solving Vibration Analysis Problem Using Matlab, 1st Edition, New Age Publication, New Delhi, 2007

[11] Brandt A., Noise and Vibration Analysis: Signal Analysis and Experimental Procedures, John Wiley and Sons, 2010.

[12] Jazar, Reza N, Advanced Vibrations, Springer

THESIS

[13] Suketu Jani, M.E. Thesis, "Simulation and Evaluation of Semi Active Suspension System for Full Car Model", Gujarat University, October 2010.